Title
Molecular Characterization of the Interaction between Bcl-2 and Nur77/Nor-1 in Apoptosis

Author
Banta, Karl

Publication Date
2017

Peer reviewed|Thesis/dissertation

Molecular Characterization of the Interaction between Bcl-2 and Nur77/Nor-1 in Apoptosis

by

Karl L. Banta

A dissertation submitted in partial satisfaction of the

requirements for the degree of

Doctor of Philosophy

in

Molecular and Cell Biology

in the

Graduate Division

of the

University of California, Berkeley

Committee in charge:

Professor Astar Winoto, Chair
Professor Kaoru Saijo
Professor Nilabh Shastri
Professor Hei Sook Sul

Fall 2017

Abstract

Molecular Characterization of the Interaction between Bcl-2 and Nur77/Nor-1 in Apoptosis

by

Karl L. Banta

Doctor of Philosophy in Molecular and Cell Biology

University of California, Berkeley

Professor Astar Winoto, Chair

As an essential safeguard against autoimmunity, apoptosis during negative selection of self-reactive T cell precursors is important in establishing a self-tolerant T cell repertoire capable of responding to a large array of foreign antigens. The fate of a thymocyte is imposed by signals through the T cell receptor (TCR). During T cell development, thymocytes expressing TCRs that strongly react to self-antigens in the thymus trigger apoptosis and die. The Nur77 family of orphan nuclear hormone receptors and the Bcl-2 family of proteins are important molecules implicated in thymocyte apoptosis and clonal deletion. Strong TCR signals induce the expression and translocation of Nur77 and Nor-1 from the nucleus to the mitochondria, where they bind Bcl-2 and expose Bcl-2's pro-apoptotic, killer BH3 domain. Through extensive Bcl-2 mutagenesis and functional assays, we identify residues within Bcl-2 that are essential for Nur77/Nor-1 interaction. We find that the Bcl-2 mutants that interfere with this interaction do not affect normal Bcl-2 anti-apoptotic function, but lose the ability to mediate Nur77/Nor-1-initiated apoptosis. This study refines the molecular details of this interaction and may assist in generating a novel tool to study the significance of this interaction *in vivo.* The importance of the Bcl-2 BH3 domain was revealed in Bcl-2 BH3 transgenic mice (BH3* Tg) where the BH3 domain is mutated. Unlike mice with a T cell-specific transgenic expression of wild-type Bcl-2, BH3* Tg mice exhibited accelerated morbidity from multi-organ autoimmunity. To further understand what might cause autoimmunity in these mice, we identified a provisional ubiquitous autoantigen found in the antisera of BH3* Tg mice. This data provides the groundwork to further study the potential cause of autoimmune syndrome in these mice. The increase of an autoreactive T cell repertoire in BH3* Tg mice may reject tumor better since self-antigens are largely shared by tumors. However, we found that the presence of an increased autoreactive T cell repertoire in BH3* Tg mice exacerbates tumor growth and morbidity. In sum, this work advances our understanding of molecular mechanisms involved in T cell negative selection and offers insights into the etiology in autoimmunity pathology and potential use for cancer immunotherapy.

DEDICATION

For my mother, Edith P. Banta,
Whose love and presence I could feel from heaven cheering me on…

&

To my husband, Jason M. Satterfield,
You are and always will be my other half.

ACKNOWLEDGEMENTS

I am incredibly thankful to my mentor and advisor, Astar Winoto, for giving me this wonderful opportunity to learn. Thank you for teaching me how to think methodically and make leaps of faith in ideas, to train my hands and perform experiments with purpose, and to "just go for it." Your voice will forever be in my head reminding me to use proper controls and focus on "key" experiments. Thank you for holding me to a higher standard that I thought was possible, and providing me with extensive support and guidance while I tried, failed, learned, and transformed into a scientist. Thank you Astar.

I am grateful to all of my committee members for their unwavering support and guidance as I juggled various projects. Nilabh Shastri, thank you for letting me drop into your office unexpectedly and have random philosophical conversations about life. Kaoru Saijo, in addition to your helpful advice about the projects, many thanks for helping me develop my ideas and become a more independent scientist. Hei Sook Sul, thank you for your helpful suggestions on my projects and many words of wisdom.

Thank you to all the members of the Winoto lab for the wonderful memories, past and present. A special heartfelt thank you goes to Zhanran Zhao. Thank you for lending your ear and listening to my countless babbles of life over lunches and libations. Most of all, thank you for your friendship. Many thanks to Jen Young, Ruchi Schock and Megan Burger for instilling a fun, but "work-hard-play-hard" lab environment. Ruchi, thanks for reminding me that it is okay to get our eyebrows done to look fabulous while doing lab work. Of course, this work could not be completed without the help of Xinyue Wang, Daniel Trisno, and Varsha Prakash. It was a pleasure to mentor and watch you grow.

I owe a great deal to Juliet Spencer for starting my journey of becoming a scientist. Thank you for your guidance and teaching me how to hold a pipette. Allan Balmain and previous members of his lab, especially, Minh To, Kuang-yu Jen, Joan Climent, Ihn Young Song, Cassandra Adams, Erik Fredlund, Jonas Sjolund, Christine Wong, and Phillips Huang, for trusting in my abilities, enriching my love for science, and letting me dabble in the inner workings of cancer genetics.

To my dearest San Francisco friends, many thanks for keeping me sane during this process and being available to grab that "one" drink whenever I needed it. I thank you for all your love and support. Your friendships mean the world to me. In no particular order, many thanks go to Stephanie Lucas, Samantha Fernandez, Sharon Li, Whitney Ray, Andy Harris, Jerry "Jer-Bear" Luke, Homer Perez, and Tony Sourmany. A special thank you goes to my "brosis" Dennis Aguiling. Thank you for having my back.

I am eternally grateful for my family as I went through this transformation. This work couldn't have been completed without your unwavering support. Maryanne 'Anne-tot' Hibner, thank you for reminding me to be headstrong in the face of adversity and to never lose sight of my goals. Vera 'B-poot' Anderson, thank you for making me laugh until I cried when days were difficult. Jasmine 'Kit-Kit' Ryczek, thank you for reminding me that I am doing something greater than myself. John J. Pinelli, thank you for being a father to me and showing me what a real father is supposed to be. Thank you all for your love.

I'd also like to thank my little fur-ball of a cat, Orion. All the cuddles and "making biscuits" on my tummy was just what I needed while I wrote this dissertation.

Finally, a deep heartfelt thank you and immense gratitude belongs to my biggest supporter of all: Jason “honey bunny” Satterfield. Your delicious home-cooked meals and bottles of wine that were readily available when I got home late never went unnoticed. When times were difficult, your unwavering support and unconditional love kept me going. Much of this PhD is because of you. Thank you for accompanying me on this journey. I love you with all my heart and can’t wait to experience more adventures with you.

TABLE OF CONTENTS

GENERAL INTRODUCTION

Apoptosis

Apoptosis is a vital and tightly regulated cell death program for maintaining normal tissue homeostasis by eliminating cells that are no longer needed or potentially dangerous[1-7]. Perturbed regulation of apoptotic pathways can lead to human pathological diseases, such as autoimmunity and cancer. The apoptotic demolition machinery is choreographed by a number of cysteine-dependent aspartate specific caspases[8,9]. Caspases are subdivided into initiator (caspase-2, -8, -9, 10) or effector caspases (caspase-3, -6, -7). In order to prevent unprovoked cell death, caspases are produced as pro-caspases, or zymogens, that must be cleaved in order to become activated[8,9]. Once activated, caspases act in a cascade manner to cleave their respective downstream substrates that ultimately lead to cell death. Two signaling mechanisms exist for the activation of caspases: the extrinsic and intrinsic pathway[10-13].

In the extrinsic pathway, apoptosis is initiated by ligation of death receptors, such as Fas and the tumor necrosis factor receptor. In the case of Fas, the ligation of the death receptor leads to trimerization and subsequent recruitment and formation of the death-inducing-signaling complex (DISC)[5,14-16]. The DISC is composed of the FADD adaptor molecule and initiator caspase, pro-caspase-8. Formation of the DISC facilitates the autocatalytic processing of pro-caspase-8 into activated caspase-8. The active form of caspase-8 can then cleave and activate the effector caspases that commits cell destruction. In some circumstances, the death signal can be boosted by caspase-8 mediated cleavage of pro-apoptotic Bcl-2 family member Bid into tBid (truncated Bid), which acts to inhibit the anti-apoptotic Bcl-2 family members[17].

In the intrinsic or mitochondrial pathway, the conserved family of Bcl-2 proteins control the life and death decision at the mitochondria by acting to protect or disrupt mitochondrial outer membrane integrity (MOMP)[4,18]. The Bcl-2 family share related regions of sequence and structural homology, and can be subdivided into groups by their function and presence of one to four conserved Bcl-2 homology (BH) domains[18]. The pro-apoptotic BH3-only molecules, such as Bcl-2 interacting mediator of cell death (e.g. Bim, Puma), sense and respond to apoptotic signals, such as cellular stress, cytokine deprivation, or DNA damage, and activate the effectors molecules, Bax/Bak[19,20]. Bax and Bak contain BH1 to BH3 domains, and can induce permeabilization of the outer mitochondrial membrane to release cytochrome-c[6]. The release of cytochrome-c leads to the recruitment of apoptotic protease activating factor-1 (APAF-1) and the formation of the apoptosome, ultimately leading to the activation of initiator capase-9 and the downstream caspases.

Apoptosis is closely intertwined with T cell development

One prerequisite for proper T cell function is the ability for its T cell receptor (TCR) to recognize an array of foreign peptide antigens, but be tolerant to self-antigens presented on self-major histocompatibility complexes (MHC). Establishing a T cell repertoire that satisfies these requirements occurs within the thymus. During T development, thymocytes undergo defined developmental stages that can be tracked by the expression of the co-receptors CD4 and CD8[21-24]. As thymocytes progress from a $CD4^-CD8^-$ double negative (DN) to $CD4^+CD8^+$ double positive (DP) stage, they begin to express unique $\alpha\beta$ TCRs on their cell surface[23]. At this stage, signals from the TCR will determine the fate of these DP thymocytes in a process called positive and negative selection[25,26]. These processes promote the survival of thymocytes with functional TCRs (positive selection), and eliminate thymocytes that react strongly to self-antigens (negative selection)[27,28]. An overwhelming majority of DP thymocytes will fail to recognize self-peptide MHC (pMHC) complexes, and consequently, will fail to receive survival signals and die by neglect. Conversely, those DP thymocytes that react with too high of an affinity to pMHC will undergo apoptotic elimination by negative selection. Only those DP thymocytes that engage pMHC with low affinity will pass positive selection and differentiate into CD4 or CD8 single positive T cells. A second round of negative selection occurs after these SP thymocytes migrate to the medulla, where they will be tested for auto-reactivity towards tissue-restricted antigens by medullary thymic epithelial cells (mTECs) under the control of the autoimmune regulatory protein (Aire)[29,30]. Thus, positive and negative selection constitute the central tolerance mechanisms that promotes the generation of a self-tolerant T cell repertoire able to recognize foreign peptides presented on self-MHCs.

Apoptosis and T cell tolerance

Defects in central tolerance have been shown to lead to T cell dysregulation and autoimmunity. This is exemplified in the case of Aire-deficient mice, which develop spontaneous multi-organ autoimmunity due to a defect in negative selection against tissue-restricted antigens[29,31]. Aire, controls the expression of tissue-restricted antigens. During apoptosis, the pro-apoptotic BH3-only Bim and Puma of the Bcl-2 family and Nur77 family of orphan nuclear hormone receptors have been shown to be implicated in the deletion of autoreactive thymocytes[32-37]. Bim-deficient mice can rescue autoreactive T cells and develop systemic lupus erythematosus-like symptoms in a mixed C57BL/6 x 129SV background[38]. Surprisingly, the disease was attenuated in an autoimmune-resistant C57BL/6 genetic background. Only with the compound loss of another BH3-only protein, Puma, could it enhance Bim-deficiency, as $Bim^{-/-}Puma^{-/-}$ mice developed multi-organ autoimmunity[35].

The Nur77 family is composed of Nur77, Nor-1 and Nurr-1. Nur77, along with Nor-1, have been shown to be involved in the thymic deletion[32,39,40]. The constitutive overexpression of Nur77 in thymocytes was shown to lead to massive apoptosis, whereas the ectopic expression of a dominate negative Nur77 protein, which can effectively block the activities of all family members, could rescue thymocytes from deletion[39,41-45]. More recent publications have alluded to additional roles of Nur77 in central tolerance, such as T cell lineage fate determination[46,47]. Nur77 expression is enhanced in thymocytes undergoing differentiation towards the natural regulatory T (Treg) cell fate[48]. Nur77 itself has been shown to bind directly to the Foxp3 promoter and induce Foxp3 expression. Surprisingly, mice lacking all Nur77 family members die faster than Foxp3-deficient mice[49]. These data suggest that Nur77 family members are indeed key players in central tolerance, both in thymic deletion and T cell lineage fate decisions.

How Nur77 and Nor-1 can initiate thymocyte apoptosis is still under investigation. Nur77 transcriptional activity has been shown to increase two components of the death receptor pathway, such as FasL and TRAIL[50,51]. However, negative selection was shown to still occur even in the absence of death receptors[52-54]. Hence, it raised the possibility that Nur77 could initiate thymocyte cell death independent of its transcriptional activity. Indeed, a Nur77 transcriptional independent mechanism that could promote apoptosis was first described in cancer cells. In these cells, an apoptotic stimulus could induce the translocation of Nur77 to the mitochondria[55,56]. At the mitochondria, Nur77 can bind Bcl-2 and expose Bcl-2's killer BH3 domain[55,56]. Importantly, this phenomenon was shown to be physiologically relevant. In thymocytes, strong TCR signals, through PKC signaling, induced the expression and translocation of Nur77 and Nor-1 to the mitochondria, where Nur77/Nor-1 interacted with Bcl-2 and exposed Bcl-2's killer BH3 domain[41,57]. Early publications of this interaction reported that Nur77 associates with Bcl-2 through a linker region between BH4 and BH3 domains (i.e. an unstructured loop domain)[56,58]. However, Nur77 is also capable of interacting with other Bcl-2 family members, Bcl-b and Bcl-2a1[59]. Given that neither Bcl-b nor Bcl-2a1 contain a BH4-BH3 linker region[60], how Nur77 may convert them into pro-apoptotic molecules is not clear. Nevertheless, the importance of the Bcl-2 BH3 domain was recently demonstrated in transgenic mice engineered to express a Bcl-2 protein with its BH3 domain mutated in T cells (BH3* Tg). Most strikingly, unlike wild-type Bcl-2

transgenic mice (Bcl-2 Tg), these mice exhibited accelerated death from multi-organ autoimmunity[61]. Why BH3* Tg, but not Bcl-2 Tg mice develop autoimmunity is of interest.

In the subsequent chapters of this work, we explore a common theme of negative selection and Nur77 biology. In Chapter 1, we delineated the critical residues within Bcl-2 for Nur77/Nor-1 interaction. We show that in contrast to previous reports, the linker region within Bcl-2 is not necessary, but the essential residues for Nur77/Nor-1 interaction are found within an intervening region between the BH1 and BH2 domains. This study, co-authored by Xingyue Wang, Phani Das, and Astar Winoto, was submitted for publication in November 2017. In Chapter 2, we dissect the autoimmune phenotype in BH3* Tg mice and identify a provisional ubiquitous, autoantigen that may be a target during autoimmune progression. In Chapter 3, we attempted to determine whether autoimmune T cells from BH3* Tg mice were capable of being used as cancer immunotherapy. Finally, we discuss remaining unanswered questions from each of these studies.

Chapter 1

Molecular Characterization of the Interaction between Bcl-2 and Nur77/Nor-1 Orphan Steroid Receptor in Apoptosis

ABSTRACT

Apoptosis can be mediated through the extrinsic or intrinsic pathway. Key regulators of the intrinsic apoptotic pathway are the family of Bcl-2 molecules. The activity of the prototypical Bcl-2 protein is traditionally considered anti-apoptotic. However, in certain circumstances, Bcl-2's activity can be converted into a potential pro-apoptotic molecule by associating with the orphan nuclear hormone receptors, Nur77 and Nor-1. Expression of Nur77 and Nor-1 can be induced by a variety of signals including those leading to apoptosis. Translocation of Nur77/Nor-1 to mitochondria can result in their association with Bcl-2, exposing the Bcl-2 BH3 domain and subsequent apoptosis. However, the molecular details of this interaction are incomplete. Through extensive Bcl-2 mutagenesis and functional assays, we have identified residues within Bcl-2 that are essential for Nur77/Nor-1 interaction. Bcl-2 consists of 4 BH domains. Despite the initial report for the requirement of a loop region between the Bcl-2 BH4 and BH3 domains, we found that it is dispensable for Nur77/Nor-1 interaction. Instead, we found important interacting residues at the BH4 domain and crucial interacting residues between the BH1 and BH2 domains. Bcl-2 alanine mutants at this region can no longer interact with Nur77/Nor-1 and can't initiate Nur77/Bcl-2-mediated cell death. However, they still retain their anti-apoptotic capability in two different death assays. These data establish a crucial site in Bcl-2 for Nur77/Nor-1 mediated apoptosis and point to a potential new strategy to manipulate the Bcl-2 function.

INTRODUCTION

Apoptosis is an essential cell death program for maintaining normal tissue homeostasis by remove unwanted and potential dangerous cells[1-7]. Dysregulation of apoptotic pathways could lead to human pathological consequences, such as autoimmunity and cancer[62-65]. Two pathways – extrinsic and intrinsic – can mediate apoptosis [10-13]. The extrinsic pathway is mediated by death receptors, such as Fas and the tumor necrosis factor receptors[5,14-16]. The intrinsic pathway is mediated by the conserved family of Bcl-2 proteins, which are important for regulating apoptosis through mitochondria[4,18,66]. The Bcl-2 family share related regions of sequence and structural homology, and can be subdivided into groups by their function and by the presence of one to four conserved Bcl-2 homology (BH) domains[18]. The pro-apoptotic BH3-only molecules, such as Bcl-2 interacting mediator of cell death (e.g. Bim, Puma), sense and respond to apoptotic signals and activate the effectors molecules, Bax/Bak[18,67-69]. Bax and Bak contain BH1 to BH3 domains, and can induce permeabilization of the outer mitochondrial membrane to release cytochrome-c, leading to activation of capase-9 and the downstream caspases[6,70-72]. The anti-apoptotic family members, which include Bcl-2 and Bcl-X, contain all four BH domains and can prevent apoptosis by sequestering and inactivating the BH3-only proteins[18,73]. This function requires intact BH1, BH2 and BH4 domains[19,20]. Over-expression of Bcl-2 protein is a common mechanism of apoptosis dysregulation[4,65]. Elevated levels of Bcl-2 protein can offer a survival advantage in cells and has been associated with resistance to chemotherapy and poor prognosis[74]. Hence, an on-going chemotherapeutic strategy in cancer has been to target Bcl-2 to restore the ability of cancer cells to undergo apoptosis[74-79].

Nur77 and Nor-1 belong to the family of orphan nuclear hormone steroid receptors, and have been implicated as pro-apoptotic factors in developing T cells and

cancer cells[39,43,80]. During T cell development, thymocytes expressing T cell receptors (TCR) with high affinity for self-antigens induces Nur77 and Nor-1 expression to a level that correlates with apoptosis accompanying negative selection[39,41,43]. Prior studies have showed that a constitutive active form of either Nur77 or Nor-1 in thymocytes led to increased apoptosis, whereas the overexpression of a dominate-negative Nur77 protein, which can effectively inhibit the activity of all Nur77 family members, can rescue thymocytes undergoing cell death during negative selection[39,41-45]. How Nur77 and Nor-1 are able to initiate apoptosis is still not completely clear and delineating the mechanism has long been under investigation. We and others have shown that Nur77 may initiate apoptosis by modulating the activity of Bcl-2[41,56,80,81]. While Bcl-2 is known as an anti-apoptotic molecule, several reports have highlighted the fact that Bcl-2 can be converted into a pro-apoptotic protein under certain circumstances[44,56,80]. In thymocytes, strong TCR signals induce Nur77 and Nor-1 translocation to the mitochondria which then associates with Bcl-2, an event originally described in several cancer cells upon apoptotic stimuli[41,56]. This association leads to a conformational change that exposes Bcl-2's BH3 domain. This may convert Bcl-2's normal anti-apoptotic activity into a killer, pro-apoptotic protein, possibly through saturation binding of Bcl-x[56,82]. The importance of the Bcl-2 BH3 domain was demonstrated in transgenic mice engineered to express a Bcl-2 protein with its BH3 domain mutated in T cells[61]. This Bcl-2 mutant exhibits increased anti-apoptotic activity and rescues more autoreactive T cells when compared to transgenic wild-type Bcl-2. Most strikingly, unlike wild-type Bcl-2 transgenic mice, these mice exhibited accelerated death from multi-organ autoimmunity[61].

Showing the *in vivo* significance of Bcl-2 conversion by Nur77/Nor-1 interaction has nevertheless been elusive, primarily because the molecular details of this interaction have not yet been fully elucidated. The essential residues within Bcl-2 for Nur77/Nor-1 interaction are unresolved. Early publications have reported that Nur77 associates with Bcl-2 through a linker region between BH4 and BH3 domains (i.e. an unstructured loop domain)[56,58]. However, Nur77 is also capable of interacting with other Bcl-2 family members, Bcl-b and Bcl-2a1[59,82]. Given that neither Bcl-b nor Bcl-2a1 contain a BH4-BH3 linker region[83-85], how Nur77 may convert them into pro-apoptotic molecules is not clear. This also raises the question whether the loop domain in Bcl-2 is even necessary for interaction with Nur77. Recently, the existence of a novel Nur77 binding pocket for Bcl-b was reported[86]. However, whether this Nur77-binding pocket pertains to Bcl-2 has not been addressed.

Here, we identify Bcl-2 mutants that abrogate the interaction for both Nur77 and Nor-1 through extensive Bcl-2 mutagenesis. In contrast to prior observations, we report that the Bcl-2 loop domain is dispensable for Nur77/Nor-1 interaction. We also find that mutating a cluster of residues located in an intervening sequence between BH1 and BH2 domain can abolish Nur77 and Nor-1 interaction. Mutations at this site do not affect the Bcl-2 normal anti-apoptotic function but can block Nur77-mediated apoptosis. Taken together, our study further refines the molecular details of Nur77/Nor-1 and Bcl-2 interaction.

RESULTS

Bcl-2 Y18 and Y21 are essential for a truncated but not the full-length Bcl-2 to interact with Nur77 and its family member Nor-1

To identify amino acids in Bcl-2 required for its interaction with Nur77 and Nor-1, we initially focused our attention on the loop between the BH4 and BH3 domain. This unstructured loop domain of Bcl-2 (amino acids 31 to 92) was reported to be a region where Bcl-2 interacts with Nur77[56,58]. However, a precise location within the loop necessary for Nur77 interaction has not been defined. To investigate this further, we engineered constructs containing a truncated Bcl-2 fused to GFP with only the BH4 and loop domain (2-92), as well as progressive C- and N-terminal deletions within this BH4-loop fragment (Figure 1A). A tagged Bcl-2 was used because we discovered that the epitope for monoclonal antibodies against Bcl-2 (clone C-2, Santa Cruz Biotechnology) is located to the Bcl-2 loop region (data not shown). For Nur77, we used a FLAG-tagged Nur77 lacking a DNA binding domain (Nur77ΔDBD) as described previously[56,81,82]. This allows us to bypass the requirement to stimulate the cells to initiate Nur77 nuclear to mitochondria translocation[57]. These constructs were then transfected into HEK293T cells and FLAG co-immunoprecipitation (FLAG-IP) assays were performed to test for the mutant Bcl-2/ Nur77ΔDBD interaction. Briefly, we used anti-FLAG antibodies to immunoprecipitate Nur77 from the cell lysates and the presence of co-immunoprecipitated Bcl-2 was detected on western blot using GFP specific antibodies. Surprisingly and in contrast to previous reports[56,58], however, the Bcl-2/F(11-60) mutant lacking much of the loop was still able to interact robustly with Nur77 (Figure 1B). Several other C-terminal deletions up to 35 amino acids also interacted strongly with Nur77 (Figure 1B).

To further locate the Nur77 interacting site(s) in this Bcl-2 region, we generated progressive N-terminal deletions (Figure 1A). As shown in Figure 1C, Bcl-2/F(2-92), Bcl-2/F(11-92) and Bcl-2/F(15-92) were able to interact with Nur77, but deletion to amino acid 21 {Bcl-2/F(21-92)} abolished its ability to interact with Nur77 (Lane 7, Figure 1C). Similar results were obtained using Nor-1, with the exception that Bcl-2/F(15-92) consistently exhibits reduced interaction with Nor-1 (Lane 11, Figure 1C). We concluded that Bcl-2 can interact with Nur77 and Nor-1 through the N terminal region at amino acids 15 through 21 in the BH4 domain, but the loop region between BH4 and BH3 domain is not required for this interaction.

To refine the region within BH4 required for interaction with Nur77/Nor-1, multiple alanine scan mutants along amino-acids 15 to 21 within the BH4-loop fragment were generated. These include Bcl-2/F(Ala(11-14)), Bcl-2/F(Ala(15-18)), and Bcl-2/F(Ala(19-21)), which respectively replace amino acids 11-14, 15-18 or 19-21 with alanines. As shown in Figure 1D, although each alanine scan mutant was able to co-immunoprecipitate with Nur77 to some extent, a consistently reduced interaction was observed with Bcl-2/F(Ala(15-18) and Bcl-2/F(Ala(19-21)) (Lane 6-7, Figure 1D). Single amino-acid alanine substitutions were then generated for residues 15 to 21, but each were able to co-immunoprecipitate with Nur77 (data not shown). Notably, Y18A or Y21A alone was observed to reduce, but not fully prevent Nur77 interaction (Lane 5 and 6, Figure 1E). A complete loss of interaction with Nur77 was only observed in the Bcl-2 BH4-loop fragment containing both the Y18A and Y21A mutations (Lane 4, Figure 1E). The Bcl-2/F(Y18A,Y21A) protein also lost its ability to interact with Nor-1 (Lane 9, Figure 1E). To see whether Y18A and Y19A within a full-length Bcl-2 protein was sufficient to

abrogate Nur77 family binding, a GFP-fused WT Bcl-2 or Bcl-2 containing the double Y18 and Y21 alanine mutation (Bcl-2/Y18A,Y21A) was generated. In contrast to the Bcl-2/F(2-92) Y18/Y21 mutant, however, an interaction with Nur77 or Nor-1 persisted in the context of full-length protein Bcl-2/Y18A,Y21A (Lane 4 and 7, Figure 2A), suggesting that there might be multiple Bcl-2 regions that interact with Nur77. We also found that deletion of the Bcl-2 loop region (Bcl-2/Δ31-51, Bcl-2/Δ52-71, and Bcl-2/Δ72-92) in the context of the full protein has no effects on its ability to interact with Nur77 (Figure 2B). Taken together, these data provide evidence that the loop domain is dispensiable, but Y18 and Y21 are essential for Nur77/Nor-1 interaction in the context of a truncated Bcl-2 protein.

Identification of Bcl-2 mutants that do not interact with Nur77 and Nor-1

Consequently, we reasoned that Bcl-2 could contain multiple interacting residues with the Nur77/Nor-1 since combined alanine substitution of Y18 and Y21 in a full length Bcl-2 protein was unable to abrogate binding. These putative alternative sites could compensate for the loss of Y18 and Y21 to allow interaction with Nur77/Nor-1. Consistent with this notion, multiple Nur77 binding sites were recently found in Bcl-b, a member of the Bcl-2 family that can also undergo anti- to pro-apoptotic conversion by Nur77[86]. Utilizing NMR spectroscopy-based methods with a Nur77 derived peptide, the authors reported that Nur77 may interact with Bcl-b through several novel interaction sites adjacent to the BAX-binding crevice[86]. We sought to test if the observation was also applicable to Bcl-2. Because Bcl-2 anti-apoptotic family members are structurally similar, we performed an amino-acid sequence alignment between Bcl-b and Bcl-2 and highlighted the Bcl-b residues involved with Nur77 interaction (Figure 3A). Interestingly, the Bcl-b residue Y19 involved in Bcl-b-Nur77 interaction aligns to Bcl-2 Y18. This is consistent with one of the two essential residues identified above using the BH4-loop fragment. The alignment also revealed other potential Bcl-2 interacting residues, which were primarily found within or flanking the BH3 domain. In addition, there are two Bcl-b Nur77-interacting residues that align to Bcl-2 residues between BH1 and BH2. To test whether analogous Bcl-2 residues could be involved in Nur77 interaction, we first generated two Bcl-2 mutants akin to the Bcl-b mutants that abolish its interaction with Nur77 (Bcl-b/Y19A,A44L to Bcl-2/Y21A,D102A,D103A & Bcl-b/R47A,E99A to Bcl-2/S105A,R106A,V159A,E160A, see Figure 3B) and performed FLAG-IPs as described before. Surprisingly, however, both Bcl-2 analogous mutants (Bcl-2/Y21A,D102A,D103A and Bcl-2/S105A,R106A,V159A,E160A) were still able to interact with Nur77 (Lane 4, Figure 3C; Lane 3, Figure 3D). We then expanded our search for potential interacting residues within the BH3 domain by generating Bcl-2 alanine scans. Bcl-2 alanine scan mutants within this domain were generated in a fashion that was N- or C-terminal to the core residues (G101, D102, D103) to avoid disrupting the potential pro-apoptotic function of BH3[44]. These included Bcl-2/Ala(93-96), Bcl-2/Ala(94-97), Bcl-2/Ala(95-98), Bcl-2/Ala(106-110), and Bcl-2/Ala(110-114) (Figure 3B). To determine whether any of these Bcl-2 alanine mutants were able to abrogate Nur77 binding, FLAG-IPs were performed as described before. Surprisingly, each mutant again interacted with Nur77 although at slightly different efficiency as that WT Bcl-2 (Figure 2C, 2E). Among these mutants, only Bcl-2/Ala(93-96) was able to consistently reduce, but not fully abolish Nur77 or Nor-1 interaction (Lane 4 and 12, Figure 3E).

Finally, we investigated potential Bcl-2 residues found to align with Bcl-b in the intervening sequence between BH1 and BH2 domains. We generated the Bcl-2 alanine scan mutants: Bcl-2/Ala(157-160), Bcl-2/Ala(158-161), and Bcl-2/Ala(159-163) (Figure 3B). Using FLAG-IP as an assay, we found that Bcl-2/Ala(158-161) and Bcl-2/Ala(159-163), and occasionally Bcl-2/Ala(157-160) could no longer co-immunoprecipitate Nur77 (Figure 3E). Similar results were also observed with Nor-1 (Lane 14 and 15, Figure 3E). Hence, amino acids 158-163 of Bcl-2 within the intervening sequences between its BH1 and BH2 domains contains essential residues important for interaction with Nur77 and Nor-1.

The BH1-BH2 intervening Bcl-2 mutants that no longer interact with Nur77 or Nor-1 still exhibit normal anti-apoptotic function

The Bcl-2 region between BH1 and BH2 is not known to be important for the Bcl-2 anti-apoptotic function[19]. To assess whether this is true, HeLa cells were transiently transfected to express either the control eGFP-C1 vector or vector encoding WT Bcl-2, Bcl-2/Ala(158-161), or Bcl-2/Ala(159-163). For comparison, we also transfected Bcl-2/Ala(93-96) or Bcl-2/Ala(94-97) with alanine mutations affecting the Bcl-2 BH3 domain. Bcl-2/Ala(93-96) but not Bcl-2/Ala(94-97) exhibited reduced interaction with Nur77. Cell viability was evaluated after apoptosis was initiated with either staurosporin (STS) or cisplatin (CIS). Cell viability of cells transfected with wild-type Bcl-2 was set at 100%. Immunoblots with the GFP-tag confirmed that each Bcl-2 mutant was expressed at similar levels to WT Bcl-2 (Figure 4A). As expected, HeLa cells expressing the control vector resulted increased cell death with 0.5 μM or 1 μM concentrations of STS (top panel, Figure 3B). Interestingly, HeLa cells expressing Bcl-2/Ala(93-96) or Bcl-2/Ala(94-97) proteins resulted in cell death indistinguishable to the empty vector control when challenged with 0.25μM, 0.5 μM or 1 μM STS. In contrast, Bcl-2/Ala(158-161) and Bcl-2/Ala(159-163) proteins exhibited protection activity to staurosporin-induced death at a similar or better level to WT Bcl-2 (top panel, Figure 4B). A similar result was obtained when cells were subjected to 30 μM CIS treatment (lower panel, Figure 4B).

We also assessed whether the 158-161 and 159-163 Bcl-2 mutants would affect anti-apoptotic function in a more physiological relevant setting by testing the Bcl-2 mutants in a classical cytokine deprivation assay. LyD9 murine hematopoietic progenitor cell line was utilized for this purpose as LyD9 cells undergo apoptosis in the absence of interleukin-3 (IL-3) [87,88]. Overexpression of Bcl-2 could protect cells from death by cytokine withdrawal[89]. To test whether Bcl-2 alanine mutants were able to offer similar protection, LyD9 cells were stably transfected with the MSCV-PIG retroviral vector, MSCV-PIG encoding an HA-tagged WT Bcl-2, Bcl-2/Ala(158-161), or Bcl-2/Ala(159-163) by viral transduction. Successful stable expression of WT Bcl-2 or each Bcl-2 mutant was confirmed by western blot analysis (Figure 3C). To assess the anti-apoptotic activities of the Bcl-2 mutants, IL-3 was withdrawn from the culture medium and cell viability was monitored over time. As expected WT Bcl-2 offered protection when cells were deprived of IL-3 compared to the control vector (Figure 4D). A similar protection was also observed for Bcl-2/Ala(158-161) and Bcl-2/Ala(159-163), although the latter exhibited slightly less protective effect (Figure 4D). Together, these results provide evidence that Bcl-2/Ala(158-161) and Bcl-2/Ala(159-163) mutants impair the

interaction with Nur77 and Nor-1, but have minor to no effect on its anti-apoptotic function.

Bcl-2 mutants that do not interact with Nur77 or Nor1 have reduced pro-apoptotic activity

The conversion of Bcl-2 from an anti- to pro-apoptotic molecule is thought to be mediated by direct Nur77 or Nor-1 interaction, which exposes its BH3 epitope[41,56,80]. We reasoned that the identified Bcl-2 mutants unable to interact with Nur77 family should exhibit reduced death mediated by Bcl-2 conversion. To test this hypothesis, HeLa cells were transiently transfected with WT Bcl-2 or Bcl-2 mutants with or without Nur77 or Nor-1. Cell death was then measured by flow cytometric analysis of cells using Annexin V. The results showed minimal death (<5%) in all single transfectants (top panel, Figure 5). To ensure equivalent loading and expression, immunoblot was used to detect the corresponding FLAG- or GFP-tag (bottom panel, Figure 5). As reported previously by others[56], co-expression of Nur77ΔDBD or Nor-1ΔDBD with WT Bcl-2 in HeLa cells significantly increased cell death. In line with our reasoning, reduced cell death was observed when Bcl-2/Ala(158-161) and Bcl-2/Ala(159-163) to some extent when they were co-expressed with Nur77. Cell rescue was also observed when these mutants were co-expressed with Nor-1. We concluded that these Bcl-2 mutants that are unable to interact with Nur77 also fail to undergo Nur77-mediated cell death.

DISCUSSION

The ability for Nur77/Nor-1 to associate and convert Bcl-2 from a normally anti-apoptotic to a killer molecule is an attractive mechanism to harness and exploit for anti-tumor chemotherapies, yet the molecular details of this interaction is not completely unclear. We therefore initiated this study to determine the precise Bcl-2 interacting residues essential for Nur77/Nor-1 interaction through extensive Bcl-2 mutagenesis. An unstructured Bcl-2 loop region (amino acids 31 to 92) between its BH4 and BH3 domain has been reported to be the site of Bcl-2/Nur77 interaction[56,58]. However, we found that this Bcl-2's unstructured loop domain is not the primary site for Nur77/Nor-1 interaction. Two observations are consistent with this notion. First, Bcl-2 mutants containing large deletions across the loop region were still able to interact with Nur77. Second, by mutagenizing a truncated Bcl-2 protein containing only the BH4-loop domains, we observed that Nur77 or Nor-1 was able to immunoprecipitate a truncated Bcl-2 protein lacking much of its loop domain. Consistent with our data, a later paper by the same group reported that a Bcl-2/Bcl-x(L) chimera without the Bcl-2 loop region was still able to bind to Nur77[86,90]. While the chimera contains a Bcl-x loop, it is known that Bcl-x(L) doesn't bind to Nur77[59,86,90].

In the context of a truncated Bcl-2 protein, we identified two important Nur77/Nor-1 interacting residues (Y18 and Y21) within the BH4 domain. Neither of these BH4 residues have been reported to be essential for the Bcl-2 anti-apoptotic activity[91,92]. Surprisingly, when these residues were replaced in the context of a full length Bcl-2 protein (Bcl-2/Y18A,Y21A), we observed that the mutant protein still interacted with Nur77/Nor-1. This might indicate the presence of additional Nur77/Nor-1 interaction sites that can compensate for the loss of Y18 and Y21. In line with this notion, a recent study performed on Bcl-b for its site of interaction with Nur77 has shown that its BH4

domain is one of the Nur77-binding sites. However, a single Bcl-b residue modification in its BH4 domain was also insufficient to affect Nur77 interaction[86].

The reported Bcl-b mutations that abolished Nur77 interaction were aimed at affecting the Nur77-binding pocket, either by hindering access by increasing Bcl-2 hydrophobicity (Bcl-b/Y19F,A44L) or by eliminating a charge residue (Bcl-b/R47A,E99A)[86]. Our mutagenesis on Bcl-2 itself either by progressive alanine scans or by mimicking these Bcl-b mutants suggests that the putative Nur77-binding pocket for Bcl-2 is not entirely similar to that of Bcl-b. This is not too surprising, since there is an apparent structural difference between Bcl-b and Bcl-2, with the latter possessing an unstructured, "linker" region between BH4 and BH3 domains that could shift the location of this Nur77-binding site. The protein alignment between Bcl-b and Bcl-2 revealed one Bcl-b residue involved in Nur77 binding that matched to a critical residue within Bcl-2 BH3 domain for pro-apoptotic function (Bcl-b/A44 to Bcl-2/D102). It would be unlikely for Nur77/Nor-1 to bind Bcl-2 at this residue since an interaction at this site would block the potential pro-apoptotic BH3 domain function. Consistent with this, we observed that the Bcl-2 mutant (Bcl-2/Y21F,D102A,D103A) corresponding to a Bcl-b mutant (Bcl-b/Y19A,A44L) was still able to interact with Nur77. Thus, D102 from Bcl-2 that corresponds to the Bcl-b BH3 site is not a critical interacting residue with Nur77. Furthermore, normal Nur77 binding can still be seen for another Bcl-2 mutant that is analogous to a Bcl-b mutant that cannot interact with Nur77. Moreover, we were unable to identify a location within the Bcl-2 BH3 domain after performing a thorough alanine scan that could lead to a consistent and/or complete loss of Nur77 binding. All these data combined highlight differences between Bcl-2 and Bcl-b in their binding sites for Nur77.

In contrast to Bcl-b, where the essential sites of interaction with Nur77 occurs over multiple domains (i.e. BH4, BH3, and BH1), we identified essential interacting residues within Bcl-2 located in an intervening sequence between BH1 and BH2 domains[86]. The mutants Bcl-2/Ala(158-161) and to a lesser extent Bcl-2/Ala(159-163), which correspond to residues CVES or VESVN, respectively, failed to interact with Nur77 and Nor-1. Unlike the Bcl-b mutants, where it was necessary to mutate discrete residues along the putative Nur77-binding pocket, the Bcl-2 mutants identified here are located within a single region. Why these mutations in Bcl-2 were sufficient to abolish Nur77 interaction instead of the mutating multiple sites similar to Bcl-b is not completely clear but might be due to the differences in the Nur77 interaction pocket between Bcl-2 and Bcl-b. One conceivable difference might be that the Nur77 interaction surface area in Bcl-b is larger than Bcl-2. In fact, it has been reported that Nur77 binds the tightest with Bcl-b compared to Bcl-2a1 and Bcl-2 *in vitro* and by fluorescence polarization assays[59,86]. Hence, mutations in Bcl-2 that affect the Nur77 binding pocket have a greater effect on Nur77-association. Alternatively, the residues are located within the central core helix (α5), a region that may play role in structural and functional importance[60]. Although we cannot completely rule out the possibility that mutating four or five residues at a time could affect Bcl-2 tertiary structure, we were still able to observe detectable levels of these Bcl-2 mutants similar to that of WT levels by probing for the GFP-fused tag by immunoblot. In addition, they exhibited little to no effect on the anti-apoptotic activities compared to WT Bcl-2. Interestingly, mutating V159 and E160 to alanines together were insufficient to abrogate Nur77 binding, suggesting that this

cluster of residues may be work synergistically to interact with Nur77 and Nor-1. These observations taken together suggest that CVES are the essential interaction residues in Bcl-2 for it to interact with Nur77/Nor-1.

In summary, we extend our findings to show an important Nur77 interacting residue cluster within Bcl-2 that is located in an intervening sequence between BH1 and BH2. We have provided evidence that these Bcl-2 mutants do not affect the normal Bcl-2 anti-apoptotic function and that these Bcl-2 mutants do not induce Nur77/Bcl-2 mediated death. These findings provide additional insights on the molecular details of the Nur77 conversion death pathway, and provide means to improve targeting Bcl-2 for anti-tumor therapy and to assess the importance of Bcl-2/Nur77 interaction in T cell negative selection.

EXPERIMENTAL PROCEDURES

Plasmid constructs

Murine N-terminal FLAG-tagged Nur77 and Nor-1 plasmids lacking a DNA binding domain (ΔDBD)[56,81] were generated by standard deletion mutagenesis by overlap extension PCR protocol using BioRad iProof High-Fidelity DNA Polymerase in pmKate2-N (Evrogen) or pCI (Promega) expression vector. The final PCR products were cloned into pmKate2-N using HindIII and EcoRI restriction sites. Nur77ΔDBD corresponds to the deletion of amino acids 169-466. Nor-1ΔDBD corresponds to the deletion of amino acids 190-460.

Human Bcl-2 mutants were generated in pEGFP-C1 (Clonetech) or MSCV-PIG in a similar fashion as described above or by Gibson cloning method[93]. All mutations were verified by DNA sequencing (UC Berkeley Sequencing Facility). Primers used to generate the Bcl-2 recombinant plasmids are available upon request.

Cell culture and transfection –HeLa or the IL-3 producing X61-IL-3 cell line were cultured and maintained at 37˚C in RPMI 1640 supplemented with 10% FBS, 2 mM L-glutamine, non-essential amino acids, 5 x 10^{-5} M 2-mercaptoethanol and 1 mM sodium pyruvate (cRPMI). The mouse multipotent IL-3 dependent LyD9 cells were cultured in cRPMI supplemented with IL-3 enriched media produced by X61-IL3 cells. Each cell line was periodically tested negative for mycoplasma. Transfection was performed using Lipofectamine 2000 (Invitrogen) according to the manufacture's recommendations.

Co-immunoprecipitation and western blot

HEK293T cells were transiently co-transfected with Nur77ΔDBD and WT Bcl-2 or Bcl-2 mutants at a 1:1 ratio. To study the interaction between Nur77 family members with human Bcl-2, cells were pelleted after 24 hours of transfection, washed with PBS, and resuspended in lysis buffer (150 mM NaCl; 50 mM Tris-HCl, pH 7.5; 20 mM EDTA; 1% NP-40; Protease Inhibitor Cocktail (Sigma); and 1 mM DTT). Lysates were clarified by high speed centrifugation and pre-cleared with Protein G agarose beads (Thermoscientific) prior to incubating with anti-FLAG or isotype with Protein G agarose overnight. Beads were washed with lysis buffer prior to being boiled in SDS sample loading buffer, ran on a 10% SDS-PAGE gel, and transferred onto nitrocellulose membranes. Membranes were blocked with 5% BSA in TBS containing 0.1% Tween and probed using anti-HA (clone HA.C5, Abcam), anti-MYC (clone E910, Clontech),

anti-FLAG (clone 5E10, Accurus), anti-GFP (clone FL, Santa Cruz Biotechnology), or anti-GAPDH (clone 14C10, Santa Cruz Biotechnology) antibodies.

LyD9 transduction of WT Bcl-2 or Bcl-2 alanine mutants

Stably expressing WT Bcl-2 or Bcl-2 alanine mutants in LyD9 cells were obtained by first transfecting Phoenix cells with 3 µg control MSCV-PIG or MSCV-PIG encoding HA-tagged WT Bcl-2 or Bcl-2 alanine mutants along with 0.5 µg VSV-G and 1 µg gag-pol helper plasmid (Nolan lab) with Lipofectamine 2000 (Invitrogen) in 6-well plates. 24 hours post-transfection, the viral supernatant was passed through a 0.2 µM syringe filter, supplemented with 10 µg/mL Polybrene (Santa Cruz Biotechnology), and added to approximately 2-4 x 10^6 LyD9 cells. The LyD9 cells were spun at 2500rpm for 1 hour at room temperature and cultured at 37˚C for 24 hours to recover. Selection of successfully transduced was obtained by supplementing the culture media with 10 µg/mL Puromycin. Stable transfection was confirmed by GFP expression using flow cytometry and/or by detecting the presence of the C-terminal HA-tag by Western Blot analysis.

Cell death from chemical apoptotic inducers or IL-3 cytokine deprivation

24 hours post-transfection of WT Bcl-2 or Bcl-2 mutants (in 6 well plates), HeLa cells were transferred to 96 well plates and allowed to settle for another 24 hours. Cell viability was determined by CellTiter-Glo (Promega) at 24, 48, or 72 hours after incubating with cRPMI supplemented with indicated concentrations of staurosporin (STS; Sigma-Aldrich) or cisplatin (CIS; Sigma-Aldrich). Relative Light Units (RLUs) were obtained by normalizing the values to the corresponding WT Bcl-2 treated sample.

To measure cell viability after interleukin-3 (IL-3) deprivation, LyD9 cells were washed three times with 1X PBS (GE HyClone) and seeded into 96 well plates at density of 1 x 10^5 cells per well with cRPMI without IL-3. Cell viability was then measured by CellTiter-Glo after indicated number of days following cytokine deprivation. CellTiter-Glo assays were performed in triplicate in 96-well plates according to the manufacture's recommendations.

Annexin V^+ staining by Flow cytometry

HeLa cells were transfected with the indicated plasmids. After 24 hours, HeLa cells were washed with 1X PBS, resuspended in Annexin V binding buffer (100 mM HEPES, pH 7.4; 140 mM NaCl; 2.5 mM $CaCl_2$), and then incubated with Pacific Blue-conjugated Annexin V antibody (BD Biosciences). Analysis of Annexin V^+ was performed on GFP^+ and $mKate^+$ cells using FlowJo 10 software (FlowJo).

FIGURE LEGENDS

FIGURE 1

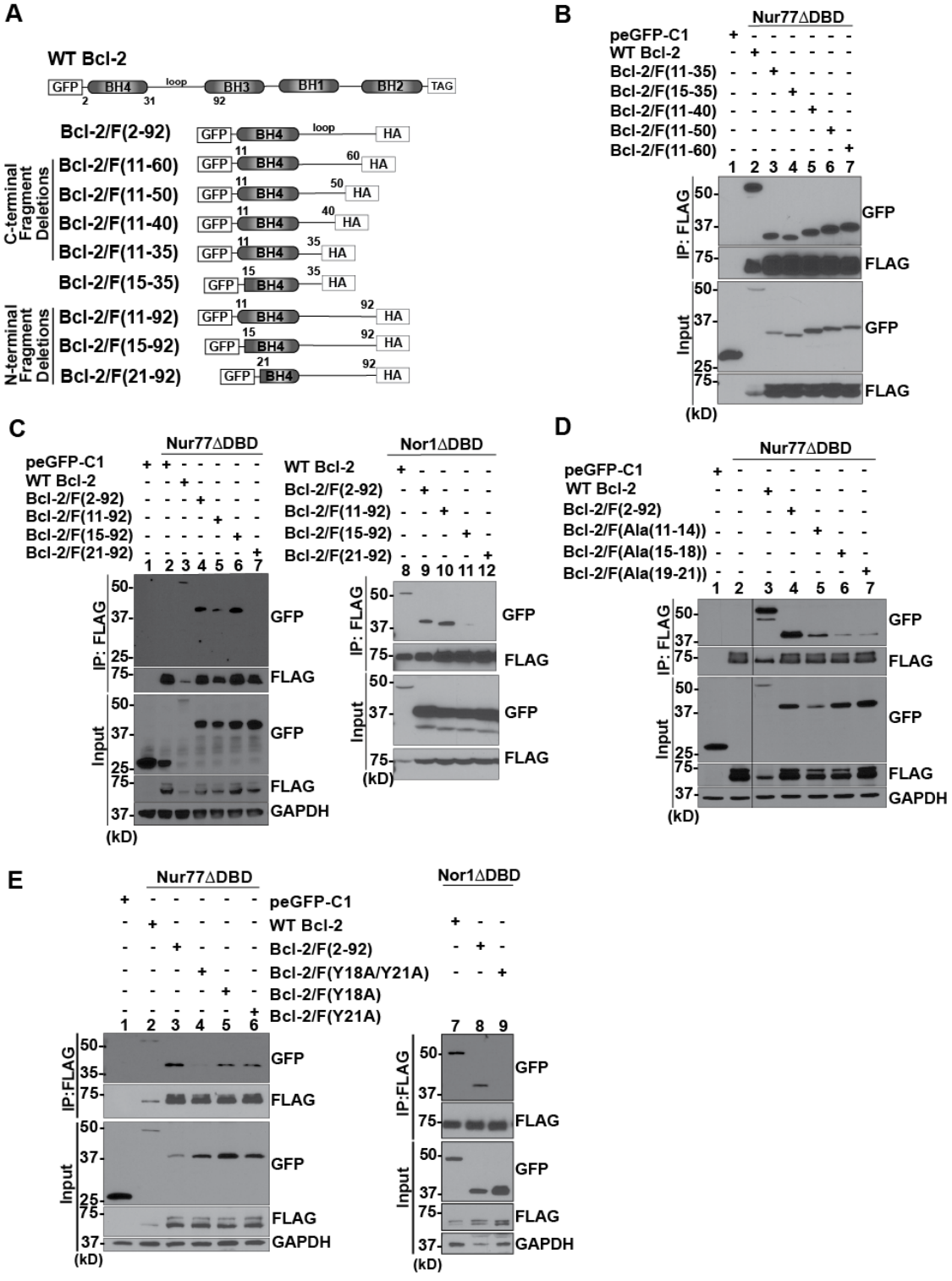

FIGURE 1. Bcl-2 Y18 and Y21 within the BH4 domain are essential for a truncated Bcl-2, but not full-length Bcl-2 to interact with the Nur77 family. *A*, A schematic diagram of GFP fused to wild-type (WT) Bcl-2 or sequential N- or C-terminal deletions of Bcl-2 containing only the BH4 and loop domains with a C-terminal hemagglutinin (HA) tag. *B*, FLAG immunoprecipitation was carried on cell lysates of HEK293T that were previously co-transfected with a FLAG-tagged Nur77 lacking a DNA binding domain (ΔDBD) and GFP fused to wild-type (WT) *Bcl-2* or the indicated *Bcl-2 C*-terminal loop deletion mutants. The immunoprecipitates were then run on the gels and blotted with antibodies to the indicated proteins (GFP or FLAG). As controls, the input extracts were also blotted with GFP, FLAG-, or GAPDH-specific antibodies. The fragments are tagged with GFP on the N-terminus and HA on the C-terminus. *C-F*, FLAG immunoprecipitations were performed similarly as in 1B using a Nur77ΔDBD or Nor-1ΔDBD construct co-transfected with the control construct containing only the eGFP (peGFP-C1) or the N-terminal deleted Bcl-2 fragments (C), alanine scan mutants within the Bcl-2 BH4-loop fragment (D), single or double alanine amino acid substitutions within the Bcl-2 fragment (E), or Y18A, Y21A mutations within the complete Bcl-2 protein (F). The immunoprecipitates were then run on the gels and blotted with antibodies to the indicated proteins (GFP or FLAG). As controls, the input extracts were also blotted with GFP-, FLAG-, or GAPDH-specific antibodies. All experiments have been repeated at least two times with similar results.

FIGURE 2

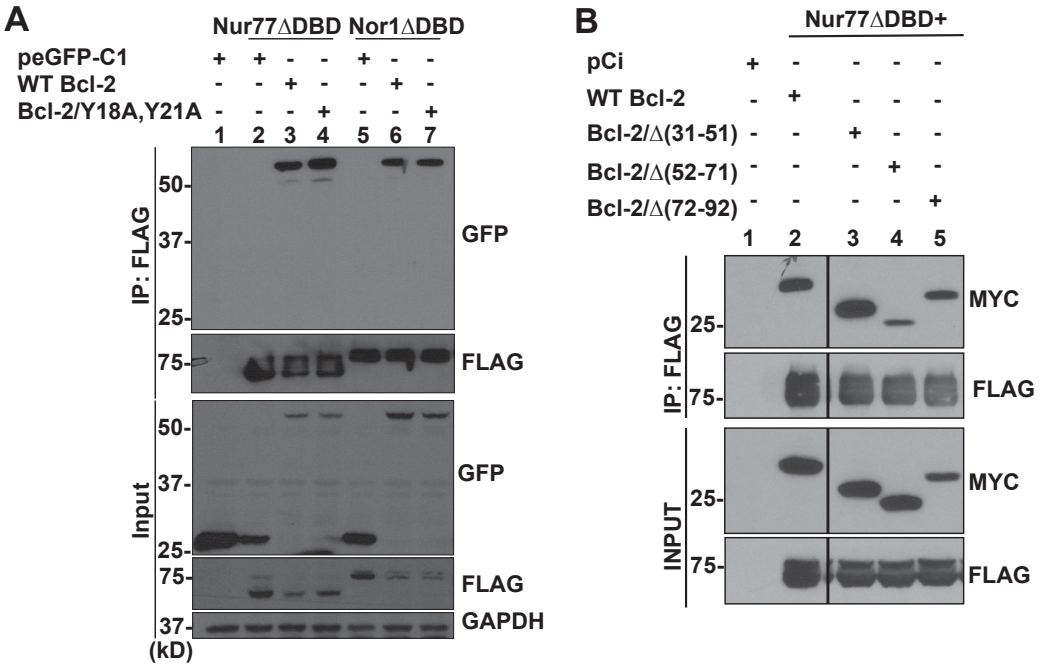

FIGURE 2. Bcl-2 Y18 and Y21 mutations or the Bcl-2 loop domain deletion within a complete full-length Bcl-2 protein are not essential for interaction with Nur77. *A,* FLAG immunoprecipitations were performed as previously described in Figure 1B using Nur77ΔDBD or Nor-1ΔDBD construct co-transfected with control construct containing only eGFP or Y18A, Y21A mutations within a complete Bcl-2 protein. The immunoprecipitates were run on gels and blotted with antibodies to the indicated proteins (GFP or FLAG). *B*, FLAG immunoprecipitations were performed using Nur77ΔDBD construct co-transfected with control vector pCI or C-terminally MYC-tagged WT Bcl-2 or the indicated Bcl-2 loop deletion mutants. The immunoprecipitates were run on gels and blotted with antibodies to the indicated proteins (MYC or FLAG). Input extracts were blotted with antibodies specific to GFP, MYC, FLAG or GAPDH as a control. All experiments have been repeated at least two times with similar results.

FIGURE 3

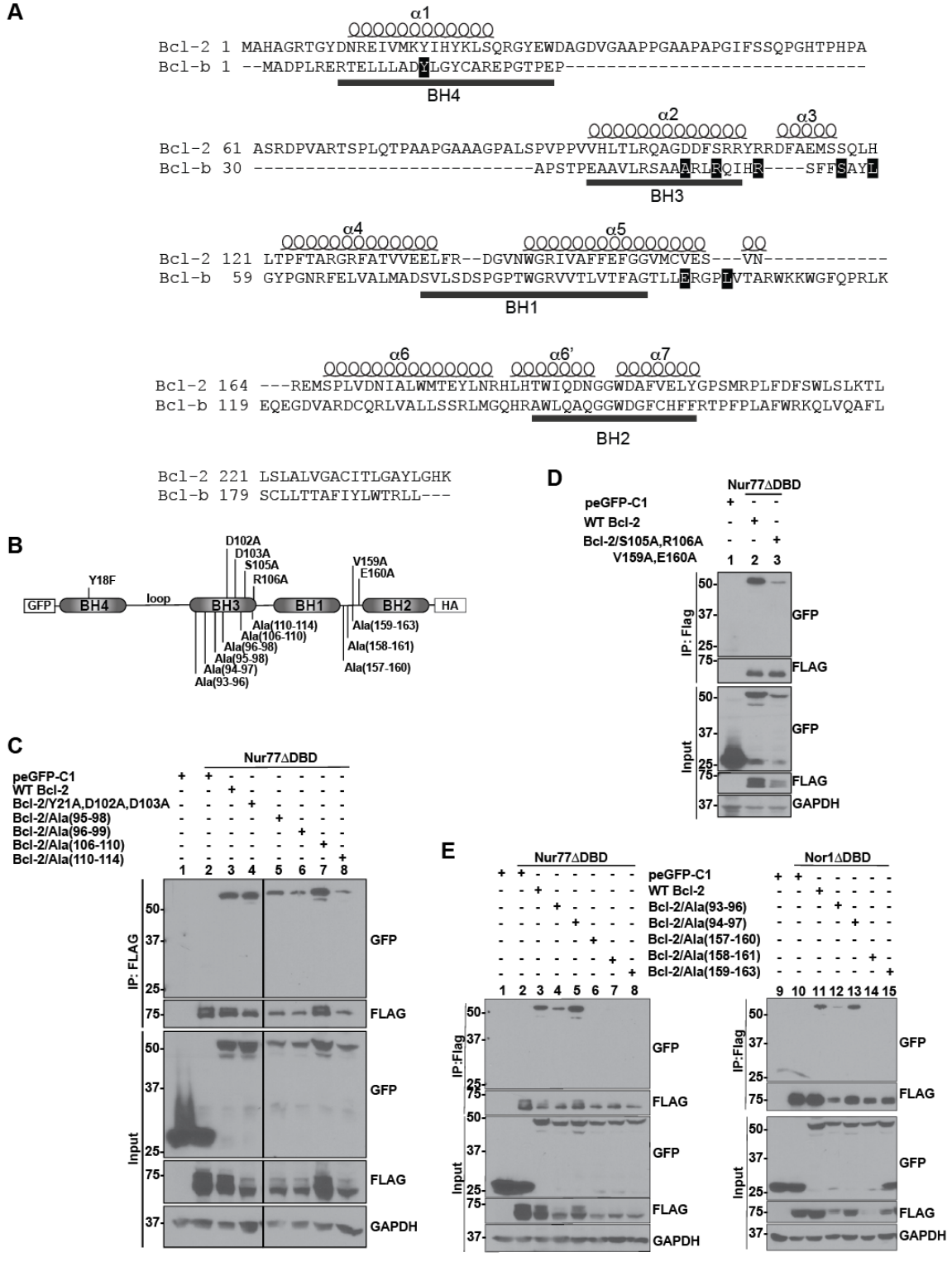
A
α1
Bcl-2 1 MAHAGRTGYDNREIVMKYIHYKLSQRGYEWDAGDVGAAPPGAAPAPGIFSSQPGHTPHPA
Bcl-b 1 --MADPLRERTELLLADYLGYCAREPGTPEP----------
BH4
α2
α3
Bcl-2 61 ASRDPVARTSPLQTPAAPGAAAGPALSPVPPVVHLTLRQAGDDFSRRYRRDFAEMSSQLH
Bcl-b 30 ----------APSTPEAAVLRSAAARLRQIHR----SFFSAYL
BH3
α4
α5
Bcl-2 121 LTPFTARGRFATVVEELFR--DGVNWGRIVAFFEFGGVMCVES---VN----------
Bcl-b 59 GYPGNRFELVALMADSVLSDSPGPTWGRVVTLVTFAGTLLERGPLVTARWKKWGFQPRLK
BH1
α6
α6'
α7
Bcl-2 164 ---REMSPLVDNIALWMTEYLNRHLHTWIQDNGGWDAFVELYGPSMRPLFDFSWLSLKTL
Bcl-b 119 EQEGDVARDCQRLVALLSSRLMGQHRAWLQAQGGWDGFCHFFRTPFPLAFWRKQLVQAFL
BH2
Bcl-2 221 LSLALVGACITLGAYLGHK
Bcl-b 179 SCLLTTAFIYLWTRLL---
B
GFP
BH4
loop
BH3
BH1
BH2
HA
Y18F
D102A
D103A
S105A
R106A
V159A
E160A
Ala(110-114)
Ala(106-110)
Ala(96-98)
Ala(95-98)
Ala(94-97)
Ala(93-96)
Ala(159-163)
Ala(158-161)
Ala(157-160)
C
Nur77ΔDBD
peGFP-C1
WT Bcl-2
Bcl-2/Y21A,D102A,D103A
Bcl-2/Ala(95-98)
Bcl-2/Ala(96-99)
Bcl-2/Ala(106-110)
Bcl-2/Ala(110-114)
1 2 3 4 5 6 7 8
IP: FLAG
Input
GFP
FLAG
GAPDH
D
Nur77ΔDBD
peGFP-C1
WT Bcl-2
Bcl-2/S105A,R106A
V159A,E160A
1 2 3
IP: Flag
Input
GFP
FLAG
GAPDH
E
Nur77ΔDBD
Nor1ΔDBD
peGFP-C1
WT Bcl-2
Bcl-2/Ala(93-96)
Bcl-2/Ala(94-97)
Bcl-2/Ala(157-160)
Bcl-2/Ala(158-161)
Bcl-2/Ala(159-163)
1 2 3 4 5 6 7 8
9 10 11 12 13 14 15
IP:Flag
Input
GFP
FLAG
GAPDH

FIGURE 3. Identification of Bcl-2 mutants that abrogate the ability to interact with Nur77 and its family member Nor-1. *A,* Sequence and structural alignment between Bcl-2 (UniProt P10415) and Bcl-b (UniProt Q9HD36) proteins. Sequences were first aligned using Clustal Omega, followed by manually adjusting the sequence after similar structural positions were identified by Phyre[2]. Coils above sequences indicate helices and labeled α1-α7. The Bcl-2 homology (BH) domains are shown below the corresponding sequences. Highlighted amino acids are Bcl-B residues involved in Nur77 family interaction as reported in Godoi et al[86]. *B*, A schematic diagram of Bcl-2 mutants used for co-immunoprecipitation assays in C-E. *C-E*, FLAG-immunoprecipitation were performed as previously described in Figure 1B to identify the potential Nur77 family interacting regions using the indicated alanine mutants (e.g. Bcl-2/Y21A,D102A,D103A) or alanine scanning mutants (e.g. Bcl-2/Ala(95-98)). All experiments have been repeated at least two times or more where indicated with similar results.

FIGURE 4

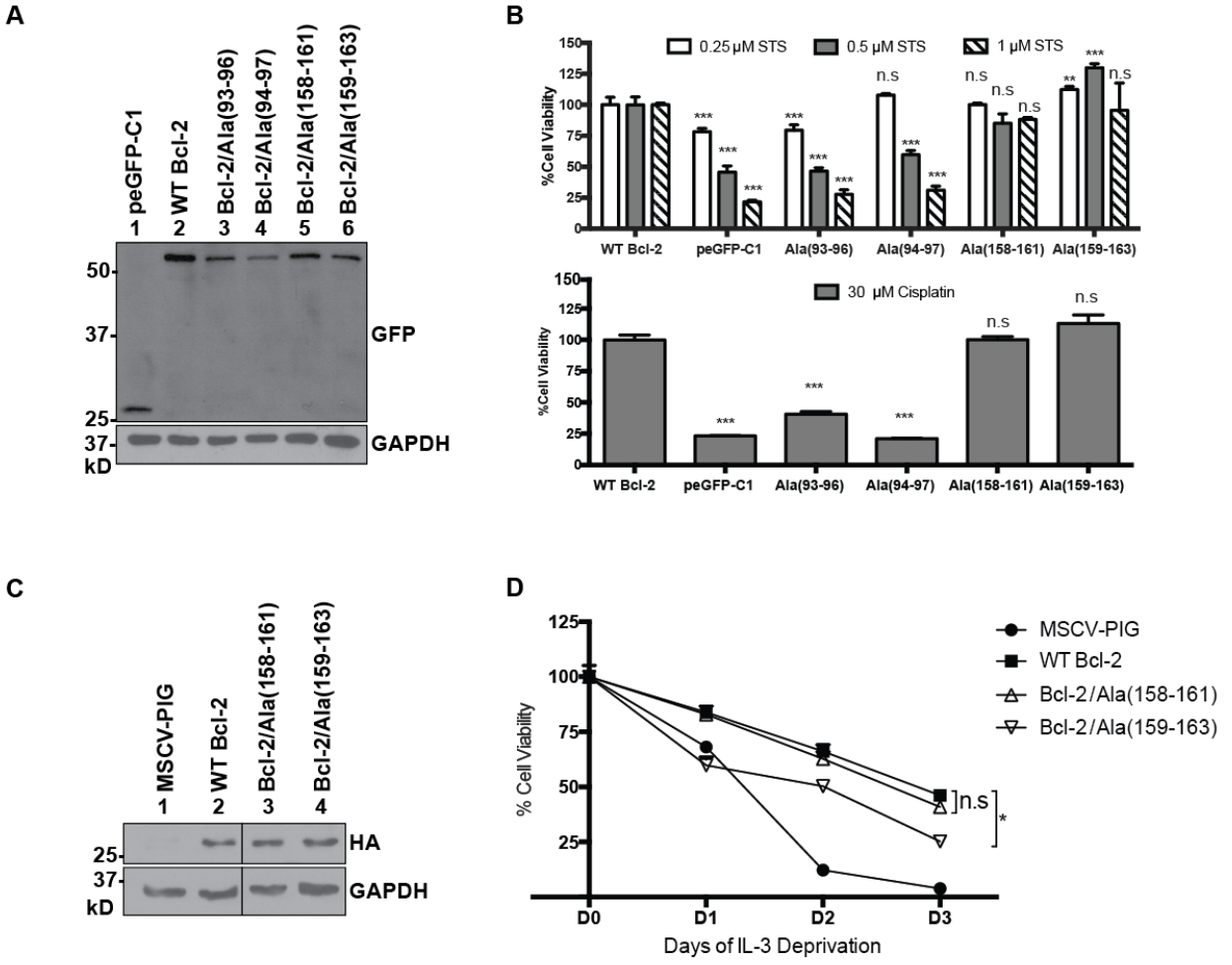

FIGURE 4. Bcl-2 mutants that do not interact with Nur77/Nor1 do not affect its anti-apoptotic function. *A*, Immunoblot analysis of transiently transfected HeLa cells with control vector (pEGFP-C1) or constructs containing GFP-fused WT Bcl-2, Bcl-2/Ala(93-96), Bcl-2/Ala(94-97), Bcl-2/Ala(158-161) or Bcl-2/Ala(159-163). Antibodies specific against GFP, and GAPDH were used to assess transfection efficiency and equal loading. *B*, HeLa cells from 3A with the indicated constructs were treated with 0.25 μM, 0.50 μM or 1 μM staurosporin (STS) for 24 hrs (upper panel) or with 30 μM Cisplatin (CIS) for 48 hrs (lower panel). Cell viability was measured by CellTiter-Glo. Results shown are referenced mean ± SD values to WT Bcl-2 and are representative of three independent experiments performed in triplicate with similar results. Statistics here were calculated by two-away analysis of variance (ANOVA), with Bonferroni's test compared to control are shown (n.s. not significant, **P* < 0.05, ***P* < 0.01, ****P* <0.001). *C*, Western Blot analysis of LyD9 cells transduced with MSCV-PIG control vector or MSCV-PIG vector encoding hemagglutinin (HA) tagged WT Bcl-2, Bcl-2/Ala(158-161) or Bcl-2/Ala(159-163). *D*, An interleukin 3-dependent (IL-3) multipotent stem cell clone, LyD9 transduced with MSCV-PIG vectors encoding WT Bcl-2 or Bcl-2 alanine mutants. Stably transduced cells were selected for resistance against puromycin. The abilities of

Bcl-2 or Bcl-2 mutants to protect cells from apoptosis were tested by depriving cells of IL-3 for the indicated days (D0, D1, D2, and D3). Cell viability was monitored by CellTiter-Glo and normalized to the initial number. All experiments have been repeated at least three times with similar results. Statistical significance was calculated by Student's t-test: n.s. not significant, $*P < 0.05$).

FIGURE 5

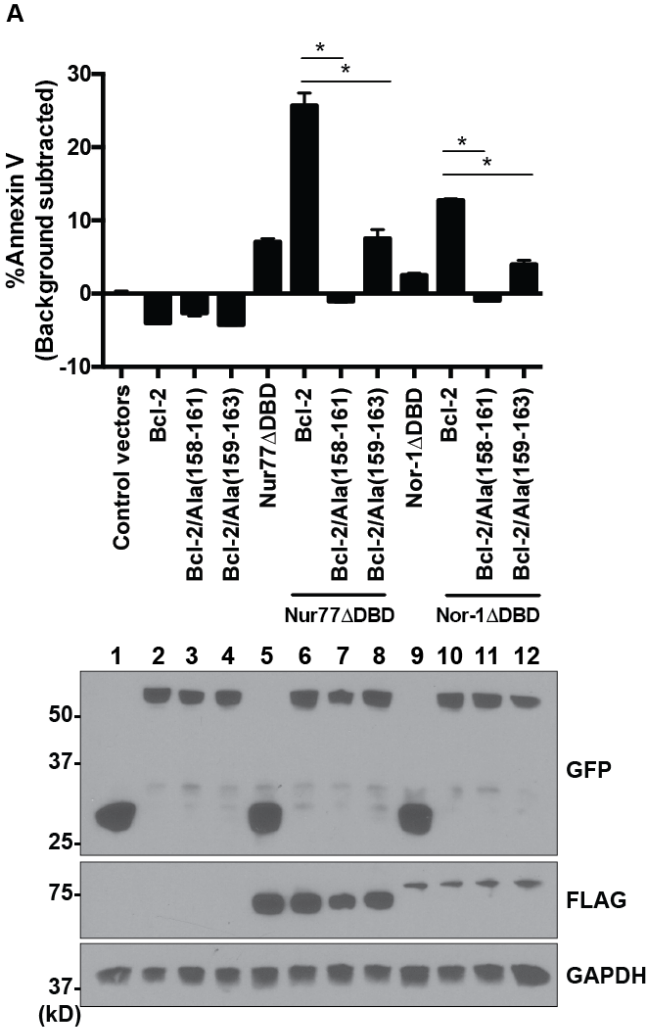

FIGURE 5. Bcl-2 mutants that cannot interact with Nur77 have reduced Nur77-mediated apoptosis. *Top,* Cell death was measured in HeLa cells by Annexin V^+ flow cytometric analysis 24 to 36 hours after transfection with or without Nur77ΔDBD or Nor-1ΔDBD along with a control construct containing only eGFP or GFP-fused WT Bcl-2, Bcl-2/Ala(158-160), or Bcl-2/Ala(159-161) as described in the texts. Results are shown as a mean percentage ± SD of Annexin V^+ from GFP^+ and $mKate^+$ positive HeLa cells. Background was subtracted. Data are representative of two independent experiments performed in duplicate with similar results. Statistical significance was calculated by one-way ANOVA, with Tukey's test compared to control are shown: n.s. not significant, **P* < 0.05. *Bottom*, Immunoblot analysis of the HeLa cells transiently transfected with the indicated plasmids shown in the top panel. Specific antibodies against FLAG, GFP, or GAPDH were used to assess transfection efficiency and equal loading.

FOOTNOTES

The abbreviations used are: Nur77ΔDBD, Nur77 lacking a DNA binding domain, Nor-1ΔDBD, Nor-1 lacking a DNA binding domain; WT, wild-type; BH, Bcl-2 homology; Bcl, B cell lymphoma; GFP, green fluorescent protein; STS, staurosporin; CIS, cisplatin

Acknowledgements: We thank Hector Nolla for help with cytometric flow analysis and members of the Winoto and Raulet labs for insightful discussions. This work was supported by the NIH grant CA66236 (to A.W.).

Conflict of interest: The authors declare no conflicts of interests with the contents of this article.

Author contributions: K.L.B. designed and performed the experiments, analyzed and interpreted the data; X.W. provided excellent technical assistance; P.D. carried out some of the initial experiments; and A.W. obtained research funding, designed the research, analyzed and interpreted the data. Drafting or revising the manuscript was prepared primarily by K.L.B and A.W., with contributions from other authors.

Chapter 2

Putative Identification of a Ubiquitous Autoantigen in Autoimmune Bcl-2-BH3* Tg Mice

INTRODUCTION

T cells undergo a rigorous developmental process to establish a diverse T cell population capable of recognizing and responding to foreign peptide antigens, but able to be tolerant self-antigens when presented on self-MHCs (major histocompatibility complexes). Failure to abide by these requirements can lead to T cell immune dysfunction and autoimmunity. An important mechanism for establishing a self-tolerant T cell repertoire is central tolerance. Central tolerance involves the removal of autoreactive T cell precursors in the thymus. Developing thymocytes that express TCRs that react strongly to self-antigens presented on MHC initiates an apoptotic program and die. Defects in thymocyte apoptosis have been shown to be sufficient in causing autoreactive T cells to escape negative selection and enter into the periphery where they can trigger autoimmunity. In particular, Aire-deficient mice have been instrumental in providing strong evidence for the importance of negative selection[29,31]. Aire controls the expression of tissue-restricted antigens presented by medullary thymic epithelial cells (mTECs). In the absence of Aire expression, spontaneous T cell mediated, multi-organ autoimmunity occurs in these mice due to a defect in negative selection against tissue-restricted antigens[29,31]. In addition to Aire, pro-apoptotic BH3-only Bim and Puma of the Bcl-2 family of proteins and the Nur77 family of orphan nuclear receptors have been implicated as important mediators of thymocyte apoptosis[32,39,94-96]. Bim has been reported to be required for the deletion of autoreactive thymocytes, but rarely do Bim-deficient mice develop autoimmunity in autoimmune resistant C57BL/6 background[94,97]. Autoimmunity is provoked in mice, however, with the compound loss of Puma, suggesting redundancy in the activities for these pro-apoptotic proteins[95,96]. Surprisingly, mice that overexpress the anti-apoptotic Bcl-2 in thymocytes (Bcl-2 Tg), which supposedly can block the pro-apoptotic activities of Bim and Puma, do not develop autoimmunity[98].

In addition to Bim/Puma, the Nur77 family is also involved in thymocyte apoptosis[37]. The ectopic overexpression of Nur77 in thymocytes can lead to massive thymocyte death. Conversely, the expression of a dominant negative Nur77 protein in thymocytes, which can block the activities all Nur77 family members, can rescue thymocytes from clonal deletion[39,41-45]. One mechanism of how Nur77 is able to elicit death in thymocytes is through a transcriptionally independent manner. Strong TCR signals induce the expression and translocation of Nur77 and Nor-1 from the nucleus to the mitochondria, where it can bind Bcl-2 and expose Bcl-2's pro-apoptotic BH3 domain[41]. Moreover, a recent mouse model demonstrating the significance of negative selection has been described. The T cell specific overexpression of a Bcl-2 protein with its BH3 domain mutated (BH3* Tg) in mice is thought to restrict the activities of Bim/Puma, but also block Nur77-mediated thymocyte apoptosis[61]. Consequently, the effectiveness of the transgene to block multiple apoptotic pathways during negative selection was underscored when BH3* Tg mice developed autoimmune symptoms that progressively worsened with age and are characterized by the presence of autoantibody reactivity and massive lymphocyte infiltration to all organs tested[61]. Interestingly, the autoimmune syndrome manifested in these mice was more severe than observed in the Aire-deficient mice[29].

Even though both Aire-deficient and BH3* Tg mouse models develop an onset of multi-organ autoimmunity, there are differences between them. In the case of Aire-

deficient mice, spontaneous autoimmunity results from defective deletion of thymocytes recognizing tissue-restricted antigens[29,30]. However, the T cell mediated autoimmunity in these mice are variable and directed to only a few organs at a time. Unlike Aire-deficient mice, the autoimmune pathology in BH3* Tg mice exhibits massive lymphocyte infiltration into each organ within an individual BH3* Tg mouse[29,61]. The differences between these mouse models might suggest that BH3* Tg mice substantially rescues autoreactive thymocytes, presumably those thymocytes that are not dependent of Aire[61]. In line this notion, BH3* Tg mice were observed to effectively rescue double positive $CD4^+CD8^+$ thymocytes from deletion, suggesting a different pool of autoantigens involved negative selection[61]. Nevertheless, it remains unclear how blocking multiple apoptotic pathways during negative selection skews the T cell repertoire towards autoimmunity in this mouse model. In particular, it is a mystery why BH3* Tg, but not Bcl-2 Tg mice, develop autoimmune pathology and succumb to autoimmunity.

Here, we further explored the autoimmune phenotype in BH3* Tg mice. To clarify how blocking multiple apoptotic pathways during negative selection can lead to autoimmunity in BH3* Tg mice, we sought to identify and define target antigens that could instigate autoimmune disease. Characterization of the autoantibodies in BH3* Tg mice showed little reactivity to Aire-dependent antigens. Instead, a predominant ubiquitous antigen, Tmod3, was identified by immunoprecipitation followed mass spectrometry. Our results are highly suggestive that BH3* Tg mice rescue a subset of T cells against ubiquitous antigens.

RESULTS

Autoimmune BH3 Tg mice minimally share autoreactive antibodies Aire-deficient mice, but can rescue Aire-dependent T cells*

Aged BH3* Tg animals were previously shown to develop multi-organ autoimmunity characterized by the accumulation of activated, autoreactive T cells and immune infiltrates in each organ[61]. In addition, autoantibodies from BH3* Tg were highly reactive to each organ tested by western blot analysis[61]. Interestingly, sera from BH3* Tg mice revealed a common banding pattern within each organ tested, suggesting the presence of a common antibody target[61]. Thus, these autoantibodies were used to as tool to define an antigen that could cause autoimmunity in BH3* Tg mice. To gain a better understanding of the autoimmune antibody repertoire, we first addressed whether BH3* Tg sera contained antibodies specific to autoantigens associated with Aire-deficiency. Because BH3* Tg mice express a Bcl-2 protein that can block the activities of multiple pro-apoptotic molecules involved during negative selection, BH3* Tg mice may also rescue self-reactive thymocytes that recognize tissue-specific antigens controlled by Aire. A radioligand binding assay (RLBA) was performed to detect antibodies specific for three previously defined AIRE autoantigens in the sera of wild-type, Bcl-2 Tg, or BH3* Tg mice. The Aire-dependent autoantigens tested were interphotoreceptor binding protein 1 (IRBP1), BPI Fold containing Family B Member 1 (BPIFB1), and vomeromodulin (VM)[29,99-101]. As expected, wild-type sera did not contain antibodies specific for any of the three antigens tested. In addition, sera from Bcl-2 Tg also did not contain antibodies reactive to any of the antigens. Surprisingly, only a couple of the BH3* Tg sera had antibodies specific to IRBP1 and BPIFB1, but none

reacted to VM (Figure 1A). Indirectly, these results suggest that BH3* Tg mice can rescue some but clearly not all tissue-restricted Aire-dependent T cells from negative selection.

Consequently, we assessed if BH3* Tg mice contained autoreactive T cells specific for the Aire-dependent autoantigen, IRBP1[101]. Two class II tetramers reagents and their corresponding peptide epitopes of IRBP1 have been previous generated and described[102]. Specifically, $CD4^+$ T cells specific for the IRBP1-derived P2 and P7 epitopes are recognized by P2-specific and P7-specific tetramers, respectively[102]. P2-specific T cells are believed to initiate autoimmune attack in Aire-deficient mice with uveitis, whereas P7-specific T cells accelerate disease pathology[102]. To enhance the detection of P2-specific T cells, a cohort of wild-type, Bcl-2 Tg or BH3*Tg mice were immunized with P2-peptide prior to tetramer analysis. Immunization with P2-peptide in CFA resulted in little expansion of P2- or P7-specific T cells in wild-type or Bcl-2 Tg mice. In contrast, a robust increase in P2- and P7-specific T cells was observed after immunization with P2-peptide (Figure 1B, Figure 1C).

Taken together, these results suggest that BH3* Tg mice can rescue tissue-restricted T cells from negative selection that are dependent on Aire. However, the majority of BH3* Tg sera contained little to no antibodies specific to each Aire-dependent antigen tested.

Autoimmune sera bind to ubiquitous antigens

I hypothesized that the rescue of thymocytes in BH3* mice might react to a ubiquitous antigen since the transgene in BH3* Tg mice were able to better protect double positive $CD4^+CD8^+$ thymocytes from apoptosis[61]. To this end, I evaluated multiple BH3* Tg sera reactivity against known organs that were significantly infiltrated by lymphocytes in these mice. Previous observations displayed massive immune infiltration and tissue damage in the kidney, liver, and lung. Single cells suspensions from each of these organs were incubated with aged-matched wild-type, Bcl-2 Tg, or BH3* Tg sera from older mice (i.e. >50-60 weeks). The cells were washed and incubated with PE-conjugated anti-mouse IgG secondary antibodies and analyzed by FACS. In each organ tested and consistent with prior observation that BH3* Tg sera harbor increased autoantibodies, BH3* Tg mice had elevated amounts of antibodies that bound to each organ, with kidney cells having significantly increased reactivity (Figure 2A). Bcl-2 Tg sera contained minimal antibody reactivity that was indistinguishable from the wild-type sera control. By using this strategy, it revealed that BH3* Tg antibodies binds presumably to a cell surface protein. Additionally, whole extracts from these tissues were also immunoblotted with sera pooled from older, aged-matched wild-type, Bcl-2 Tg, or BH3* Tg mice. Like before, sera from Bcl-2 Tg and wild-type mice reacted very little to the kidney, liver or lung extracts, whereas BH3* Tg displayed a similar banding pattern between each of tissues tested (Figure 2B). In particular, sera from BH3* Tg mice, but not wild-type or Bcl-2 Tg, reacted strongly against multiple bands with two predominate antigens that migrated around 37 and 75 kD. This is consistent with the hypothesis that the Bcl-2 BH3* autoantigens are common, ubiquitous antigens.

Identification of Tmod3 a potential autoantigen candidate

We performed immunoprecipitation on columns containing BH3* Tg sera covalently cross-linked to protein agarose to identify the autoantigens. Since kidney cells contained a significant increase in autoantibody reactivity with BH3* Tg sera, kidney extracts were used. As a control to identify nonspecific background, immunoprecipitation on kidney extracts were precleared through wild-type or Bcl-2 Tg sera coupled to protein agarose column prior to passing the extracts through the BH3* Tg column matrix. Elutions from wild-type, Bcl-2 Tg and BH3* Tg were collected, concentrated, and proteins were resolved on a SDS-PAGE gel. The eluates immunoprecipitated from BH3* Tg, but not wild-type or Bcl-2 Tg columns had a strong, observable band that migrated around 37 kD by coomassie stain (Figure 3A). This band could be observed in two independent experiments. In both cases, the distinct band was sliced and sent to protein identification by mass spectrometry (MS). As an added control to identify nonspecific background, slices of the same “gel area” in the control lanes were also processed.

Unexpectedly, MS did not identify a single predominate protein from the slice. Instead, MS results identified a large number (525) of unfiltered protein candidates (Figure 3B). The protein candidate list was initially filtered to remove cytoskeletal and immunoglobulin (Ig) related proteins and proteins that were present in the controls (i.e. proteins that were identified in the Bcl-2 and wild-type slices). To increase stringency, the list was also filtered through CRAPome[103], a database of known MS contaminants (Figure 3B). Finally, the analysis was focused on the higher number of peptide spectrum matches (PSM) (i.e. the abundance of an identified peptide sequence for the protein) in the data. Eight candidates were obtained after meeting the criteria and all were within the appropriate molecular weights (Figure 3C).

Out of the eight candidates, Tropomodulin-3 (Tmod3) was the highly abundant protein identified in MS. Indeed, peptides identified by MS mapped and nearly aligned to the entire Tmod3 amino acid sequence (highlighted in red, Figure 4A). To determine where Tmod3 and the other candidates were expressed in mice, RNA was obtained from multiple mouse organs and reverse transcription polymerase chain reaction (RT-PCR) for full length cDNA of each candidate was performed. For each candidate, we observed that each candidate was amplified in every tissue (Figure 4B). This result suggests that these candidates are ubiquitously expressed and consistent with the hypothesis that BH3* Tg may rescue self-reactive thymocytes against a ubiquitous antigen. To provisionally confirm Tmod3 or any other candidates were the target antigens, successful GST-recombinant proteins for V-type proton ATPase subunit C1 (ATP6v1c1), Fructose-1,6-bisphosphatase 1 (Fbp1), 26S proteasome non-ATPase regulatory subunit 13 (Psmd13), and Tropomodulin-3 (Tmod3) were purified and immunoblotted with wild-type or BH3* Tg serum. Ponceau S stain was performed prior to the immunoblot to confirm successful transfer of the recombinant proteins onto a membrane. Immunoblot using wild-type or Bcl-2 Tg sera showed no reactivity to the recombinant proteins; however, sera from BH3* Tg mice only reacted to Tmod3 (Figure 4C).

Consequently, my next goal to was confirm the existence of T cell population that could react to Tmod3 in BH3* Tg mice, but not control wild-type or Bcl-2 Tg mice. To this end, BMDCs were used to process Tmod3 protein and present peptides that could stimulate a T cell response. The T cell response was determined by the production of

IFNγ by intracellular cytokine staining (ICS). To enhance the T cell response to Tmod3, a cohort of BH3* Tg mice were immunized with GST-only or GST-Tmod3 in CFA. After 10 days, T cells were obtained from each mouse and co-cultured with BMDCs pulsed with PBS, GST- or GST-Tmod3. In each condition, $CD4^+$ or $CD8^+$ lymphocytes cultured with control BMDC pulsed with PBS did not produce IFNγ. Surprisingly, little $CD4^+IFN\gamma^+$ T cells were detected in immunized with GST or GST-Tmod3 mice (Figure 4D). In contrast, $CD8^+$ T cells from immunized GST-Tmod3 group produced an elevated level of IFNγ when pulsed with BMDCs with same peptide. However, these results were overshadowed by the presence of $CD8^+IFN\gamma^+$ producing cells in the immunized cohort of GST-Tmod3 T cells pulsed with GST, suggesting the GST protein is masking the results (Figure 4E). Taken together, these results are highly suggestive for Tmod3 to act as a putative ubiquitous autoantigen targeted by BH3* Tg T cells but additional experiments are needed to confirm this.

DISCUSSION

Here we investigated why and how autoimmunity occurs in BH3* Tg, but not Bcl-2 Tg mice. One obvious, but unlikely explanation for autoimmunity in BH3* Tg mice is the failure of regulatory T cell suppressive activity in these mice. Previous reports unquestionably showed that the suppressive activity of Tregs from Bcl-2 Tg, *Bim*$^{-/-}$, or Bim$^{-/-}$Puma$^{-/-}$ mice were similar to wild-type Tregs[104]. We also showed that Tregs from BH3* Tg mice are still capable of immunosuppressive function in a classical Treg suppression assays (Supplemental Figure 1). Further, Tregs numbers are actually elevated in both Bcl-2 Tg and BH3* Tg[61]. Therefore, we do not favor a hypothesis in which a failure in Treg function is the primary reason why BH3* Tg mice develop autoimmunity.

One hypothetical explanation for the development of autoimmunity in BH3* Tg, but not Bcl-2 Tg mice may be because the inhibition of negative selection of self-reactive thymocytes in BH3* Tg mice is much more complete. Unlike Bcl-2 Tg mice, BH3* Tg mice presumably blocks not only Bim-mediated apoptosis, but also Nur77-mediated apoptosis during negative selection. Thus, the rescue of a specific group of autoreactive T cells in BH3* Tg mice may escape clonal deletion in the thymus, enter the periphery and lead to autoimmunity. However, determining this specific group of autoreactive T cells has been difficult to ascertain given the controversial requirements for the apoptotic factors that mediated negative selection of auto-reactive thymocytes recognizing ubiquitous or tissue-restricted antigens. The BH3-only Bim protein was shown to be a critical molecule in thymocyte apoptosis, especially for the deletion of autoreactive thymocytes to tissue-restricted, but not ubiquitous antigens[34,94,105]. Though, multi-organ autoimmunity phenotype was largely absent in Bim-deficient mice. However, the combined deficiency of Nur77 and Bim was shown to induced diabetes[106]. Also, the additional loss of Puma can enhance Bim-deficiency and lead to autoimmunity, but surprisingly, the autoimmunity that developed in these double knockout mice were reported to be different than *Aire*$^{-/-}$ mice[35]. Thus, whether Bim promotes tolerance by mediating deletion of ubiquitous or tissue-restricted antigens is unclear. Here, our data show that BH3* Tg mice, which can block the pro-apoptotic activities of Bim and act similar to Bim-deficient mice, can rescue populations of auto-reactive T cells to tissue-restricted antigens. Using autoantibodies from BH3* Tg mice

as a method to initially probe for tissue-specific reactivity, we demonstrated that BH3* Tg mice contain autoantibodies that were reactive, albeit to a low level, to some (IRBP1, BPIFB1), but not all Aire-dependent antigens (VM). Additionally, we were able to demonstrate that when immunized, BH3* Tg, but not wild-type or Bcl-2 Tg mice could rescue Aire-mediated deletion of autoimmune IRBP specific T cells by tetramer analysis. The observation that Bcl-2 Tg mice cannot rescue Aire-dependent antigens is perplexing given that if Bim were sufficiently responsible for the deletion of tissue-restricted antigens, the overexpression of the Bcl-2 transgene would have presumably rescued these cells undergoing negative selection. Nevertheless, our tetramer analysis in Bcl-2 Tg mice is in accord with $Bim^{-/-}Puma^{-/-}$ mice. Whether BH3* Tg mice can rescue T cells specific for Aire-dependent antigens, VM or BPIFB1, is uncertain since no experimental tools currently exist. Together, these results suggest BH3* Tg mice can rescue autoreactive T cells that are tissue-restricted.

While both BH3* Tg and $Aire^{-/-}$ mice develop multi-organ autoimmunity, there are apparent differences. First, the penetrance for the autoimmune phenotype in BH3* Tg mice is greater than in $Aire^{-/-}$ mice. Each BH3* Tg mouse accumulates activated T cells and has observable massive lymphocyte infiltration into each organ. Second, BH3* Tg mice, when crossed to the Nur77-GFP reporter mouse, showed an increased rescue of post-selected DP thymocytes, a discrete developmental stage where thymocytes are thought to undergo negative selection against ubiquitous antigens [107]. Third, our Surf-blot analysis shows that the autoantibody sera from BH3* Tg mice potentially reacts to a common antigen. Taken together, these data strongly suggested that BH3* Tg mice may rescue autoreactive T cells that recognize a ubiquitous antigen. Surprisingly, HY-tetramer analysis in a cohort of unimmunized wild-type, Bcl-2 Tg, or BH3* Tg mice staining showed similar numbers of HY specific $CD8^+$ T cells from Bcl-2 Tg and BH3* Tg male mice (Supplemental Figure 2). For some reasons, why BH3* Tg mice were unable to rescue autoreactive T cells to the ubiquitous male antigen is unknown and perhaps immunizing the mice with an HY-peptide prior to tetramer analysis would increase the limit of detection. Nevertheless, we sought to identify the predominate common antigen detected by the autosera from BH3* Tg mice in our Surf-Blot analysis. By performing immunoprecipitation using autosera from BH3* Tg mice, we identified Tmod3 as a provisional ubiquitous autoantigen. The preliminary results are promising as sera from only BH3* Tg, but not wild-type littermate mice reacted to Tmod3. Even so, further validation is required. Specifically, determining if Tmod3 is a bonafide autoantigen that is sufficient to break tolerance and induce autoimmunity in BH3* Tg, but not in control mice. Moreover, this work provides the groundwork to develop tetramer reagents that can track and characterize an autoreactive T cell population.

MATERIALS & METHODS

Mice

C57BL/6 wild-type (WT), congenic Ly5.1 (CD45.1), RagKO or T cell specific wild-type *Bcl2* transgenic line (Bcl-2 Tg) or *Bcl2* BH3 mutant transgenic (BH3* Tg) were generated as previously described[61,108]. All experiments in mice were compliant with and approved by the UC Berkeley Animal Care and Use Committee (ACUC).

Flow cytometry

Single cell suspension of mouse splenocytes or lymph nodes were obtained by dissociating the tissue through a 40 μM cell strainer followed by lysing red blood cells by 1X ACK buffer (10X: 1.5M NH_4Cl, 0.1M $KHCO_3$, 1M EDTA, pH 7.2). Cells were stained with a viability dye (Tonbo) and commercial antibodies against CD45 (eBioscience), CD45.1 (eBioscience), CD3 (Biolegend), CD4 (Biolegend), CD8 (Biolegend), CD44 (Tonbo), CD62L (Tonbo), B220 (eBioscience), Ly6C (eBioscience), Ly6G (eBioscience), GR-1 (eBioscience), CD11b (eBioscience), CD11c (Tonbo), NK1.1 (eBioscience), or PD-1 (eBioscience) where indicated. For intracellular cytokine staining, cells were stimulated with 2 μg/mL CD3 (2C11) and 2 μg/mL CD28 (PV-1) 4-5 hr at 37˚C in the presence of GolgiStop (BD Bioscience) and GolgiPlug (BD Bioscience). Alternatively, bone marrow derived dendritic cells (BMDCs) were pulsed overnight with purified GST-only or GST-candidate gene. Further maturation of DCs was initiated by adding 10 ng/mL LPS for 1 hour, followed by multiple PBS (>4) washes before co-culturing them with T cells overnight at 37˚C. After stimulation, cells were surfaced stained as described, fixed, and permeablized with BD Cytofix/Cytoperm Kit (BD Bioscience) according to manufacturer's instructions. Fixed cells were stained with antibodies against IFNγ (eBioscience), IL-4 (eBioscience), IL-10 (eBioscience), or IL-17A (eBioscience) where indicated. For intracellular transcription factor staining, cells were surface stained as described, fixed, and permeabilized with FoxP3 Staining Kit (eBioscience). Fixed cells were stained with antibodies against Bcl-6 (BD Bioscience), FoxP3 (eBioscience), T-bet (Biolegend), and RORyt (BD Bioscience) where indicated.

CFSE Treg Suppression Assays

Suppression assays were performed as described[104,109]. Briefly, total conventional T cells (Tconv; $CD8^+$ and $CD4^+CD25^-$) were obtained from congenic Ly5.1 mice using $CD3^+$ T cell enrichment columns (R&D Systems) and depleted of Tregs by using PE conjugated anti-CD25 and EasySep Immunomagnetic Mouse PE Positive Selection Kit (StemCell Technologies). Tconv were then labeled with 1 μM Cell Trace CFSE (Invitrogen) according to manufacturer's recommendations. Tregs (CD4+CD25+) from Ly5.2 wild-type littermate, Bcl-2 Tg, or BH3* Tg mice underwent two rounds of selection: first, negatively selecting on $CD4^+$ T cells by staining with PE-conjugated antibodies to B220, CD8, CD11b, CD11c, F4/80, NK1.1, Ter-119 and using the EasySep Immunomagnetic Mouse PE Positive Selection Kit (StemCell Technologies); second, positive selection for Tregs by staining for APC-conjugated CD25 and using EasySep Immunomagnetic Mouse APC Positive Selection Kit (StemCell Technologies). In a 96-well round-bottom plate, Tconv (2.5×10^4) were stimulated with anti-CD3 (2μg/mL) and co-cultured with irradiated splenocytes from RagKO mice (5×10^4) and titrated amounts of Tregs. CFSE dilution was measured by FACS. Percent suppression was assessed by (Tconv only total CFSE dilution – [Tconv + Treg total CFSE dilution])/Tconv only total CFSE dilution.

Tetramer Staining

Tetramer staining was performed as described in Moon et al[110,111]. HY:H-$2D^b$ tetramers were a gift from the Shastri lab that were originally obtained from NIH Tetramer Core Facility and were used to detect endogenous T cells specific for ubiquitous male HY antigen in aged BH3* Tg mice. P2-I-A^b and P7-I-A^b tetramers were

a gift from the Anderson lab at UCSF and were used to detect Aire-dependent autoreactive T cell receptors against IRBP. P2-specific CD4+ T cells are expanded in autoimmune BH3* Tg mice, but not in control Bcl-2 Tg or littermate mice. Mice were harvested 10 days after immunizing with 100 µg P2 peptide emulsified in 100 µL CFA. Magnetic separation was performed to enrich tetramer positive cells on pooled spleen and peripheral lymph nodes (i.e. cervical, submandibular, axillary, inguinal, and mesenteric) after an hour incubation with HY:H-2D^b tetramer on ice or with P2-I-A^b and P7-I-A^b tetramers at room temperature. Positively selected cells were stained and live gated on CD3$^+$CD4$^+$CD8$^-$B220$^-$CD11b$^-$CD11c$^-$F480$^-$. Absolute tetramer-positive cells were quantified using FACS analysis using counting beads (AccuCheck, Invitrogen).

Autoantibody Assay

Autoantibody assay using ^{35}S-Radiolabeled BPIFB1, IRBP, and VM were previously described[100]. Sera from aged-matched wild-type, Bcl-2 Tg, or BH3* Tg mice were sent to Mark Anderson's lab to determine antibody reactivity to these autoantigens found in Aire$^{0/0}$ mice. In brief, *in vitro* transcription, translation, and labeling with ^{35}S-methionine of BPIFB1, IRBP, and VM were performed using the TNT system kit (Promega). Radiolabeled proteins immunoprecipitated with serum were performed in triplicate in 96-well PVDF filtration plates (Millipore). The radioactivity of the immunoprecipitated protein was evaluated by scintillation counter (Beckman Coulter). Autoantibody index was assessed and calculated by: [cpm in the unknown sample – cpm in the negative standard] ÷ [cpm in the positive standard– cpm in the negative standard] x 100), where positive standard values from Aire$^{0/0}$ sera.

Immunoaffinity purification of candidate antigens

The immunoprecipitation of BH3* Tg candidate autoantigens were performed on RagKO kidney lysates (50 mM Tris-HCl, pH 7.5, 150 mM NaCl, 2 mM EDTA, 0.1% CHAPS, 1 mM DDT, Sigma protease inhibitor cocktail, along with phosphatase inhibitors 1 mM $NaVO_4$, 1 mM NaF, and 1 mM PMSF). Sera from older, aged-matched wild-type littermate, Bcl-2 Tg, or BH3* Tg was obtained from cardiac puncture. Serum was obtained after blood was allowed to coagulate overnight at 4˚C. BH3* Tg serum that were previously identified to have similar banding pattern were pooled and covalently cross-linked using dimethyl pimelimidate (DMP) to Protein G-agarose beads (Thermoscientific). Kidney lysates were pre-cleared with Protein G-agarose for 1 hour at 4˚C prior to incubating Protein G-agarose coupled to WT, Bcl-2 Tg, or BH3* Tg sera overnight at 4˚C. Beads were transferred into a column and washed extensively with CHAPS lysis buffer. Elution was performed by passing 0.5 mL of 0.1 M glycine, pH 3.0, through the column and collecting flow through. Multiple eluates were pooled, concentrated, and dialyzed with 50 mM Tris-CL, pH 7.5 with 1 mM DTT using Amicon Ultra 3K spin columns according to manufacturer's instructions.

Mass Spectrometry

BH3* Tg candidate autoantigens were immunoprecipitated and resolved by a 4-20% Mini-PROTEAN TGX gel (Bio-Rad) and stained with Colloidal Blue Staining Kit (Invitrogen). Excised bands that were unique BH3* Tg immunoprecipitates were digested with trypsin, and batch fractionated on a Poros 50 R2 RP micro-tip, and

resulting peptide pools were analyzed by matrix-assisted laser desorption ionization reflectron time-of-flight (MALDI-reTOF) mass spectrometry (MS) using BRUKER UltraFlex TOF/TOF instrument (Bruker Daltronics) as described (REFS 39 and 40 JBC Jen's). Selected experimental masses (*m/z)* were taken to search non-redundant protein database utilizing the Mascot Peptide Mass Fingerprint program (REF 41 of Jen's Paper), with a restriction better than 35 ppm and maximum of one missed cleavage site allowed per peptide. Tentative confirmation (Mascot score ≥ 30) of a Peptide Mass Fingerprint result, thus, obtained was verified by comparing the computer-generated fragments on series of the predicted tryptic peptide with the experimental MS/MS data. Peptide Mass Fingerprint results with ≤ 40 were confirmed by mass spectrometric sequencing of selected peptides using MALDI-TOF/TOF (MS/MS) analysis on the same prepared samples using the UltraFlex instrument in "LIFT" mode. Fragment ion spectra were taken to search nonredundant using the MASCOT MS/MS ion search program (Matrix Science Ltd.).

Preparation of cDNA from organs and Real-time PCR (RT-PCR)

RagKO mice were profused with 1X PBS and their organs collected (i.e. brain, eye, heart, kidney, liver, lung, pancreas, and stomach). 30 mg of organ tissue were mechanically disassociated using orange-colored gentleMACS M tubes and the gentleMACS Octo Dissociator (Miltenyi Biotec) in 600 µL of Buffer RPE (Qiagen) supplemented with ß-ME. RNA was purified and subjected to on-column DNase-treatment using RNeasy Mini Kit (Qiagen) according to manufacturer's recommendations. RNA was then reverse transcribed into cDNA using Superscript III (Invitrogen) and poly-dT primers. Specific primers used to amplify ATP6v1c1, Fbp1, Psmd13, Lrpap1, Tp52, Tmod3, or GAPDH cDNA for 30 cycles are found in Supplemental Table 1.

Production of GST-fused proteins

GST recombinant proteins for ATP6v1c1, Fbp1, Psmd13, Lrpap1, Tp52, and Tmod3 were produced by inserting full-length each candidate cDNA sequences into pGEX-4T-1 expression vector. Primers to amplify each candidate gene cDNA for pGEX-4T-1 insertion are located in Supplemental Table 2. PCR products were cloned into pGEX-4T-1 by Gibson cloning method and transformed into BL21-RIL bacteria (Stratagene) for protein expression. Protein was harvested according to the manufacturer's instructions (GE Healthcare). Briefly, bacterial starter cultures were grown overnight, and a 1:20 – 1:50 dilution of the overnight culture was inoculated into a 100 mL of LB Broth containing appropriate antibiotic (i.e. Ampicillin) and placed on shaker at 37˚C. Protein expression was initiated by adding 0.5 mM IPTG when cultures reached an OD_{600} between 0.5 and 1. Cultures remained at 37˚C for an additional 3-4 hours or overnight at 25˚C. Bacteria was pelleted, weights measured, and flash frozen to improve bacterial lysis. Pellets were resuspended at approximately 3-5 mL of 1X GST resuspension buffer supplemented with 1 mM DTT per gram of pellet (5X: 250 mM Tris-Cl pH 8.5, 500 mM NaCl, 5 mM EDTA). 1 mg/mL of Lysozyme and 1 mM of PMSF was added to the sample and incubated on ice for 30' with intermittent swirling. 1% Triton X-100 was added after samples were sonicated on ice until the solution became fluid (multiple pulses of 10 to 30 seconds at 25% output). Samples were then clarified by

high speed centrifugation at 4˚C, and supernatant was incubated with 1 mL of swollen glutathione-agarose beads (Sigma-Aldrich) per liter of bacterial culture overnight at 4˚C. Beads were washed with 1X extraction buffer with 0.5% Triton X-100 and PMSF, then washed with extraction buffer containing 0.1% Triton X-100. Elution was performed in extraction buffer with 10 mM glutathione. Multiple eluted fractions were pooled, concentrated and dialyzed with 50 mM Tris-Cl, pH 7.5 and 1 mM DTT using Amicon Ultra 3K (Millipore) spin columns according to manufacturer's instructions.

Western Blotting

Single cell suspensions of organs from RagKO mice were obtained by using purple-colored gentleMACS C tubes and the gentleMACS Octo Dissociator (Miltenyi Biotec). Dissociated tissues were pelleted, washed with PBS, and lysed in RIPA buffer (50 mM Tris-HCL, pH 7.6, 150 mM NaCl, 2 mM EDTA, 1% NP-40, 0.05% SDS, 1 mM DDT, Sigma protease inhibitor cocktail, along with phosphatase inhibitors 1 mM $NaVO_4$, 1 mM NaF, and 1 mM PMSF). Quantification of protein was obtained using Bio-Rad *DC* Protein Assay (Bio-Rad), and 150 µg of protein was loaded into a single well 10% SDS-PAGE gel. Proteins were transferred on nitrocellulose membranes and blocked with 5% non-fat milk in 1% Tween TBS (TBST). Membranes were placed in a Surf-Blot apparatus (Idea Scientific) and probed with serum diluted to 1:200 for 2 hrs at room temperature. Membranes were incubated with HRP-conjugated anti-mouse IgG antibody (1:7500, GE Healthcare) following three washes with TBST. Visualization of bands was performed using SuperSignal West Pico Chemiluminescent Substrate (Thermoscientific) by autoradiography.

FIGURES

Figure 1

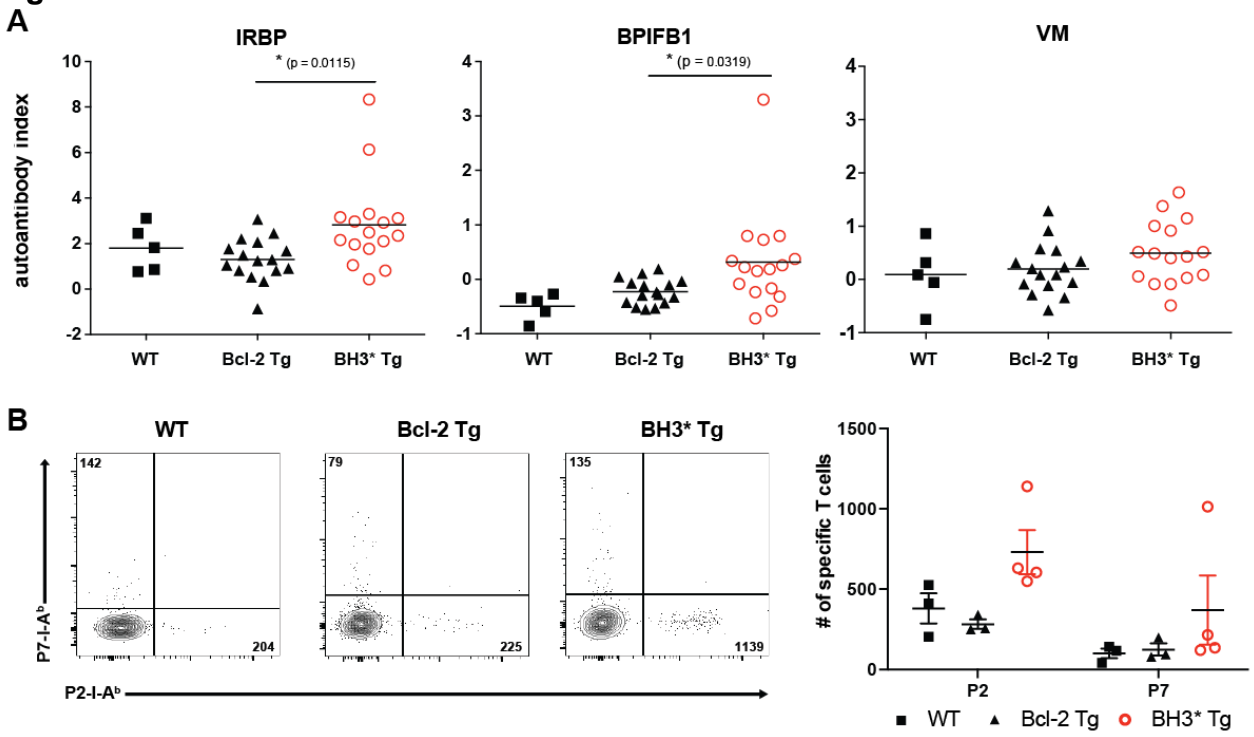

Figure 1. BH3* Tg mice contain autoantibodies that react to Aire-dependent autoantigens and can rescue Aire-dependent T cells from negative selection. *A,* Sera from older, aged-matched wild-type, Bcl-2 Tg, or BH3* Tg mice were screened for reactivity against Aire-dependent autoantigens by radioligand binding assay (RLBA). Statistics obtained by one-way analysis of variance (ANOVA), * $p < 0.05$. *B,* FACS plots representative (left) or absolute cell number (right) of tetramer enriched, peripheral $CD4^+$ T cells specific to IRBP-derived P2 or P7 epitope. Absolute number is provided in FACS plot (left). Each data point represents one mouse (right). A cohort of wild-type (WT), Bcl-2 Tg, or BH3* Tg mice were immunized with P2 peptide. After 10 days, peripheral lymphoid organs were obtained and stained with tetramers specific for P2 or P7, respectively. IRBP, interphotoreceptor retinoid binding protein; BPIFB1, BPI Fold containing Family B Member 1; VM, vomeromodulin.

FIGURE 2

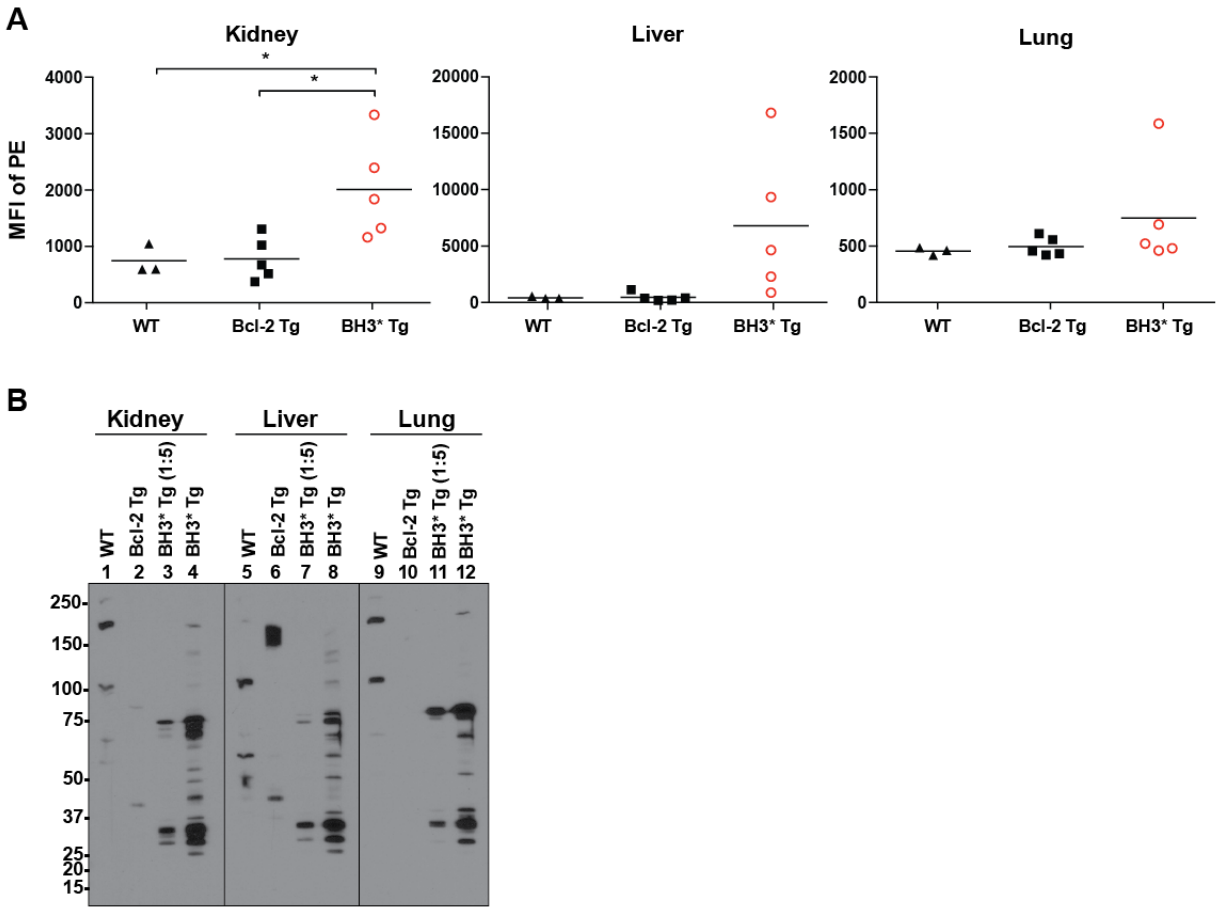

Figure 2. **Autoantibodies from BH3* Tg sera target a common, ubiquitous antigen.** *A,* Single cells of indicated organ (i.e. kidney, liver, or lung) obtained from RagKO were incubated with 1:200 dilution of sera collected from wild-type (WT), Bcl-2 Tg, or BH3* Tg mice. The cells were then washed and stained with an Phycoerythin (PE)-conjugated mouse IgG-specific antibody and analyzed by flow cytometry. Statistics obtained by one-way analysis of variance (ANOVA), * $p < 0.05$. *B,* Sera from wild-type, Bcl-2 Tg, BH3* Tg mice were used to probe antibody reactivity in whole cell extracts from kidney, liver, or lung by western blot. Antisera from BH3* Tg were used undiluted or diluted 1 to 5 (1:5).

FIGURE 3

A

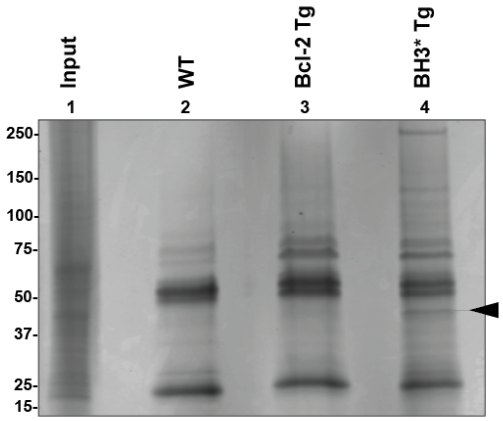

B

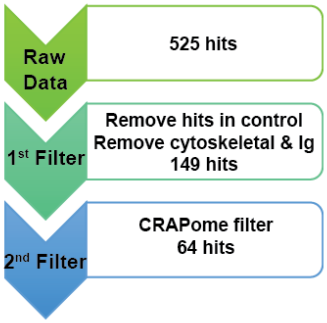

C

Candidate	Gene Name	Protein Size
Tropomodulin-3 OS	Tmod3	40 kDa
26S proteasome non-ATPase regulatory subunit 6 OS	Psmd6	46 kDa
Aminoacylase-1 OS	Acy1	46 kDa
Fructose-1,6-bisphosphatase 1 OS	Fbp1	37 kDa
26S proteasome non-ATPase regulatory subunit 13 OS	Psmd13	43 kDa
V-type proton ATPase subunit C 1 OS	Atp6v1c1	44 kDa
Acetyl-CoA acetyltransferase, mitochondrial OS	Acat1	45 kDa
26S proteasome non-ATPase regulatory subunit 7 OS	Psmd7	37 kDa

Figure 3. **Identification of autoantigen candidates by immunoprecipitation followed by mass spectrometry.** *A,* Sera from wild-type littermate, Bcl-2 Tg, or BH3* Tg were coupled to protein agarose and used to immunoprecipitate antigens from whole kidney extract. Protein eluates were resolved on a SDS-PAGE gel and visualized by coomassie stain. Data are representative from two independent experiments. Arrow depicts the band that is detected by the BH3* Tg antisera but not antisera from Bcl-2 Tg or wild-type (WT). Slice of bands were analyzed by mass spectrometry. *B,* Schematic used to filter proteins identified by mass spectrometry as described in the text. C, Top eight candidates obtained after stringently filtering the data as depicted in figure 3B.

FIGURE 4

A

MALPFRKDLGDYKDLDEDELLGKLSE
SELKQLETVLDDLDPENALLPAGFRQKNQTS
KSATGPFDRERLLSYLEKQALEHKDR
DDYVPYTGEKKGKIFIPKQKPAQTLTEETISL
DPELEEALTSASDTELCDLAAILGMHNLIADT
PFCDVLGSSNGVNQERFPNVVKGEKILPV
FDEPPNPTNVEESLKRIRENDARLVEVNLNN
IKNIPIPTLKDFAKTLEANTHVKHFSLAATRSND
PVAVAFADMLKVNKTLKSLNMESNFITGAGVLA
LIDALRDNETLMELKIDNQRQQLGTSVELEMAK
MLEENTNILKFGYQFTQQGPRTRAANAITKNN

B

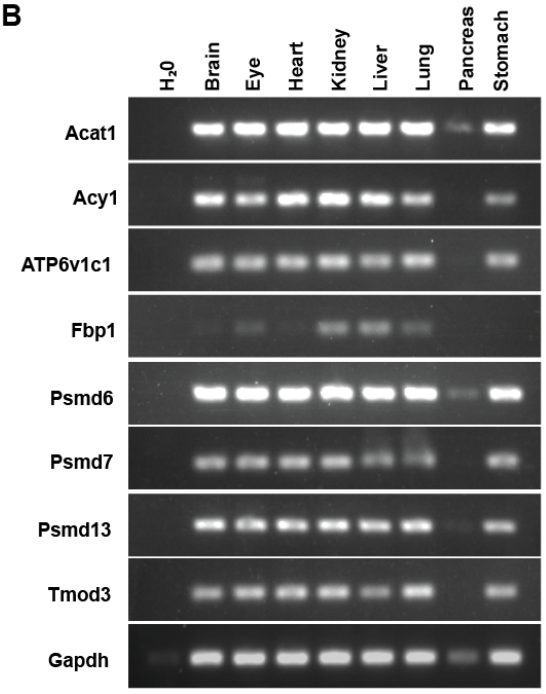

C

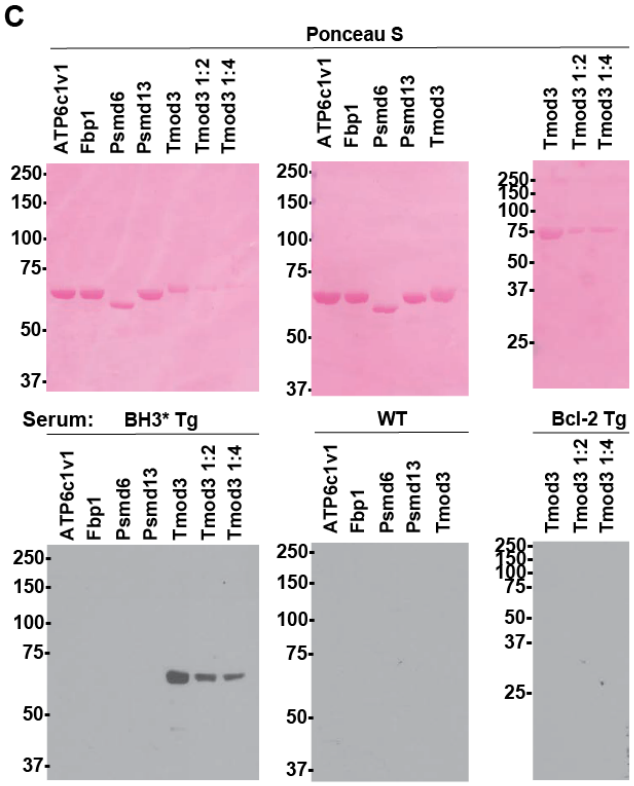

D

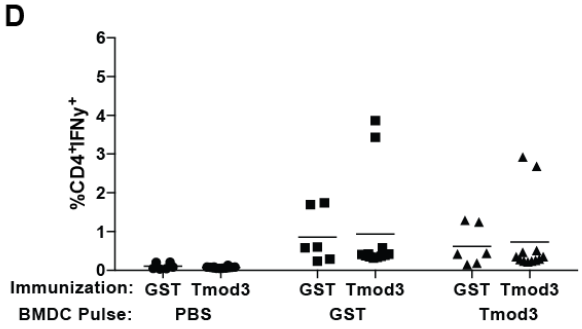

E

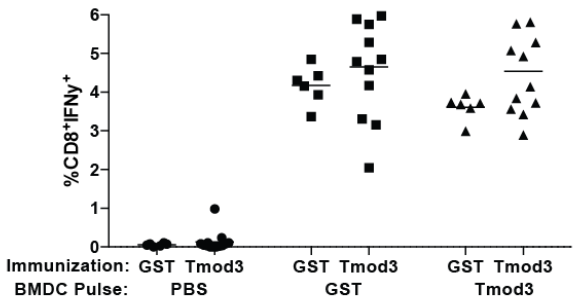

Figure 4. **Identification of Tmod3 as a putative autoantigen in BH3* Tg mice**. *A,* Amino acid sequence of Tmod3 (UniProt U9JHJ0). Peptides identified (red) by MS were mapped to Tmod3. *B,* RT-PCR of indicated candidate genes in the indicated tissue. *C,* Immunoblot using sera from wild-type, Bcl-2 Tg or BH3* Tg mice to probe reactivity towards indicated recombinant proteins (bottom). Ponceau S stain was used to confirm efficient transfer of recombinant proteins to a nitrocellulose membrane (top). Recombinant Tmod3 was undiluted or diluted 1 to 2 (1:2) or 1 to 4 (1:4). *D-E,* FACS analysis for detecting IFNγ production by intracellular staining in $CD4^+$ (D) or $CD8^+$ T cells. T cells were purified from peripheral lymphoid organs from a cohort of BH3* Tg immunized mice with GST or GST-Tmod3. At 10 days after immunization, T cells were incubated with BMDCs pulsed with PBS, GST, or GST-Tmod3 where indicated and IFNγ production was analyzed by FACS.

SUPPLEMENTAL FIGURE 1

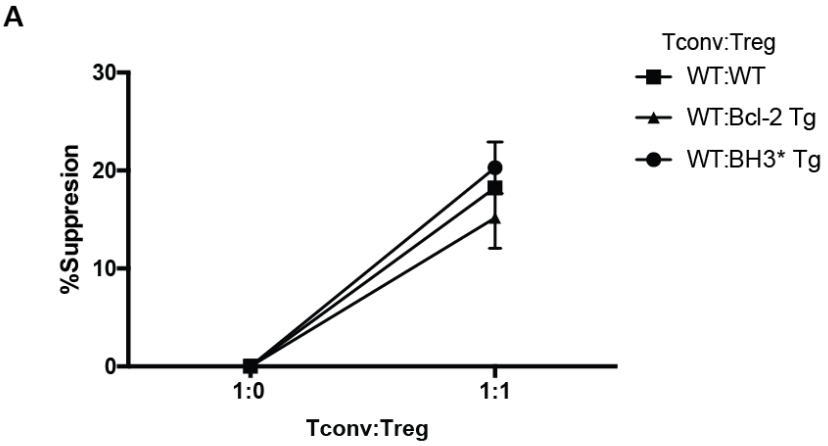

Figure S1. Tregs from BH3* Tg mice maintain their suppressive activity. *A*, CFSE labeled Tconv ($CD8^+CD25^-$) obtained from congenic Ly5.1 mice were stimulated with 2µg/mL CD3 (clone 2C11) and 2µg/mL CD28 (PV1) with or without Tregs ($CD4^+CD25^+$) obtained from Ly5.2 wild-type, Bcl-2 Tg, or BH3* Tg mice. Irradiated RagKO splenocytes were used as feeder cells. Data shown are percent suppression relative to stimulated Tconv only (1:0) as described in Materials and Methods.

SUPPLEMENTAL FIGURE 2

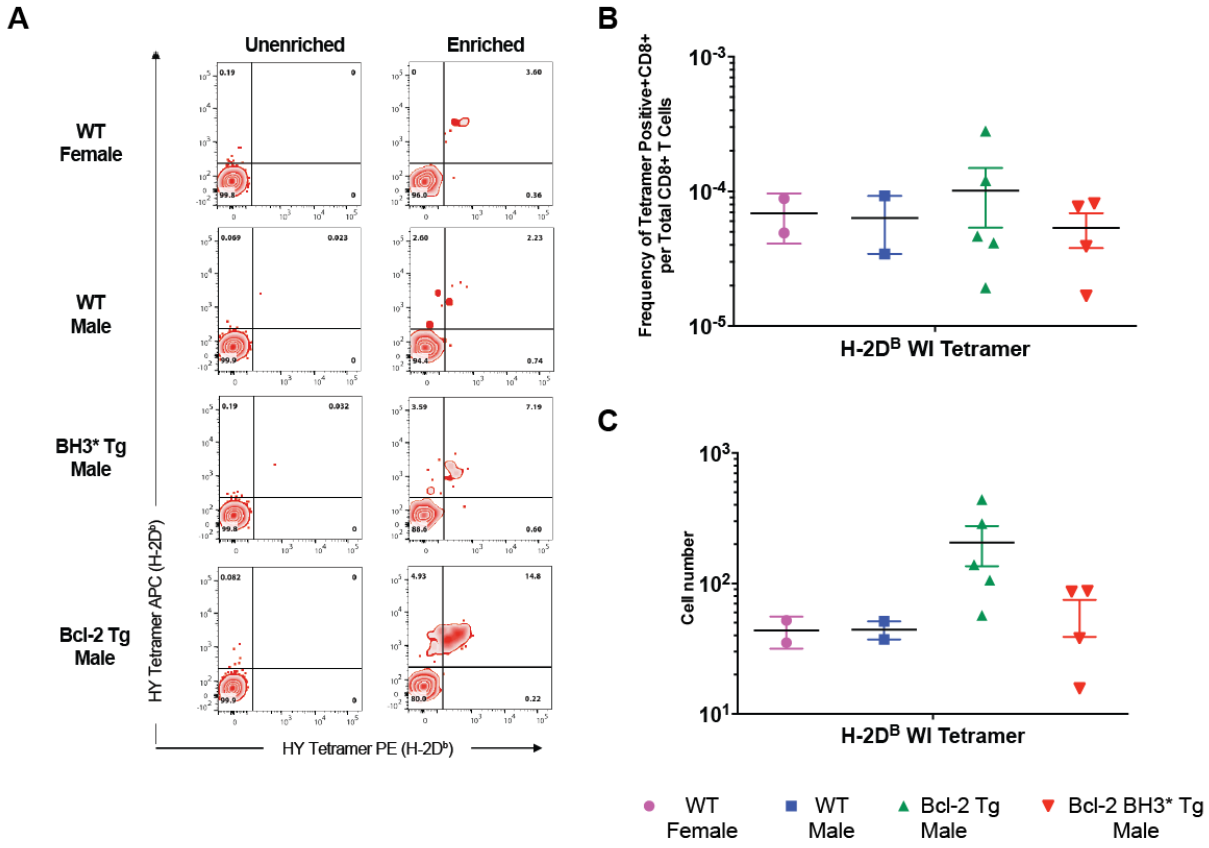

Figure S2. Assessing the rescue of HY-specific T cells in WT, Bcl-2 Tg, or BH3* Tg from male mice. *A-C,* Frequencies of endogenous HY-specific T cells were determined in a cohort of wild-type, Bcl-2 Tg, or BH3* Tg mice. All peripheral lymphoid organs were pooled and stained with HY tetramers. Data are shown as representative FACS plots of tetramer-enriched (A), frequency of $CD8^+tetramer^+$ within a $CD8^+$ population (B), or absolute number of HY-specific $CD8^+$ T cells (C) for each genotype and sex.

SUPPLEMENTAL TABLE 1

Gene	Primer Name	Sequence	Tm*	Expected Size (Bp)
Tmod3	mTmod3-F	aattcccgggtcgactcgagGCACTGCCGTTCCGGAAG	64	1106
Tmod3	mTmod3-R	cagtcagtcacgatgcggccgcTTACTGGTGGTCTCCTTCAATTCG	64	1106
Psmd6	mPsmd6-F	aattcccgggtcgactcgagCCGCTAGAAAACCTAGAAGAAG	56	1216
PSmd6	mPsmd6-R	cagtcagtcacgatgcggccgcTTACATGTTAATTACTCTGGATAATTTC	56	1216
Fbp1	mFbp1-F	aattcccgggtcgactcgagGCGAACCATGCGCCCTTC	66	1056
Fbp1	mFbp1-R	cagtcagtcacgatgcggccgcTCACTTGGCTTTGTGCTTCCTG	66	1056
ATP6v1c1	mATP6v1c1-F	aattcccgggtcgactcgagACTGAGTTCTGGCTCATATCTG	56	1210
ATP6v1c1	mATP6v1c1-R	cagtcagtcacgatgcggccgcTTACTTGAATTCCAGCAAGTTG	56	1210
Acy1	mAcy1-F	aattcccgggtcgactcgagACCACCAAGGATCCCGAG	57	1274
Acy1	mAcy1-R	cagtcagtcacgatgcggccgcTCAGCTTTCACTAGGCAGG	57	1274
Acat1	mAcat1-F	aattcccgggtcgactcgagGCTGCCCTGGTGGCTCTG	64	1330
Acat1	mAcat1-R	cagtcagtcacgatgcggccgcCTACAGCTTCTCAATCAGCAGGG	64	1330
Psmd7	mPsmd7-F	aattcccgggtcgactcgagCCGGAGCTGGCGGTGCAG	68	1028
Psmd7	mPsmd7-R	cagtcagtcacgatgcggccgcTTACTTTTTCTCCTTTTTCTCTTCTTTCTTCGC	68	1028

Supplemental Table 1. Primers used to generate recombinant GST proteins identified by mass spectrometry. pGEX-4T-1 vector was linearized using XhoI and NotI enzymes. Templates for the PCR products for each candidate gene were obtained from kidney RNA that was reverse transcribed into cDNA by Superscript III (Invitrogen). PCR products contained 5' and 3' overlapping ends to the linearized pGEX-4T-1 vector. PCR products were cloned into the vector by the Gibson cloning method[93].

SUPPLEMENTAL TABLE 2

Gene	GenBank	Primer Name	Sequence	Tm	Expected Size	Notes
Tmod3	NM_016963	rtTmod3-F	CTCCTTGGCAAGCTGTCCG	63	128	Location 58-76
Tmod3	NM_016964	rtTmod3-R	CCCGTGGCAGACTTTGATGT	63	128	Location 185-166
Psmd6	NM_025550.2	rtPsmd6-F	ATGCCGCTAGAAAACCTAGAAGA	61	186	Location 1-23
PSmd6	NM_025550.2	rtPsmd6-R	GTCGAGGGATTTACACAAGGC	60	186	Location 186-166
Fbp1	NM_019395.3	rtFbp1-F	AGTCGTCCTACGCTACCTGTG	63	102	Location 260-280
Fbp1	NM_019395.3	rtFbp1-R	GGGGATCGAAACAGACAACAT	60	102	Location 361-341
ATP6v1c1	NM_025494.3	rtATP6-F	ACTGAGTTCTGGCTCATATCTGC	61	106	Location 4-26
ATP6v1c1	NM_025494.3	rtATP6-R	TGGAAGAGACGGCAAGATTATTG	61	106	Location 109-87
Acy1	NM_025371	rtAcy1-F	CAACCCAATCCAGACTATGGAGG	62	157	Location 76-98
Acy1	NM_025371	rtAcy1-R	GTGGGAGTTTAGCAAGATGGAG	62	157	Location 240-219
Psmd13	NM_011875	rtPsmd13-F	TTTGGCACCGTTTGGAAGAG	60	170	Location 62-81
Psmd13	NM_011875	rtPsmd13-R	TACCAGGGACAGAGGGTTTAC	60	170	Location 231-211
Acat1	NM_144784	rtAcat1-F	CAGGAAGTAAGATGCCTGGAAC	60	228	Location 61-82
Acat1	NM_144784	rtAcat1-R	TTCACCCCCTTGGATGACATT	61	228	Location 288-268
Psmd7	NM_010817	rtPsmd7-F	GGTGGATCATTTCAACCGAATTG	60		Location 57-79
Psmd7	NM_010817	rtPsmd7-R	AAGGTACTGCAAAACTGTTGGAT	60		Location 172-150
Lrp2	NM_001081088.1	rtLrp2-F	AAAATGGAAACGGGGTGACTT	60	170	Location 13418-13438
Lrp2	NM_001081088.1	rtLrp2-R	GGCTGCATACATTGGGTTTTCA	60	170	Location 13587-13566
Tpd52	NM_001025261.1	rtTpd52-F	GGAGAGGATGCTGTTACCATGC	62	127	Location 169-190
Tpd52	NM_001025261.1	rtTpd52-R	TTGCGGCCAATACTTGGGAC	62	127	Location 295-276

Supplemental Table 2. Primers used for RT-PCR.

Chapter 3

Assessing a Block in Thymic Central Tolerance to Improve T cell Anti-tumor Responses

INTRODUCTION

The attempt to harness and direct immune responses towards cancer is a primary goal of cancer immunotherapy[112,113]. For the most part, cancer immunotherapies largely target peripheral tolerance mechanisms that unleash potent T cell cytotoxic functions. Prime examples of approved cancer immunotherapies aimed at bypassing critical immune checkpoints include ipilimumab, an antibody directed against cytotoxic T lymphocyte-antigen 4 (CTLA-4), and prembrolizumab, an antibody that inhibits the programmed cell death 1 (PD-1) [114]. Together, both of these immunotherapies target the co-inhibitory receptors involved in T cell activation and have been shown to promote antitumor activity in patients with advanced melanoma and lung cancer[115]. However, it remains unclear why only a minority of patients respond to immunotherapies[112,113]. In addition to lack of mutations in some tumor types that render them invisible to the immune system, another potential factor is the limited availability of tumor-reactive T cells in a self-tolerant T cell repertoire.

T cell tolerance is an important mechanism for preventing and controlling autoimmunity. Both central and peripheral tolerance mechanisms are essential for establishing a self-tolerant T cell repertoire that is able to respond against foreign pathogens. Central tolerance or negative selection involves the apoptotic deletion of self-reactive T cell precursors in the thymus[116,117]. Developing thymocytes that harbor self-reactive T cell receptors (TCRs) and bind strongly to self-peptides presented on major histocompatibility complexes (MHC) receive strong signals and trigger apoptosis and clonal deletion[28,37,118]. Defects in negative selection pathways have been shown to lead to spontaneous multi-organ autoimmunity. This has been exemplified in multiple mouse model strains, such as mice deficient in Aire or mice deficient in pro-apoptotic molecules involved during negative selection (i.e. Bim/Puma)[29,95]. More recently, Burger et al[61] generated a mouse model (Bcl-2-BH3* Tg) overexpressing a mutant form of anti-apoptotic Bcl-2 that can block the activities of multiple pro-apoptotic molecules, such as Bim/Puma. This Bcl-2 mutant protein was also resistant to cell death induced by Nur77 conversion. Consequently, like mice deficient in Aire, the block in multiple negative selection pathways in the Bcl-2 BH3* Tg mice led to accelerated death from multi-organ autoimmunity. Together, these data highlight the importance of central tolerance as an important safeguard for removing autoreactive T cells.

However, central tolerance mechanisms are imperfect and a minority of autoreactive T cells can escape deletion and enter the periphery[119-123]. Peripheral tolerance mechanisms, such as anergy and FoxP3 expressing regulatory T cells (Tregs), can hinder and suppress autoreactive T cells from becoming fully activated in the periphery[124]. The importance of Tregs as a predominant peripheral tolerance mechanism was underscored in FoxP3-deficient mice, which succumbed to a quick onset of T cell mediated multi-organ autoimmunity within one month[125]. In addition, T cell intrinsic mechanisms also play a role in preventing autoimmunity. The expression of T cell co-inhibitory receptors, such as CTLA-4 or PD-1, are essential regulatory systems that serve to maintain peripheral tolerance by attenuating co-stimulatory/activating signals[126]. Taken together, the cooperation of both central and peripheral T cell tolerance mechanisms are important for controlling autoimmunity.

Despite these tolerance mechanisms for protecting against autoimmunity, they may simultaneously inhibit the generation and activation of T cells necessary for

productive anti-tumor responses. Indeed, many tumors antigens that are targeted by T cells are also self-antigens shared by normal cells, such as TRP-1 epitope derived from tyrosinase, a self-antigen in melanocytes but also a tumor antigen in melanoma[127,128]. Given how T cell self-tolerance is established early on in the thymus, the deletion of effector T cells capable of responding to tumor antigens may be clonally deleted during negative selection. A prior report demonstrated that modulating the activity of Aire, and thereby, altering the negative selection of T cells expressing tissue restricted antigens (TSA), led to better melanoma rejection in a TRP-1 transgenic mouse model[129,130]. This revealed the possibility that a break in tolerance could increase autoreactive T cells capable of recognizing tumor antigens and provided a novel therapeutic strategy to increase tumor recognition and antitumor response.

To more fully assess an autoimmune T cell response on tumor progression, we tested whether autoreactive T cells from BH3* Tg mice could improve anti-tumor responses. To this end, BH3* Tg mice were inoculated with multiple syngeneic tumor models and interrogated for their ability of BH3* Tg mice to reject tumors. In contrast to our hypothesis (that autoreactive T cells may provide additional anti-tumor immunity), we found that tumor progression was starkly enhanced in autoimmune BH3* Tg mice. The accelerated tumor growth could be deterred when Tregs cell were depleted, but nevertheless, BH3* Tg T cells could not provide additional protection. Our data suggest that an increase an autoimmune T cell repertoire does not provide a benefit against anti-tumor responses.

RESULTS

Autoimmune BH3 Tg mice have increased serum antibodies against tumor cells, but they do not confer additional protection*

Unlike wild-type Bcl-2 transgenic mice, T cells in the Bcl-2 BH3* Tg (BH3* Tg) mice are highly resistant to apoptosis accompanying negative selection during T cell development and lead to the accumulation of autoreactive T cells in the periphery. Consequently, these mice die early from multi-organ autoimmunity. A striking feature of these mice is the increased presence of autoreactive antibodies directed to multiple organs[61]. Because of this observation, we assessed whether this increase in antibody reactivity could translate into improved tumor recognition. To this end, sera reactivity from each mouse genotype were tested against syngeneic sarcoma-derived MCA303 or melanoma-derived B16 tumor cell lines by FACS. The tumor cell lines were stained with PE-conjugated anti-mouse IgG specific antibodies after incubating them with sera from aged matched wild-type (WT) littermate, Bcl-2 Tg, or BH3* Tg mice. Results are displayed as the median fluorescence intensity (MFI) of PE fluorophore. Sera from WT and Bcl-2 Tg resulted in no statistical difference in antibody reactivity against MCA303 cells (Figure 1A). In contrast, sera from BH3* Tg mice resulted in a statistically significant increase in antibody reactivity towards MCA303 (Figure 1A). We also observed an increase in protein banding patterns by western blot of MCA303 lysates probed with sera from BH3* Tg mice, but not sera from Bcl-2 Tg or wild-type control (Figure 1B). Interestingly, in each BH3* Tg sera tested, a common banding pattern was detected. Although WT and Bcl-2 Tg sera did contain antibodies that were reactive to MCA303 lysate, only a minimal binding pattern was observed. A similar result was observed when the B16 tumor cell line was used (Figure 1B, Figure 1D). Together, the

results reveal the possibility that sera from BH3* Tg mice could provide increased recognition to tumor cells and lead to improved anti-tumor rejection.

The increased antibody reactivity against two different tumor cell lines in the BH3* Tg mice may provide increased tumor recognition and lead to better tumor rejection. Consistent with this hypothesis, the administration of tumor-specific antibodies has been demonstrated to enhance tumor-specific T cell responses[131]. In fact, monoclonal antibodies that target six tumor-associated proteins have been established as immune treatments for solid and hematological cancers[112]. To test whether antibodies from BH3* Tg mice could improve tumor rejection, antibodies were isolated from WT, Bcl-2 Tg, or BH3* Tg sera, then injected into wild-type mice 1 day prior and 3 days after MCA303 tumor inoculation (Figure 1E). Tumor growth was assessed daily and mice were killed upon reaching experimental endpoint. WT mice injected with PBS were used as a control. By day 14, tumor progression to endpoint was observed in WT mice receiving PBS or WT antibodies (Figure 1F). Interestingly, mice receiving Bcl-2 Tg or BH3* Tg antibodies could delay tumor progression up until day 20. However, tumor progression occurred by day 27 in these mice (Figure 1F). While transfer of Bcl-2 Tg or BH3* Tg antibodies into WT mice could delay tumor progression, no statistically significant difference was observed with tumor growth sizes (Figure 1F). Although Bcl-2 Tg or BH3* Tg antibodies transferred into WT mice were able to provide a survival benefit when compared to mice receiving WT sera, but BH3* Tg antibodies did not offer a statistically significant increase in overall survival against tumor challenge compared to Bcl-2 Tg antibodies (Figure 1G). Together, these results suggest that while there is an increase in antibody reactivity towards tumor cells and lysate, BH3* Tg antibodies do not offer additional anti-tumor immunity.

Decreased anti-tumor immunity in aged, autoimmune BH3 Tg mice*

The increased antibody reactivity towards tumor cells in BH3* Tg mice sera suggested the presence of a T cell population able to recognize and respond to tumor antigens. This is based on the assumption that an existing tumor-specific $CD4^+$ T cell provides “help” to a B cell to produce antibodies that may react with a tumor antigen. To test whether an increased autoreactive T cell population in BH3* Tg mice could respond to tumor antigens *ex-vivo*, T cells were purified from littermate control or BH3* Tg mice, stimulated with bone marrow derived dendritic cells (BMDCs) pulsed with or without MCA 303 tumor lysates, and IFNγ production was measured by intracellular cytokine staining (ICS). As shown in Figure 2A, IFNγ production was detected in both WT and BH3* Tg $CD8^+$ T cells, but IFNγ production was elevated in BH3* Tg T cells. For some reasons, we did not detect IFNγ production from WT or BH3* Tg $CD4^+$ T cells (data not shown). Why IFNγ production was not detected in CD4+ T cells is unclear, but is unlikely due to a technical issue as IFNγ production was observed in $CD8^+$ T cells from the same well.

To directly test the hypothesis that the presence of an autoreactive T cell repertoire could be effective against tumor progression, we injected MCA303 syngeneic tumor cells into a cohort of wild-type littermate, Bcl-2 Tg, or BH3* Tg mice. We inoculated MCA303 tumor cells into younger mice, defined by 6 to 20 weeks of age, and tumor growth was assessed daily until experimental endpoint. No statistically significant differences in tumor growth were observed between any the mouse genotypes by day

15 (Figure 2B). These results were also observed in TrampC2 tumor-bearing young mice (Figure 2C). Since no differences in tumor progression were observed in younger mice, we reasoned that aged BH3* Tg mice containing more autoreactive T cells could elicit better tumor rejection. In older BH3* Tg mice, the onset of autoimmune symptoms, such as increased activated T cells ($CD44^+CD62L^-$) in the blood, occurs by 25 weeks of age. To test this hypothesis, a cohort of older, aged-matched mice from WT, Bcl-2 Tg, or BH3* Tg were inoculated with MCA303 cells and tumor growth was assessed over time. Two weeks postinoculation, tumors grew at a rate indistinguishable between aged WT littermate and Bcl-2 Tg control mice. Unexpectedly, MCA303 tumor inoculation into BH3* Tg mice led to a striking enhancement in tumor growth (Figure 2D). This result could also be observed in B16 tumor-bearing BH3* Tg mice (Figure 2E). To preliminary determine whether enhanced tumor growth was T cell dependent, T cells were purified from WT, Bcl-2 Tg, or BH3* Tg mice and adoptively transferred into T/B cell deficient RagKO mice. RagKO mice were then challenged with MCA303 cells and tumor growth was monitored daily. By day 15, there was no difference between tumor growth in RagKO tumor-bearing mice receiving T cells from WT littermates or Bcl-2 Tg mice (Figure 2F). However, tumors grew larger in RagKO receiving BH3* Tg T cells compared to control WT littermate or Bcl-2 Tg (Figure 2F) although more mice are needed to get statistically significant data.

Taken together, although autoimmune BH3* Tg mice are able to respond to tumors *ex-vivo*, they are unable to mount a protective antitumor immune response *in-vivo*.

Contribution of immunosuppressive Tregs hinder BH3 Tg mice from mounting a productive anti-tumor response*

Highly immunosuppressive tumor microenvironments are permissive for tumor growth and can elicit profound myeloid and T cell dysregulation[132,133]. Given the prior observation that older BH3* Tg mice have an inflammatory phenotype and increased number of immunosuppressive Treg cells, we hypothesized whether either of these factors could contribute to tumor escape in the BH3* Tg mice. To assess the contribution of inflammatory $Ly6c^{lo}CD11b^+$ neutrophils, older, aged-matched WT littermates or BH3* Tg mice were inoculated with B16 cells and subjected to temporary neutrophil ablation using Gr-1 (Ly6c/Ly6g) depleting antibodies (Figure 3A). Successful depletion of neutrophils was confirmed 4 days after tumor inoculation by FACS (data not shown). By day 15 as expected, B16-tumor bearing BH3* Tg mice injected with PBS had a significant increase in tumor growth compared to WT mice injected with PBS (Figure 3B). Tumor growth was not affected in Gr-1 depleted WT mice. Interestingly, tumor growth in BH3* Tg mice depleted of Gr-1 neutrophils was indistinguishable to that of BH3* Tg mice injected with PBS (Figure 3B). These data suggest that neutrophils have no appreciable effects on the accelerated tumor growth phenotype in BH3* Tg mice.

Given that Treg cells can suppress T cell function and promote tumor evasion, we tested tumor bearing mice in which Treg cells were depleted and assessed the ability for autoreactive T cells from BH3* Tg mice to reject tumors. T cells that were purified from WT, Bcl-2 Tg, or BH3* Tg mice were depleted of $CD4^+CD25^+$ Tregs and adoptively transferred into RagKO mice (Figure 3C). Successful depletion of Tregs was

confirmed by FACS (data not shown). These mice were then challenged with MCA303 cells and tumor progression was monitored daily. RagKO mice that received conventional $CD4^+$ and $CD8^+$ T cells from WT or Bcl-2 Tg displayed no differences in tumor growth (Figure 3D). Surprisingly, tumor growth in mice that received T cells depleted of Tregs from BH3* Tg mice grew at a similar rate to that observed in mice receiving WT and Bcl-2 Tg T cells. This result indicates a possible contribution of Tregs in the accelerated tumor growth phenotype in BH3* Tg mice, but further experiments with more mice are needed to verify their role.

We then characterized the tumor infiltrating lymphocyte (TILs) populations by FACS two weeks after tumor inoculation in the Treg depleted tumor-bearing mice. By two weeks, an overall significant increase in the number of $CD3^+$ infiltrating T cells in tumors of RagKO mice receiving BH3* Tg compared to WT or Bcl-2 Tg T cells (Figure 3E). This increase of $CD3^+$ T cells in these mice were predominately $CD8^+$; however, a slight, but not significant increase was observed in $CD4^+$ T cells (Figure 3F). Further, there was a presence of polarized Th1, Th17, and $FoxP3^+$ $CD4^+$ T cells that were slightly increased in the tumors of mice that received BH3* Tg, but not WT or Bcl-2 Tg T cells (Figure 3G). Although there was an increased presence of $FoxP3^+$ T cells in mice receiving BH3* Tg T cells, the CD8+/Treg ratio was no different than the controls (Figure 3H). Surprisingly, $CD8^+$ T cells from BH3* Tg mice expressed PD-1 relatively higher than WT or Bcl-2 Tg $CD8^+$ T cells (Figure 3I). Together, these results suggest that autoreactive T cells do not contribute to anti-tumor immunity.

DISCUSSION

We have shown that BH3* Tg mice are not effective in provoking productive anti-tumor responses. Increased tumor size and outgrowth occurred in BH3* Tg tumor-bearing mice with multiple syngeneic tumor models. We demonstrated that this outcome can be replicated in T cell adoptive transfers into RagKO mice, strongly suggesting T cell dysregulation. Whether T cell dysregulation was preempted by the immunosuppressive nature of tumor microenvironments or enhanced peripheral tolerance mechanisms from altering negative selection in these mice is not completely clear. Nevertheless, we demonstrated that BH3* Tg T cells, specifically $CD8^+$ T cells, were able to produce IFNγ in the presence of antigen-presenting cells (APC) presenting B16 tumor antigens, suggesting BH3* Tg T cells have the capacity to respond to tumors. Even with a tumor reactive T cells population in BH3* Tg mice, the ability for these T cells to mount an effective anti-tumor response *in vivo* may be countered by the increased peripheral tolerance mechanisms, such as increased Tregs or anergic T cells, which existed prior to tumor inoculation. Fascinatingly, the adoptive transfer of Treg-depleted T cells purified from BH3* Tg mice into RagKO hosts ablated the accelerated tumor growth phenotype. Interestingly, the depletion of Tregs in within the pool of BH3* Tg T cells did not offer greater tumor protection. One likely factor for this observation may be also the increased number of already existing anergic T cells ($FR4^+CD73^+$) in periphery of the BH3* Tg mice[61]. In addition, increased levels T cell exhaustion marker, PD-1, has also been observed in these T cells upon ex-vivo stimulation assays (data not shown). Together, our results suggest that overcoming multiple several immune checkpoints that are enhanced in BH3* Tg mice serves as cardinal impediment for producing or utilizing autoimmune T cells as an effective anti-tumor therapy, and

attempting to circumvent these processes by using checkpoint blockade therapies may open the possibility for improved anti-tumor responses in these mice.

MATERIALS AND METHODS

Cells

TrampC2 cells were purchased from ATCC and maintained in DMEM supplemented with 5% fetal calf serum, 5% NuSerum (Collaborative Biochemical), 5 ug/mL insulin, 0.01 nM dihydrotestosterone (Sigma), and 100 U/ml penicillin/100 µg/mL streptomycin. MCA303 or B16-BL6 cells were maintained in DMEM supplemented with 5% fetal calf serum, 2 mM L-glutamine, non-essential amino acids, 1 mM sodium pyruvate, and 100 U/ml penicillin/100 µg/mL streptomycin at 37˚C. Cells were routinely tested negative for mycoplasma. For tumor injection, only early passages (<10) were used.

Syngeneic tumor studies

C57BL/6 wild-type (WT), RagKO or T cell specific wild-type *Bcl2* transgenic line (Bcl-2 Tg) or *Bcl2* BH3 mutant transgenic (BH3* Tg) mice were inoculated subcutaneously (s.c.) in the right flank with 5 x 10^6 TrampC2 (males only), 1 x 10^5 MCA303, or 2-2.5 x 10^4 B16-BL6 syngeneic tumor cells resuspended in 1X PBS. Age 6 to 20-week-old mice were designated young. Aged mice were defined as being over the age of 25 weeks. For serum transfer experiments, mouse serum was pooled from three mice of each genotype obtained from cardiac puncture or saphenous vein bleeds. Blood was allowed to coagulate for 1 hour to overnight at 4˚C, and subjected to low temperature high speed centrifugation to obtain serum supernatant. Antibodies were isolated from total serum by Protein A/G agarose bead capture, followed by briefly eluting with 100 mM Glycine, pH 2.5-3.0 after washing beads three times with binding buffer (1X PBS). WT mice were injected with 150 µg of isolated antibodies intraperitoneal (i.p.) 1 day before and 3 days after tumor inoculation. For T cell adoptive transfer experiments, RagKO mice were inoculated with indicated tumor cells after 3 to 5 days after receiving 1-3 x 10^6 T cells by tail vein injection. T cells were pooled from spleen and peripheral lymph nodes and enriched by T cell enrichment columns (R&D Systems). Where indicated, Tregs were depleted by PE conjugated anti-CD25 (clone PC1, eBioscience) positive selection and magnet separation using EasySep Mouse PE Selection Kit (StemCell Technologies) according to manufacturer's recommendations. For myeloid-derived suppressor cell (MDSCs) depletion, 250 µg of anti-Gr1 antibody was injected i.p four times after tumor injection every three days. Mice were monitored for tumor growth by palpitation and tumor size was obtained by taking two perpendicular measurements by Vernier calipers. Mice were monitored and euthanized when tumor volumes reached ≥ 2 cm^3 ($0.5(L \times W^2)$), ulceration, or moribund. All experiments involving these animals were approved by the UC Berkeley Animal Care and Use Committee (ACUC).

Flow cytometry

For tumor cell staining, single cell suspension of MCA303 or B16-BL6 tumor cells were stained with 1:200 of serum in FACS buffer (1X PBS, 2% FCS, 0.05% $NaNH_3$) for 15 minutes on ice. After incubation, cells were washed with FACS buffer and incubated

with PE-conjugated secondary antibody against mouse IgG (eBioscience). Data shown is depicted as the Median Fluorescence Intensity (MFI) of PE.

Single cell suspension of mouse splenocytes or lymph nodes were obtained by dissociating the tissue through a 40 μM cell strainer followed by lysing red blood cells by 1X ACK buffer (10X: 1.5M NH_4Cl, 0.1M $KHCO_3$, 1M EDTA, pH 7.2). Tumor infiltrating lymphocytes (TILs) were obtained as previously described. Briefly, tumors were minced by mechanical disruption (i.e. scissors), and DNase I (Thermoscientific) and Collagenase IV (Sigma-Aldrich) digested for 30 minutes at 37˚C. Tumors were mashed with an end of a syringe plunger, and passed through a 40 μM cell strainer to obtain single cell suspensions and red blood cells were lysed with 1X ACK buffer. When necessary, TILs were enriched by Lympholyte M (Cedarlane) according to the manufacturer's instructions. Cells were stained with a viability dye (Tonbo) and commercial antibodies against CD45 (eBioscience), CD45.1 (eBioscience), CD3 (Biolegend), CD4 (Biolegend), CD8 (Biolegend), CD44 (Tonbo), CD62L (Tonbo), B220 (eBioscience), Ly6C (eBioscience), LyGC (eBioscience), GR-1 (eBioscience), CD11b (eBioscience), CD11c (Tonbo), NK1.1 (eBioscience), or PD-1 (eBioscience) where indicated. For intracellular cytokine staining, cells were stimulated with 2 μg/mL CD3 (2C11) and 2 μg/mL CD28 (PV-1) 4-5 hr at 37˚C in the presence of GolgiStop (BD Bioscience) and GolgiPlug (BD Bioscience). Alternatively, bone marrow derived dendritic cells (BMDCs) were pulsed overnight with tumor lysate produced by three consecutive rounds of flash-freeze in LN_2 and thaw. Further maturation of DCs was initiated by adding 10 ng/mL LPS for 1 hour, followed by multiple PBS (>4) washes before co-culturing them with T cells overnight at 37˚C. After stimulation, cells were surfaced stained as described, fixed, and permeablized with BD Cytofix/Cytoperm Kit (BD Bioscience) according to manufacturer's instructions. Fixed cells were stained with antibodies against IFNγ (eBioscience), IL-4 (eBioscience), IL-10 (eBioscience), or IL-17A (eBioscience) where indicated. For intracellular transcription factor staining, cells were surface stained as described, fixed, and permeabilized with FoxP3 Staining Kit (eBioscience). Fixed cells were stained with antibodies against Bcl-6 (BD Bioscience), FoxP3 (eBioscience), T-bet (Biolegend), and RORyt (BD Bioscience).

Western Blotting

Single cell suspensions of MCA303 or B16-BL6 tumor cells were pelleted, washed with PBS, and lysed in RIPA buffer (50 mM Tris-HCL, pH 7.6, 150 mM NaCl, 2 mM EDTA, 1% NP-40, 0.05% SDS, 1 mM DDT, Sigma protease inhibitor cocktail, along with phosphatase inhibitors 1 mM $NaVO_4$, 1 mM NaF, and 1 mM PMSF). Quantification of protein was obtained using Bio-Rad *DC* Protein Assay (Bio-Rad), and 150 μg of protein was loaded into a single well 10% SDS-PAGE gel. Proteins were transferred on nitrocellulose membranes and blocked with 5% non-fat milk in 1% Tween TBS (TBST). Membranes were placed in a Surf-Blot apparatus (Idea Scientific) and probed with serum diluted to 1:200 for 2 hrs at room temperature. Membranes were incubated with HRP-conjugated anti-mouse IgG antibody (1:7500, GE Healthcare) following three washes with TBST. Visualization of bands were performed using SuperSignal West Pico Chemiluminescent Substrate (Thermoscientific) by autoradiography.

FIGURES
FIGURE 1

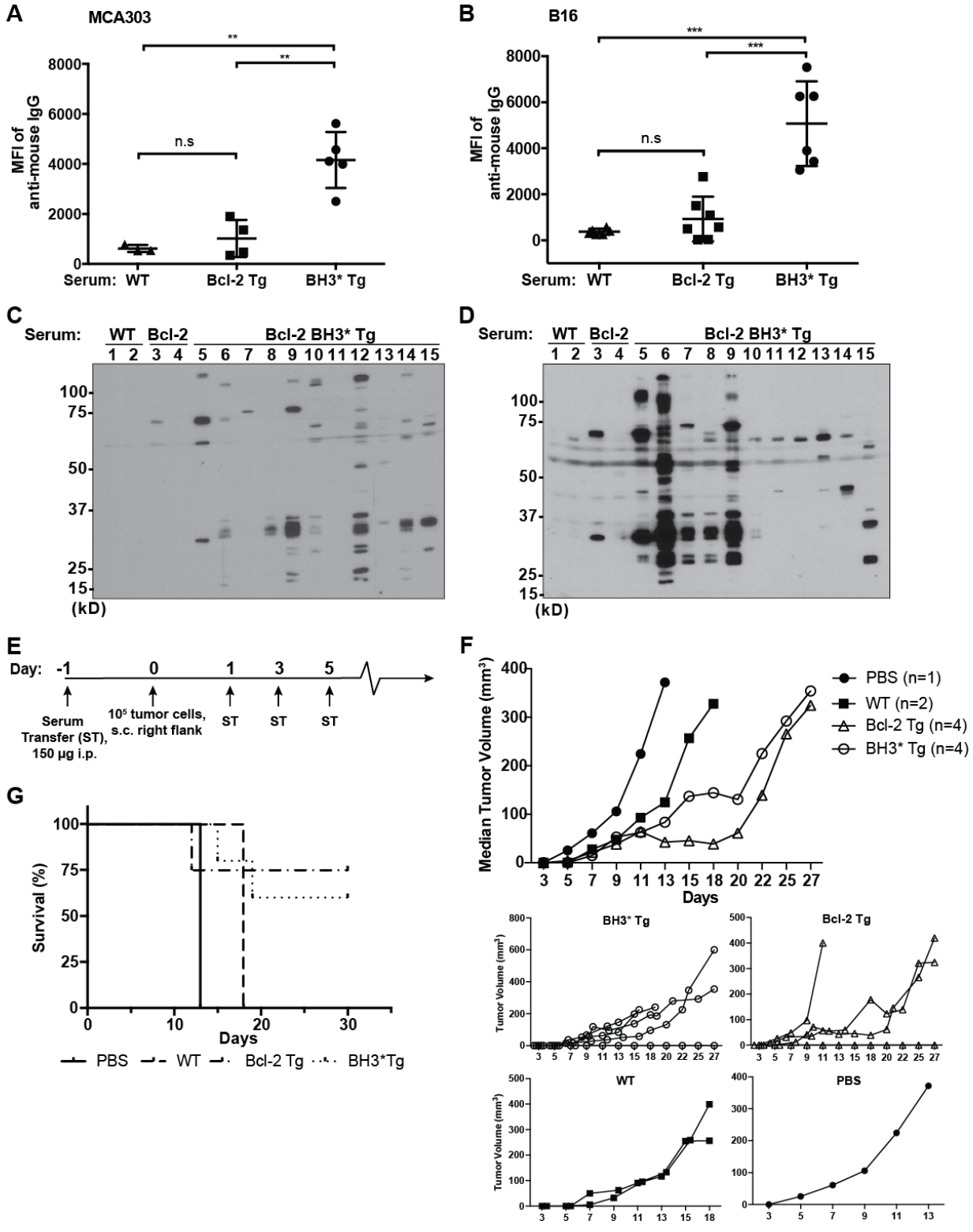

Figure 1. Increased endogenous tumor-specific autoantibody reactivity in autoimmune mice. *A-B,* MCA303 sarcoma (*A*) or B16 melanoma (*B*) tumor cells incubated with 1:200 dilution of sera collected from wild-type (WT), Bcl-2 Tg, or BH3* Tg tumor free, naïve mice. The cells were then washed and stained with an Phycoerythin (PE)-conjugated mouse IgG-specific antibody and analyzed by flow cytometry. *C-D*, Sera western blots for detecting antibody reactivity in whole cell MCA303 (C) or B16 (D) tumor lysates. Each lane represents sera from an individual WT (n=2), Bcl-2 Tg (n=2), or BH3* Tg (n=11) mouse. *E,* Schematic of serum transfer tumor model. WT mice were injected intraperitoneal (i.p.) with PBS (n=1) or serum from aged (>50 weeks) WT (n=2), Bcl-2 Tg (n=5), or BH3* Tg (n=4) mice one day prior and three days after subcutaneous (s.c.) inoculation with 10^6 MCA303 tumor cells into the flanks of mice. *F,* Tumor sizes of mice transferred with sera as outlined in 1E. Depicted are compiled median tumor volume (top) or individual tumor growth means for each group (bottom). *G*, Percent survival over time as outlined in 1E. n.s. not significant, * $p<0.5$ by Student t-test.

FIGURE 2

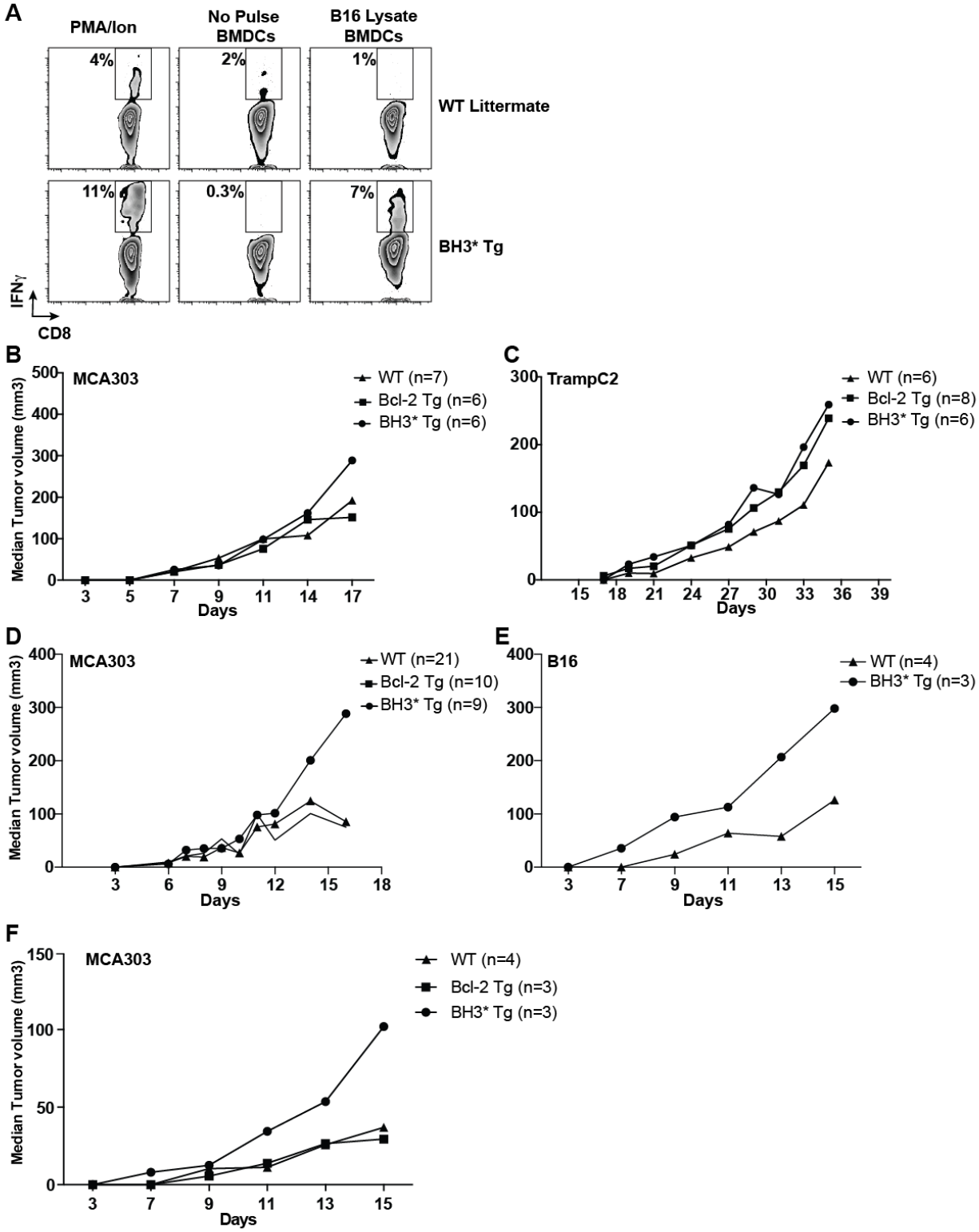
A
PMA/Ion
No Pulse BMDCs
B16 Lysate BMDCs
4%
2%
1%
WT Littermate
11%
0.3%
7%
BH3* Tg
IFNγ
CD8
B
MCA303
WT (n=7)
Bcl-2 Tg (n=6)
BH3* Tg (n=6)
Median Tumor volume (mm3)
Days
C
TrampC2
WT (n=6)
Bcl-2 Tg (n=8)
BH3* Tg (n=6)
Days
D
MCA303
WT (n=21)
Bcl-2 Tg (n=10)
BH3* Tg (n=9)
Median Tumor volume (mm3)
Days
E
B16
WT (n=4)
BH3* Tg (n=3)
Days
F
MCA303
WT (n=4)
Bcl-2 Tg (n=3)
BH3* Tg (n=3)
Median Tumor volume (mm3)
Days

Figure 2. Aged BH3* Tg mice exhibit faster tumor growth. *A,* T cells purified from WT littermate or BH3* Tg mice stimulated with bone-marrow derived dendritic cells (BMDCs) pulsed with B16 tumor lysate or not in the presence of Brefeldin A and monensin. Phorbol myristate acetate (PMA) and ionomycin (Ion) were used as a positive control. Shown are representative flow cytometry plots for intracellular cytokine staining to detect B16 tumor specific $CD8^+$ T cells producing IFNγ (n=2 per each group). *B,C,* Tumor growth over time in young (<20 week) mice inoculated with 10^5 MCA303 (B) or 5 x 10^6 TrampC2 (C) tumors cells. Shown are the median tumor growth volumes for each mouse genotype. *D,E,* Tumor growth in aged (>25 week) mice challenged with 10^5 MCA303 (D) or 2.5 x 10^4 B16 (E) tumor cells. Shown are the median tumor growth volumes for each genotype. *F*, RagKO mice adoptively transferred with purified T cells from WT (n=4), Bcl-2 Tg (n=3), or BH3* Tg (n=3) were challenged with 10^5 MCA303 tumor cells. Depicted are median tumor growth.

FIGURE 3

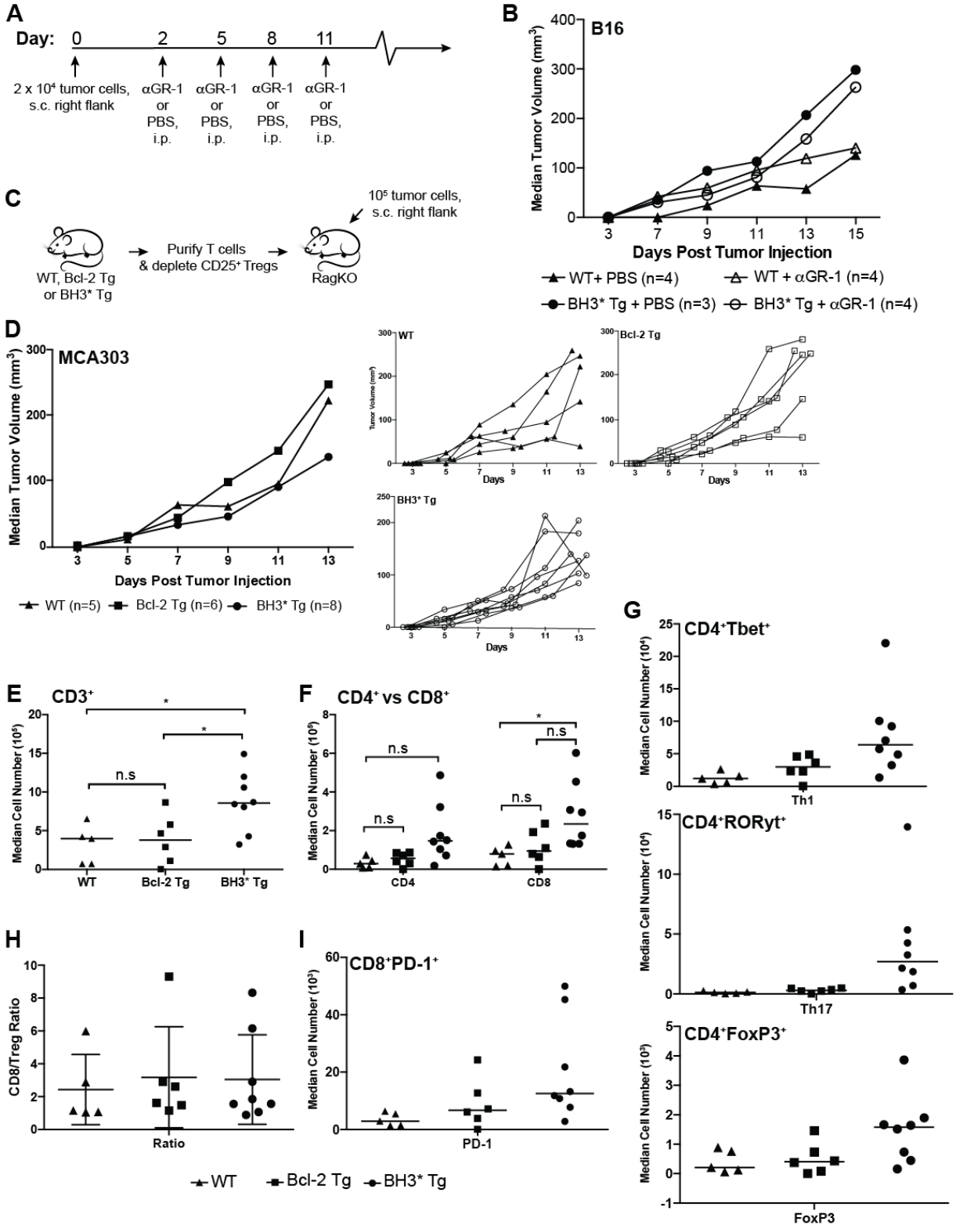
A
Day: 0 2 5 8 11
2 x 10⁴ tumor cells, s.c. right flank
αGR-1 or PBS, i.p.
B
B16
Median Tumor Volume (mm³)
Days Post Tumor Injection
WT+ PBS (n=4)
WT + αGR-1 (n=4)
BH3* Tg + PBS (n=3)
BH3* Tg + αGR-1 (n=4)
C
10⁵ tumor cells, s.c. right flank
WT, Bcl-2 Tg or BH3* Tg
Purify T cells & deplete CD25⁺ Tregs
RagKO
D
MCA303
Median Tumor Volume (mm³)
Days Post Tumor Injection
WT (n=5)
Bcl-2 Tg (n=6)
BH3* Tg (n=8)
WT
Bcl-2 Tg
BH3* Tg
Days
E
CD3⁺
Median Cell Number (10⁵)
n.s
WT
Bcl-2 Tg
BH3* Tg
F
CD4⁺ vs CD8⁺
CD4
CD8
G
CD4⁺Tbet⁺
Th1
CD4⁺RORγt⁺
Th17
CD4⁺FoxP3⁺
FoxP3
H
CD8/Treg Ratio
Ratio
I
CD8⁺PD-1⁺
PD-1

Figure 3. **Contributions of tumor suppressive networks on BH3* Tg accelerated tumor growth.** *A*, Schematic for older, aged-matched WT littermate or BH3* Tg mice inoculated with B16 melanoma. Mice were treated with aGR-1 antibody temporarily depleted or not of pro-inflammatory Gr-1$^+$ (Ly6c$^+$Ly6g$^+$) cells every three days after tumor injection. *B,* Tumor growth of mice treated with or without GR-1 depleting antibody. Depicted are median tumor growth volume. *C-G,* RagKO mice were adoptively transferred with CD4$^+$CD25$^+$ Treg cells from a pool of purified T cells obtained from WT, Bcl-2 Tg or BH3* Tg mice. Five days post adoptive transfer, 10^5 MCA303 tumor cells were s.c. injected into the back flanks of mice. WT→RagKO (n=5), Bcl-2→RagKO (n=6), and BH3* Tg→RagKO (n=8). *C,* Schematic for adoptively transferring Treg-depleted T cells. *D,* Median (left) and individual (right) MCA303 tumor volumes over time. *E-G,* FACS analysis of tumor infiltrating lymphocytes of MCA303 tumor bearing mice as described in 3C for total CD3$^+$ T cell population (E), CD4$^+$ or CD8$^+$ T cell subsets (F), polarization of Th1 (top), Th17 (middle), or Tregs (bottom) CD4$^+$ T cell populations (G), CD8$^+$/Treg ratio (H), or the expression of PD-1 exhaustion marker on CD8$^+$ T cells (I). Data shown are the median cell number of indicated cell type. In E and F, n.s. or * $p < 0.5$ by Student's t-test.

GENERAL DISCUSSION AND OUTLOOK

The overall theme surrounding my dissertation has been learning and exploring the mediators of apoptosis in T cells, which involve the complex biology of the enigmatic protein Nur77 and its relationship with Bcl-2. Chapter 1 described and characterized the Nur77 and Bcl-2 interaction, where I identified critical residues within Bcl-2 essential for Nur77/Nor-1 interaction. Chapter 2 explored how blocking multiple negative selection pathways, which includes Nur77-mediated apoptosis, can lead to autoimmunity. In this chapter, I putatively identified a potential target autoantigen, Tmod3. Chapter 3 investigated whether the rescue of BH3* Tg T cells could be utilized for cancer immunotherapies. Here, I will discuss the limitations and reflect on remaining unanswered questions for each study.

Characterizing the interaction between Nur77 and Bcl-2 was of great interest because results from this study could offer new insights in therapeutically targeting Bcl-2 overexpression commonly observed cancers. In Chapter 1, we demonstrated that Nur77 and Bcl-2 interaction relies on a cluster of residues found between the Bcl-2 BH1 and BH2 domains (i.e. Bcl-2/Ala(158-161)). The Bcl-2 mutant that abrogated Nur77 interaction did not affect the anti-apoptotic function of Bcl-2, but can affect Nur77/Nor-1 mediated apoptosis. While these results provide the critical residues for Nur77 interaction, the mechanism of how Nur77 can convert Bcl-2 into a pro-apoptotic molecule becomes more obscure. In particular, it is not entirely clear how Nur77 can elicit extensive conformational changes in Bcl-2, especially since the putative Nur77 binding pocket contains numerous salt-bridges. In addition, Godoi et al[86] reported that they did not observe any overall conformational changes by NMR in any of the Bcl-2 family members they tested. Perhaps another unidentified protein is required to assist conformational changes in the Nur77:Bcl-2 complex. Nevertheless, the identification of these critical residues provides an opportunity to study the significance of Nur77:Bcl-2 interaction *in vivo*.

One interesting and perplexing puzzle emerged when we studied Bcl-2 BH3* Tg mice. Specifically, why do BH3* Tg, but not Bcl-2 Tg mice developed autoimmunity and die quicker. The autoimmune phenotype in these mice was also characterized by the increased presence of autoantibodies directed to antigens found within tested with very little variability. In Chapter 2 of this work, we attempted to dissect the autoimmune phenotype in BH3* Tg mice. Using antibodies as a tool to identify a common target antigen, we first showed that potential targets were presumably cell surface antigens. Unexpectedly, the IP-MS using BH3* Tg sera did not identify any cell surface proteins. Two experimental repeats, however, identified a ubiquitously expressed intracellular protein, Tmod3. If Tmod3 is a target antigen, it remains unclear how autoimmunity could initiate from an antibody directed to an intracellular protein. Whether Tmod3 is an initiator of autoimmunity or a byproduct of epitope spreading remains to be determined. Nevertheless, my data strongly suggest that Tmod3 is a potential autoantigen. Regardless, the candidate(s) and subsequent reagent(s) to further study the autoimmune phenotype are available to answer these remaining questions.

Finally, in Chapter 3 of this work, we explored whether the increase in self-reactivity could improve tumor recognition and rejection. Using syngeneic tumor cells as a model, aged, tumor-bearing BH3* Tg mice contained increased antibodies reactivity to tumor cells, suggestive of increased recognition. Despite this observation, BH3* Tg

mice were unable to provoke an effective anti-tumor response when challenged with tumors. Tumors grew bigger and faster in these mice. While multiple factors could attribute to the increased tumor progression in BH3* Tg mice, two plausible and non-mutually exclusive elements may attribute to this phenotype. First, aged BH3* Tg mice develop inflammation characterized by increased inflammatory monocytes and neutrophils. During tumor progression, these myeloid derived suppressor cells (MDSCs) may promote a microenvironment that is more conducive for tumor growth. Second, Tregs may be playing a role in increased tumor progression. Tregs have been shown to promote tolerance to tumors through immune suppression[133]. Malchow et al[134] provided an interesting hypothesis that tumors may recruit thymic-derived Tregs that recognize self-antigens, and tumors coopt their immunosuppressive mechanisms to elicit immune tolerance. Along these lines, it would be of interest to characterize the nature these Tregs in BH3* Tg mice, as identification of the Treg and its corresponding target antigen could be a targeted approach to improve cancer immunotherapies. Nevertheless, the advent of successful cancer immunotherapy has drastically influenced the course of cancer treatment, yet improving cancer immunotherapy response rates to ≥30% involves further delineating the basic biology of the immune system to harness the full potential of anti-tumor immunity.

REFERENCES

1. Strasser, A., O'Connor, L. & Dixit, V. M. Apoptosis signaling. *Annu. Rev. Biochem.* **69,** 217–245 (2000).
2. Cory, S. & Adams, J. M. The Bcl2 family: regulators of the cellular life-or-death switch. *Nat Rev Cancer* **2,** 647–656 (2002).
3. Sprick, M. R. & Walczak, H. The interplay between the Bcl-2 family and death receptor-mediated apoptosis. *Biochimica et biophysica acta* **1644,** 125–132 (2004).
4. Youle, R. J. & Strasser, A. The BCL-2 protein family: opposing activities that mediate cell death. *Nature Publishing Group* **9,** 47–59 (2008).
5. Wilson, N. S., Dixit, V. & Ashkenazi, A. Death receptor signal transducers: nodes of coordination in immune signaling networks. *Nat Immunol* **10,** 348–355 (2009).
6. Tait, S. W. G. & Green, D. R. Mitochondria and cell death: outer membrane permeabilization and beyond. *Nature reviews. Molecular cell biology* **11,** 621–632 (2010).
7. Nagata, S. & Tanaka, M. Programmed cell death and the immune system. *Nature Reviews Immunology* **17,** nri.2016.153–340 (2017).
8. Imawati Budihardjo, Holt Oliver, Michael Lutter, Xu Luo, A. & Wang, X. Biochemical Pathways of Caspase Activation During Apoptosis. *http://dx.doi.org/10.1146/annurev.cellbio.15.1.269* **15,** 269–290 (2003).
9. Wolf, B. B. & Green, D. R. Suicidal tendencies: apoptotic cell death by caspase family proteinases. *Journal of Biological Chemistry* **274,** 20049–20052 (1999).
10. Delbridge, A. R. D., Grabow, S., Strasser, A. & Vaux, D. L. Thirty years of BCL-2: translating cell death discoveries into novel cancer therapies. *Nat Rev Cancer* **16,** nrc.2015.17–109 (2016).
11. Strasser, A., Jost, P. J. & Nagata, S. The Many Roles of FAS Receptor Signaling in the Immune System. *Immunity* **30,** 180–192 (2009).
12. Walczak, H. Death Receptor-Ligand Systems in Cancer, Cell Death, and Inflammation. *Cold Spring Harbor Perspectives in Biology* **5,** a008698–a008698 (2013).
13. Wallach, D., Kang, T. B., Dillon, C. P. & Green, D. R. Programmed necrosis in inflammation: Toward identification of the effector molecules. - PubMed - NCBI. *Science* **352,** aaf2154–aaf2154 (2016).
14. Wajant, H. The Fas Signaling Pathway: More Than a Paradigm. *Science* **296,** 1635–1636 (2002).
15. Wang, S. & El-Deiry, W. S. TRAIL and apoptosis induction by TNF-family death receptors. *Oncogene* **22,** 1207232–8633 (2003).
16. Cohen, P. L. & Eisenberg, R. A. Lpr and gld: single gene models of systemic autoimmunity and lymphoproliferative disease. *Annu. Rev. Immunol.* **9,** 243–269 (1991).
17. Marsden, V. S. & Strasser, A. Control of apoptosis in the immune system: Bcl-2, BH3-only proteins and more. *Annu. Rev. Immunol.* **21,** 71–105 (2003).
18. Chipuk, J. E., Moldoveanu, T., Llambi, F., Parsons, M. J. & Green, D. R. The BCL-2 family reunion. *Molecular Cell* **37,** 299–310 (2010).

19. Yin, X. M., Oltvai, Z. N. & Korsmeyer, S. J. Bh1 and Bh2 Domains of Bcl-2 Are Required for Inhibition of Apoptosis and Heterodimerization with Bax. *Nature* **369,** 321–323 (1994).
20. Kawatani, M. & Imoto, M. Deletion of the BH1 domain of Bcl-2 accelerates apoptosis by acting in a dominant negative fashion. *Journal of Biological Chemistry* **278,** 19732–19742 (2003).
21. Robey, E. Selective events in T cell development. *Annu. Rev. Immunol.* (1994).
22. Palmer, E. Negative selection--clearing out the bad apples from the T-cell repertoire. *Nature Reviews Immunology* **3,** 383–391 (2003).
23. Koch, U. & Radtke, F. Mechanisms of T cell development and transformation. *Annu. Rev. Cell Dev. Biol.* **27,** 539–562 (2011).
24. Carpenter, A. C. & Bosselut, R. Decision checkpoints in the thymus. *Nat Immunol* **11,** 666–673 (2010).
25. Hogquist, K. A., Baldwin, T. A. & Jameson, S. C. Central tolerance: learning self-control in the thymus. *Nature Reviews Immunology* **5,** 772–782 (2005).
26. Moran, A. E. & Hogquist, K. A. T-cell receptor affinity in thymic development. *Immunology* **135,** 261–267 (2012).
27. Stritesky, G. L., Jameson, S. C. & Hogquist, K. A. Selection of self-reactive T cells in the thymus. *Annu. Rev. Immunol.* **30,** 95–114 (2012).
28. Klein, L., Kyewski, B., Allen, P. M. & Hogquist, K. A. Positive and negative selection of the T cell repertoire: what thymocytes see (and don't see). *Nature Reviews Immunology* **14,** 377–391 (2014).
29. Anderson, M. S. *et al.* Projection of an immunological self shadow within the thymus by the aire protein. *Science* **298,** 1395–1401 (2002).
30. Metzger, T. C. & Anderson, M. S. Control of central and peripheral tolerance by Aire. *Immunol. Rev.* **241,** 89–103 (2011).
31. Mathis, D. & Benoist, C. A decade of AIRE. *Nature Reviews Immunology* **7,** 645–650 (2007).
32. Calnan, B. J., Szychowski, S., Chan, F. K., Cado, D. & Winoto, A. A role for the orphan steroid receptor Nur77 in apoptosis accompanying antigen-induced negative selection. *Immunity* **3,** 273–282 (1995).
33. Zhou, T. *et al.* Inhibition of Nur77/Nurr1 leads to inefficient clonal deletion of self-reactive T cells. *J. Exp. Med.* **183,** 1879–1892 (1996).
34. Suen, A. Y. W. & Baldwin, T. A. Proapoptotic protein Bim is differentially required during thymic clonal deletion to ubiquitous versus tissue-restricted antigens. *Proc. Natl. Acad. Sci. U.S.A.* **109,** 893–898 (2012).
35. Gray, D. H. D. *et al.* The BH3-only proteins Bim and Puma cooperate to impose deletional tolerance of organ-specific antigens. *Immunity* **37,** 451–462 (2012).
36. Strasser, A. The role of BH3-only proteins in the immune system. *Nature Reviews Immunology* **5,** 189–200 (2005).
37. Sohn, S. J., Thompson, J. & Winoto, A. Apoptosis during negative selection of autoreactive thymocytes. *Curr. Opin. Immunol.* **19,** 510–515 (2007).
38. Bouillet, P. *et al.* Proapoptotic Bcl-2 relative Bim required for certain apoptotic responses, leukocyte homeostasis, and to preclude autoimmunity. *Science* **286,** 1735–1738 (1999).
39. Woronicz, J. D., Calnan, B., Ngo, V. & Winoto, A. Requirement for the orphan

steroid receptor Nur77 in apoptosis of T-cell hybridomas. *Nature* **367,** 277–281 (1994).
40. Youn, H. D. & Liu, J. O. Cabin1 represses MEF2-dependent Nur77 expression and T cell apoptosis by controlling association of histone deacetylases and acetylases with MEF2. *Immunity* **13,** 85–94 (2000).
41. Thompson, J. & Winoto, A. During negative selection, Nur77 family proteins translocate to mitochondria where they associate with Bcl-2 and expose its proapoptotic BH3 domain. *J. Exp. Med.* **205,** 1029–1036 (2008).
42. Cheng, L. E., Chan, F. K., Cado, D. & Winoto, A. Functional redundancy of the Nur77 and Nor-1 orphan steroid receptors in T-cell apoptosis. *The EMBO Journal* **16,** 1865–1875 (1997).
43. Liu, Z.-G., Smith, S. W., McLaughlin, K. A., Schwartz, L. M. & Osborne, B. A. Apoptotic signals delivered through the T-cell receptor of a T-cell hybrid require the immediate–early gene nur77. *Nature* **367,** 281–284 (1994).
44. Cheng, E. H. *et al.* Conversion of Bcl-2 to a Bax-like death effector by caspases. *Science* **278,** 1966–1968 (1997).
45. Zhou, T. *et al.* Inhibition of Nur77/Nurr1 leads to inefficient clonal deletion of self-reactive T cells. *J. Exp. Med.* **183,** 1879–1892 (1996).
46. Hu, Q. N., Suen, A. Y. W., Caviedes, L. M. H. & Baldwin, T. A. Nur77 Regulates Nondeletional Mechanisms of Tolerance in T Cells. *J Immunol* **199,** 3147–3157 (2017).
47. Nowyhed, H. N. *et al.* The Nuclear Receptor Nr4a1 Controls CD8 T Cell Development Through Transcriptional Suppression of Runx3. *Scientific Reports* **5,** S57 (2015).
48. Sekiya, T. *et al.* Nr4a receptors are essential for thymic regulatory T cell development and immune homeostasis. *Nature Publishing Group* **14,** 230–237 (2013).
49. Sekiya, T. *et al.* Nr4a receptors are essential for thymic regulatory T cell development and immune homeostasis. *Nat Immunol* **14,** 230–237 (2013).
50. Rajpal, A. *et al.* Transcriptional activation of known and novel apoptotic pathways by Nur77 orphan steroid receptor. *The EMBO Journal* **22,** 6526–6536 (2003).
51. Weih, F., Ryseck, R. P., Chen, L. & Bravo, R. Apoptosis of nur77/N10-transgenic thymocytes involves the Fas/Fas ligand pathway. *Proc Natl Acad Sci U S A* **93,** 5533–5538 (1996).
52. Villunger, A. *et al.* Negative selection of semimature CD4(+)8(-)HSA+ thymocytes requires the BH3-only protein Bim but is independent of death receptor signaling. *Proc Natl Acad Sci U S A* **101,** 7052–7057 (2004).
53. Cretney, E. *et al.* Normal thymocyte negative selection in TRAIL-deficient mice. *J. Exp. Med.* **198,** 491–496 (2003).
54. Cretney, E., Uldrich, A. P., McNab, F. W., Godfrey, D. I. & Smyth, M. J. No requirement for TRAIL in intrathymic negative selection. *International immunology* **20,** 267–276 (2008).
55. Li, H. *et al.* Cytochrome c release and apoptosis induced by mitochondrial targeting of nuclear orphan receptor TR3. *Science* **289,** 1159–1164 (2000).
56. Lin, B. *et al.* Conversion of Bcl-2 from protector to killer by interaction with

nuclear orphan receptor Nur77/TR3. *Cell* **116,** 527–540 (2004).
57. Thompson, J., Burger, M. L., Whang, H. & Winoto, A. Protein kinase C regulates mitochondrial targeting of Nur77 and its family member Nor-1 in thymocytes undergoing apoptosis. *Eur. J. Immunol.* **40,** 2041–2049 (2010).
58. Ferlini, C. *et al.* Paclitaxel directly binds to Bcl-2 and functionally mimics activity of Nur77. *Cancer Res.* **69,** 6906–6914 (2009).
59. Luciano, F. *et al.* Nur77 converts phenotype of Bcl-B, an antiapoptotic protein expressed in plasma cells and myeloma. **109,** 3849–3855 (2007).
60. Petros, A. M., Olejniczak, E. T. & Fesik, S. W. Structural biology of the Bcl-2 family of proteins. *Biochimica et Biophysica Acta (BBA) - Molecular Cell Research* **1644,** 83–94 (2004).
61. Burger, M. L., Leung, K. K., Bennett, M. J., Winoto, A. & Mathis, D. T cell-specific inhibition of multiple apoptotic pathways blocks negative selection and causes autoimmunity. *eLife Sciences* **3,** e03468 (2014).
62. Merino, D. & Bouillet, P. The Bcl-2 family in autoimmune and degenerative disorders. *Apoptosis : an international journal on programmed cell death* **14,** 570–583 (2009).
63. Tischner, D., Woess, C., Ottina, E. & Villunger, A. Bcl-2-regulated cell death signalling in the prevention of autoimmunity. *Cell Death Dis* **1,** e48–e48 (2010).
64. Hanahan, D. & Weinberg, R. A. The Hallmarks of Cancer. 1–14 (1999).
65. Kelly, P. N. & Strasser, A. The role of Bcl-2 and its pro-survival relatives in tumourigenesis and cancer therapy. *Cell Death Differ* **18,** 1414–1424 (2011).
66. Czabotar, P. E., Lessene, G., Strasser, A. & Adams, J. M. Control of apoptosis by the BCL-2 protein family: implications for physiology and therapy. *Nature reviews. Molecular cell biology* **15,** nrm3722–63 (2013).
67. Willis, S. N. & Adams, J. M. Life in the balance: how BH3-only proteins induce apoptosis. *Curr. Opin. Cell Biol.* **17,** 617–625 (2005).
68. Bouillet, P. & Strasser, A. BH3-only proteins - evolutionarily conserved proapoptotic Bcl-2 family members essential for initiating programmed cell death. *J Cell Sci* **115,** 1567–1574 (2002).
69. Kelekar, A. & Thompson, C. B. Bcl-2-family proteins: the role of the BH3 domain in apoptosis. *Trends in Cell Biology* **8,** 324–330 (1998).
70. Adams, J. M. Ways of dying: multiple pathways to apoptosis. *Genes Dev.* **17,** 2481–2495 (2003).
71. Chipuk, J. E., Bouchier-Hayes, L. & Green, D. R. Mitochondrial outer membrane permeabilization during apoptosis: the innocent bystander scenario. *Cell Death Differ* **13,** 4401963–1402 (2006).
72. Shi, Y. G. Mechanisms of caspase activation and inhibition during apoptosis. *Molecular Cell* **9,** 459–470 (2002).
73. Cheng, E. H. *et al.* BCL-2, BCL-X(L) sequester BH3 domain-only molecules preventing BAX- and BAK-mediated mitochondrial apoptosis. *Molecular Cell* **8,** 705–711 (2001).
74. Lessene, G., Czabotar, P. E. & Colman, P. M. BCL-2 family antagonists for cancer therapy. *Nat Rev Drug Discov* **7,** 989–1000 (2008).
75. Letai, A. G. Diagnosing and exploiting cancer's addiction to blocks in apoptosis. *Nat Rev Cancer* **8,** 121–132 (2008).

76. Kang, M. H. & Reynolds, C. P. Bcl-2 inhibitors: targeting mitochondrial apoptotic pathways in cancer therapy. *Clin. Cancer Res.* **15,** 1126–1132 (2009).
77. Adams, J. M. & Cory, S. Bcl-2-regulated apoptosis: mechanism and therapeutic potential. *Curr. Opin. Immunol.* **19,** 488–496 (2007).
78. Vogler, M., Dinsdale, D., Dyer, M. J. S. & Cohen, G. M. Bcl-2 inhibitors: small molecules with a big impact on cancer therapy. *Cell Death Differ* **16,** cdd2008137–367 (2008).
79. Ruefli-Brasse, A. & Reed, J. C. Therapeutics targeting Bcl-2 in hematological malignancies. *Biochem. J.* **474,** 3643–3657 (2017).
80. Moll, U. M., Marchenko, N. & Zhang, X.-K. p53 and Nur77/TR3 - transcription factors that directly target mitochondria for cell death induction. *Oncogene* **25,** 4725–4743 (2006).
81. Li, H. *et al.* Cytochrome c release and apoptosis induced by mitochondrial targeting of nuclear orphan receptor TR3. *Science* **289,** 1159–1164 (2000).
82. Kolluri, S. K. *et al.* A short Nur77-derived peptide converts Bcl-2 from a protector to a killer. *Cancer Cell* **14,** 285–298 (2008).
83. Ke, N., Godzik, A. & Reed, J. C. Bcl-B, a novel Bcl-2 family member that differentially binds and regulates Bax and Bak. *Journal of Biological Chemistry* **276,** 12481–12484 (2001).
84. Vogler, M. BCL2A1: the underdog in the BCL2 family. *Cell Death Differ* **19,** 67–74 (2011).
85. Rautureau, G. J. P. *et al.* The restricted binding repertoire of Bcl-B leaves Bim as the universal BH3-only prosurvival Bcl-2 protein antagonist. *Cell Death Dis* **3,** e443 (2012).
86. Godoi, P. H. C. *et al.* Orphan Nuclear Receptor NR4A1 binds a novel protein interaction site on anti-apoptotic B-cell lymphoma gene-2 family proteins. *J. Biol. Chem.* jbc.M116.715235 (2016). doi:10.1074/jbc.M116.715235
87. Palacios, R. & STEINMETZ, M. Il3-Dependent Mouse Clones That Express B-220 Surface-Antigen, Contain Ig Genes in Germ-Line Configuration, and Generate Lymphocytes-B Invivo. *Cell* **41,** 727–734 (1985).
88. Kinashi, T. *et al.* Differentiation of an interleukin 3-dependent precursor B-cell clone into immunoglobulin-producing cells in vitro. *Proc Natl Acad Sci U S A* **85,** 4473–4477 (1988).
89. Vaux, D. L., Cory, S. & Adams, J. M. Bcl-2 gene promotes haemopoietic cell survival and cooperates with c-myc to immortalize pre-B cells. *Nature* **335,** 440–442 (1988).
90. Petros, A. M. *et al.* Solution structure of the antiapoptotic protein bcl-2. *Proc Natl Acad Sci U S A* **98,** 3012–3017 (2001).
91. Lee, L. C., Hunter, J. J., Mujeeb, A., Turck, C. & Parslow, T. G. Evidence for alpha-helical conformation of an essential N-terminal region in the human Bcl2 protein. *Journal of Biological Chemistry* **271,** 23284–23288 (1996).
92. Huang, D. C., Adams, J. M. & Cory, S. The conserved N-terminal BH4 domain of Bcl-2 homologues is essential for inhibition of apoptosis and interaction with CED-4. *The EMBO Journal* **17,** 1029–1039 (1998).
93. Gibson, D. G. *et al.* Enzymatic assembly of DNA molecules up to several hundred kilobases. - PubMed - NCBI. *Nat. Methods* **6,** 343–345 (2009).

94. Bouillet, P. *et al.* BH3-only Bcl-2 family member Bim is required for apoptosis of autoreactive thymocytes. *Nature* **415,** 922–926 (2002).
95. Gray, D. H. D. *et al.* The BH3-Only Proteins Bim and Puma Cooperate to Impose Deletional Tolerance of Organ-Specific Antigens. *Immunity* **37,** 451–462 (2012).
96. Erlacher, M. *et al.* Puma cooperates with Bim, the rate-limiting BH3-only protein in cell death during lymphocyte development, in apoptosis induction. *J. Exp. Med.* **203,** 2939–2951 (2006).
97. Labi, V. *et al.* Deregulated cell death and lymphocyte homeostasis cause premature lethality in mice lacking the BH3-only proteins Bim and Bmf. *Blood* (2014). doi:10.1182/blood-2013-11-537217
98. Sentman, C. L., Shutter, J. R., Hockenbery, D., Kanagawa, O. & Korsmeyer, S. J. bcl-2 inhibits multiple forms of apoptosis but not negative selection in thymocytes. *Cell* **67,** 879–888 (1991).
99. Shum, A. K. *et al.* Identification of an autoantigen demonstrates a link between interstitial lung disease and a defect in central tolerance. *Sci Transl Med* **1,** 9ra20–9ra20 (2009).
100. Shum, A. K. *et al.* BPIFB1 is a lung-specific autoantigen associated with interstitial lung disease. *Sci Transl Med* **5,** 206ra139–206ra139 (2013).
101. DeVoss, J. *et al.* Spontaneous autoimmunity prevented by thymic expression of a single self-antigen. *J. Exp. Med.* **203,** 2727–2735 (2006).
102. Taniguchi, R. T. *et al.* Detection of an autoreactive T-cell population within the polyclonal repertoire that undergoes distinct autoimmune regulator (Aire)-mediated selection. *Proc. Natl. Acad. Sci. U.S.A.* **109,** 7847–7852 (2012).
103. Mellacheruvu, D. *et al.* The CRAPome: a Contaminant Repository for Affinity Purification Mass Spectrometry Data. *Nat. Methods* **10,** 730–736 (2013).
104. Szymczak-Workman, A. L., Delgoffe, G. M., Green, D. R. & Vignali, D. A. A. Cutting edge: regulatory T cells do not mediate suppression via programmed cell death pathways. *J. Immunol.* **187,** 4416–4420 (2011).
105. Hu, Q., Sader, A., Parkman, J. C. & Baldwin, T. A. Bim-mediated apoptosis is not necessary for thymic negative selection to ubiquitous self-antigens. *J. Immunol.* **183,** 7761–7767 (2009).
106. Hu, Q. N. & Baldwin, T. A. Differential Roles for Bim and Nur77 in Thymocyte Clonal Deletion Induced by Ubiquitous Self-Antigen. *J. Immunol.* **194,** 1400030–2653 (2015).
107. McCaughtry, T. M., Baldwin, T. A., Wilken, M. S. & Hogquist, K. A. Clonal deletion of thymocytes can occur in the cortex with no involvement of the medulla. *J. Exp. Med.* **205,** 2575–2584 (2008).
108. Linette, G. P., Hess, J. L., Sentman, C. L. & Korsmeyer, S. J. Peripheral T-cell lymphoma in lckpr-bcl-2 transgenic mice. *Blood* **86,** 1255–1260 (1995).
109. Collison, L. W. & Vignali, D. In vitro Treg suppression assays. *Regulatory T Cells: Methods and Protocols* **372,** 95–106 (2011).
110. Moon, J. J. *et al.* Tracking epitope-specific T cells. *Nature Protocols* **4,** 565–581 (2009).
111. Moon, J. J. *et al.* Naive CD4+ T Cell Frequency Varies for Different Epitopes and Predicts Repertoire Diversity and Response Magnitude. *Immunity* **27,** 203–213

(2007).
112. Mellman, I., Coukos, G. & Dranoff, G. Cancer immunotherapy comes of age. *Nature* **480,** 480–489 (2011).
113. Chen, D. S. & Mellman, I. Oncology meets immunology: the cancer-immunity cycle. *Immunity* **39,** 1–10 (2013).
114. Pardoll, D. M. The blockade of immune checkpoints in cancer immunotherapy. *Nat Rev Cancer* **12,** 252–264 (2012).
115. Hodi, F. S. *et al.* Improved Survival with Ipilimumab in Patients with Metastatic Melanoma. *N Engl J Med* **363,** 711–723 (2010).
116. Hogquist, K. A., Baldwin, T. A. & Jameson, S. C. Central tolerance: learning self-control in the thymus. *Nature Reviews Immunology* **5,** 772–782 (2005).
117. Sohn, S. J., Rajpal, A. & Winoto, A. Apoptosis during lymphoid development. *Curr. Opin. Immunol.* **15,** 209–216 (2003).
118. Stritesky, G. L., Jameson, S. C. & Hogquist, K. A. Selection of self-reactive T cells in the thymus. *Annu. Rev. Immunol.* **30,** 95–114 (2012).
119. Gallegos, A. M. & Bevan, M. J. Central tolerance: good but imperfect. *Immunol. Rev.* **209,** 290–296 (2006).
120. Gallegos, A. M. & Bevan, M. J. Central tolerance to tissue-specific antigens mediated by direct and indirect antigen presentation. *J. Exp. Med.* **200,** 1039–1049 (2004).
121. Legoux, F. P. *et al.* CD4+ T Cell Tolerance to Tissue-Restricted Self Antigens Is Mediated by Antigen-Specific Regulatory T Cells Rather Than Deletion. *Immunity* **43,** 896–908 (2015).
122. Zehn, D. & Bevan, M. J. T Cells with Low Avidity for a Tissue-Restricted Antigen Routinely Evade Central and Peripheral Tolerance and Cause Autoimmunity. *Immunity* **25,** 261–270 (2006).
123. Yu, W. *et al.* Clonal Deletion Prunes but Does Not Eliminate Self-Specific αβ CD8+ T Lymphocytes. *Immunity* **42,** 929–941 (2015).
124. Ohkura, N., Kitagawa, Y. & Sakaguchi, S. Development and Maintenance of Regulatory T cells. *Immunity* **38,** 414–423 (2013).
125. Fontenot, J. D., Gavin, M. A. & Rudensky, A. Y. Foxp3 programs the development and function of CD4+CD25+ regulatory T cells. *Nat Immunol* **4,** 330–336 (2003).
126. Mueller, D. L. Mechanisms maintaining peripheral tolerance. *Nat Immunol* **11,** 21–27 (2010).
127. Caspi, R. R. Immunotherapy of autoimmunity and cancer: the penalty for success. *Nature Reviews Immunology* **8,** 970–976 (2008).
128. Träger, U. *et al.* The Immune Response to Melanoma Is Limited by Thymic Selection of Self-Antigens. *PLoS ONE* **7,** e35005 (2012).
129. Zhu, M.-L., Nagavalli, A. & Su, M. A. Aire deficiency promotes TRP-1-specific immune rejection of melanoma. *Cancer Res.* **73,** 2104–2116 (2013).
130. Khan, I. S. *et al.* Enhancement of an anti-tumor immune response by transient blockade of central T cell tolerance. *Journal of Experimental Medicine* **211,** 761–768 (2014).
131. Rafiq, K., Bergtold, A. & Clynes, R. Immune complex-mediated antigen presentation induces tumor immunity. *J. Clin. Invest.* **110,** 71–79 (2002).

132. Zou, W. Immunosuppressive networks in the tumour environment and their therapeutic relevance. *Nat Rev Cancer* **5,** 263–274 (2005).
133. Rabinovich, G. A., Gabrilovich, D. & Sotomayor, E. M. Immunosuppressive strategies that are mediated by tumor cells. *Annu. Rev. Immunol.* **25,** 267–296 (2007).
134. Malchow, S. *et al.* Aire-dependent thymic development of tumor-associated regulatory T cells. *Science* **339,** 1219–1224 (2013).
135. Watkins, C. L. *et al.* Co-operative Membrane Disruption Between Cell-penetrating Peptide and Cargo: Implications for the Therapeutic Use of the Bcl-2 Converter Peptide D-NuBCP-9-r8. *Molecular Therapy* 1–9 (2009).
136. Rong, Y.-P. *et al.* The BH4 domain of Bcl-2 inhibits ER calcium release and apoptosis by binding the regulatory and coupling domain of the IP3 receptor. *Proc. Natl. Acad. Sci. U.S.A.* **106,** 14397–14402 (2009).
137. Shimizu, S., Konishi, A., Kodama, T. & Tsujimoto, Y. BH4 domain of antiapoptotic Bcl-2 family members closes voltage-dependent anion channel and inhibits apoptotic mitochondrial changes and cell death. *Proc Natl Acad Sci U S A* **97,** 3100–3105 (2000).
138. Ono, M. *et al.* BH4 peptide derivative from Bcl-xL attenuates ischemia/reperfusion injury thorough anti-apoptotic mechanism in rat hearts. *Eur J Cardiothorac Surg* **27,** 117–121 (2005).
139. Sugioka, R. *et al.* BH4-domain peptide from Bcl-xL exerts anti-apoptotic activity in vivo. *Oncogene* **22,** 8432–8440 (2003).
140. Rong, Y.-P. *et al.* Targeting Bcl-2-IP3 Receptor Interaction to Reverse Bcl-2's Inhibition of Apoptotic Calcium Signals. *Molecular Cell* **31,** 255–265 (2008).
141. Monaco, G. *et al.* The BH4 domain of anti-apoptotic Bcl-XL, but not that of the related Bcl-2, limits the voltage-dependent anion channel 1 (VDAC1)-mediated transfer of pro-apoptotic Ca2+ signals to mitochondria. *Journal of Biological Chemistry* jbc.M114.622514 (2015).

Appendix A

The Effectiveness of Inducing Apoptosis by a Nur77-derived Bcl-2 Converting Peptide, NuBCP-9, in vitro

INTRODUCTION

The discovery a novel Bcl-2 pathway has revealed a unique opportunity to target Bcl-2 overexpression and exploit Bcl-2's activity as a killer, pro-apoptotic molecule[41,56,81]. Prior reports demonstrated Bcl-2 can be converted into a pro-apoptotic molecule upon interacting with Nur77 or Nor-1[41,56,81]. Characterization of this association has mapped the minimal Nur77 interaction residues to 478-504 (FRSLHSLL)[82]. Coupling this sequence with an arginine-rich cell penetrating peptide (CPP, D-Arg octomer), now available commercially as the Bcl-2 converter peptide D-NuBCP-9-r8 (NuBCP-9), was reported to induce cell death in a Bcl-2 dependent manner in several human cancer cell lines and block the anti-apoptotic activity of Bcl-x [82]. In addition, NuBCP-9 was also reported to possess anti-tumorigenic effects, as NuBCP-9 could inhibit tumor growth when injected directly into breast cancer xenografts[82]. Despite these promising indications that this Nur77-peptide could be used as a chemotherapeutic agent, NuBCP-9 has not been assessed in any clinical trial since its discovery.

Here, we initially revisited the ability for NuBCP-9 to induce cell death in a panel of cancer cell lines to gain additional insights on the mechanisms of Nur77-mediated cell death. In contrast to the initial report[82], the data suggests that NuBCP-9 can induce apoptosis independent of Bcl-2. Further, NuBCP-9 was still able to induce cell death in T cells expressing Bcl-2 with its BH3 domain mutated. Together, these results question NuBCP-9 specificity and caution the use of this peptide as a chemotherapeutic agent due to cytotoxic issues.

RESULTS

NuBCP-9 induces apoptosis in a panel of cancer cell lines in vitro independent of Bcl-2

The presence of Bcl-2 was shown to be essential for cancer cells to undergo NuBCP-9 induced apoptosis[82]. To confirm this, we first examined the presence of endogenous Bcl-2 protein in a panel of six human cancer cell lines to predict the efficacy of NuBCP-9. The cell lines that were used were breast cancer cell lines SKBR3, MDA-MB-231, and MCF7, cervical cancer cell line HeLa, lung cancer cell line H460, and prostate cancer cell line LnCAP. Cell lysates from each cell line were obtained and the presence of Bcl-2 was detected by immunoblot using Bcl-2 specific antibodies. As a control, lysates from T cells overexpressing the wild-type Bcl-2 transgene were used. As expected, high levels of Bcl-2 were detected in T cells expressing the Bcl-2 transgene. Of the six cancer cell lines used, high levels of Bcl-2 were detected in H460, followed by moderate levels of Bcl-2 in HeLa, and minimal levels of Bcl-2 in MCF-7 (Figure 1A). Undetectable levels of Bcl-2 were observed in LnCAP, MDA-MB-231, or SKBr3 cell lines (Figure 1A).

Based on the varied expression levels of endogenous Bcl-2 in this cell panel, we predicted the cell lines H460, HeLa, and MCF-7 would be most sensitive than LnCAP, MDA-MB-231, and SKBr3 to cell death by NuBCP-9. To test this prediction, cell viability in each cell line was evaluated after inducing apoptosis by staurosporin (STS) or titrated amounts of NuBCP-9 (2, 4, 6, 10, or 15 μM). Cell viability was normalized to the vehicle control (DMSO). As an additional control, the pan-caspase inhibitor, zVAD-fmk, was included in each condition to inhibit apoptosis. As expected and for each cell line, the addition of 1 μM STS was able to induce apoptosis, while the addition of 20 μM

zVAD-fmk in the presence of the apoptotic inducers was able to rescue from cell death in most treatments. As shown in Figure 1B and in line with our prediction, NuBCP-9 treatment in H460 and HeLa resulted in cell death in a dose dependent manner compared to the vehicle control (top left and middle panels, Figure 1B). MDA-MB-231 and SKBr3 cells, which we anticipated to be relatively resistant to cell death by NuBCP-9, was in line with our prediction and had minimal cell death compared vehicle control even when subjected to the highest dose of NuBCP-9 (bottom middle and right panels, Figure 1B). Interestingly, MCF-7 expressed low levels of Bcl-2, but these cells did not exhibit increased cell death in the presence of NuBCP-9 as observed in H460 and HeLa cells (top right panel, Figure 1B). Moreover, LnCAP cells, which had undetectable Bcl-2 protein levels, were nevertheless sensitive to NuBCP-9 induced cell death (bottom left panel, Figure 1B). Interestingly, death induced by NuBCP-9 in HeLa, MCF7 or LnCAP cells couldn't be rescued by addition of zVAD, suggesting that NuBCP-9 doesn't induce apoptosis. Together, these results highlight that NuBCP-9 could induce cell death *in vitro* regardless of Bcl-2 status and that NuBCP-9 induced death is not apoptosis.

NuBCP-9 may induce apoptosis independent of Bcl-2 BH3 domain exposure

NuBCP-9 has been shown to induce Bcl-2's pro-apoptotic function by exposing Bcl-2's killer BH3 domain[82]. Since we observed cell death inconsistent with a principle tenent of this peptide (i.e. dependent on the presence of Bcl-2) in a panel of cancer cell lines, we investigated the ability for NuBCP-9 peptide to elicit cell death in T cells obtained from wild-type littermate, Bcl-2 Tg, or mice expressing a transgene for *Bcl-2* containing a mutant BH3 domain (Bcl-2 BH3* Tg). In the latter, the mutation corresponds to GDD101-103 → AAA, which effectively disrupts Nur77 conversion death pathway[44,61]. Cell viability was assessed by Annexin V and 7-aminoactinomycin-D (7-AAD) over time in total thymocytes subjected to 10 μM NuBCP-9. As expected, NuBCP-9 induced cell death in total WT thymocytes, with cell death occurring maximally at 8 hours after adding the peptide (Figure 2A). Surprisingly, the addition of NuBCP-9 to Bcl-2 Tg or Bcl-2 BH3* Tg thymocytes resulted in death that was indistinguishable to WT littermates (Figure 2A). Similar results were obtained when performed on peripheral CD4 or CD8 T cells obtained from different mouse genotypes (Figure 2B). Taken together, we conclude that NuBCP-9 can induce cell death independent of Bcl-2 and Bcl-2 BH3 domain exposure.

DISCUSSION

The reports that observed a Nur77-derived peptide could induce the pro-apoptotic function of Bcl-2 highlights that this pathway can be targeted for cancer therapy[41,56,81]. Our initial rationale for using NuBCP-9 peptide was to further clarify the mechanism of Nur77 conversion. While Nur77 has been reported to interact with an unstructured loop region within Bcl-2, Nur77 has also been reported to interact and convert anti-apoptotic Bcl-b and Bcl-2a1 into pro-apoptotic molecules[59]. However, how this is achieved with either Bcl-2a1 or Bcl-b is not entirely clear since neither contain a loop domain. NuBCP-9 was also an attractive molecule to utilize and assess whether this peptide could cooperatively induce cell death by interacting with Bcl-2a1 in cancer cell lines. This is an attractive hypothesis supported by the observation that NuBCP-9 could elicit cell death in cancer cells that express little to no Bcl-2. However, in this

report, we demonstrate that NuBCP-9 peptide has unanticipated cytotoxic effects independent of this peptide's proposed mechanism. This is supported by the cell death induced by NuBCP-9 in T cells obtained *ex-vivo* from BH3* Tg mice, which has been shown to effectively block Nur77 conversion pathway in T cells. In light of producing these results, Watkins et al[135] reported that the Nur77-derived sequence could enhance the ability for the cell penetrating peptide (CPP) sequence to interact with the plasma membrane and causes cell death independent of Bcl-2 expression. Therefore, our data casts doubt on the specificity and use of NuBCP-9.

MATERIAL & METHODS

Mice

C57BL/6 wild-type (WT) or C57BL/6 mice engineered to express wild-type Bcl-2 or Bcl-2 with its BH3 domain mutated (BH3* Tg) transgenes have been previous described[61,108]. Single cell suspension of mouse thymus, spleen, or lymph nodes were obtained by dissociating the tissue through a 40 μM cell strainer followed by lysing red blood cells using ACK Buffer (0.15M NH_4Cl, 1 mM $KHCO_3$, 0.1 mM EDTA, pH adjusted to 7.2-7.4 with 1N HCl, filter sterilized). Cells were then used for cell viability assays described below. The UC Berkeley Animal Care and Use Committee (ACUC) have approved all experiments involving these animals.

Cell culture and reagents

SKBr3, MCF-7, and MDA-MB-231 cells were maintained at 37˚C in DMEM supplemented in 10% fetal bovine serum (FBS), 2 mM L-glutamine, non-essential amino acids, and 1 mM sodium pyruvate (cDMEM). HeLa, H460, and LnCAP cells were cultured and maintained at 37˚C in RPMI-1640 supplemented with 10% FBS, 2 mM L-glutamine, non-essential amino acids, 5 x 10^{-5} M 2-mercaptoethanol and 1 mM sodium pyruvate (cRPMI). D-NuBCP-9-r8 (NuBCP-9) was purchased from Cal-Biochem, resuspended in DMSO at a stock concentration of 1 mM and stored in aliquots at -80˚C. Staurosporin (STS) was purchased from Sigma-Alridch.

Western Blot and antibodies

Whole cell extracts were obtained for each cancer cells cultured from a 10 cm dish of 75-80% confluence. Cells were washed with PBS, and resuspended in standard radioimmunoprecipitation assay (RIPA; 150 mM NaCl; 50 mM Tris-HCl, pH 7.5; 1 mM EDTA; 1% NP-40; 0.5% SDS; Protease Inhibitor Cocktail (Sigma); and 1 mM DTT). Lysates were clarified by high-speed centrifugation. Protein concentration was obtained using Bio-Rad *DC* protein assay. 20 μg of total protein was loaded into a 10% SDS-PAGE gel, and transferred onto nitrocellulose membranes. Membranes were blocked with 5% BSA in TBS containing 0.1% Tween. Membranes were probed using anti-Bcl-2 (clone 6C8BD, Pharmingen) and anti-B-actin (Sigma) antibodies.

Cell viability via CellTiter-Glo

Each cell line was seeded at 1 x 10^5 cells per well in 96-flat bottom plates one day prior to the addition of indicated concentrations of STS or NuBCP-9. Cell viability was measured 24 hours after the addition of these drugs or indicated time using CellTiter-glo (CTG) according to the manufacture's recommendations with one

exception: dilute CTG 1:1 with 1X PBS to extend the use of the reagent. Relative Light Units (RLUs) were normalized to the vehicle control sample to compare the apoptotic induction.

Annexin V & 7-aminoactinomycin D staining by flow cytometry

Single cells suspension from thymocytes and peripheral lymph nodes of indicated mouse genotype were obtained as previously described above. After resting cells for 1 hour at 37˚C in cRPMI, cells were seeded at 1-5 x 10^5 cells per well in a 96-flat bottom plate. NuBCP-9 was added at indicated concentration. Cells were harvested at indicated time points, washed with 1X PBS, resuspended in Annexin V binding buffer (100 mM HEPES, pH 7.4; 140 mM NaCl; 2.5 mM $CaCl_2$), and then incubated with Annexin V-FITC (BD Pharmingen) and 7-AAD (BD Pharmingen).

FIGURE 1

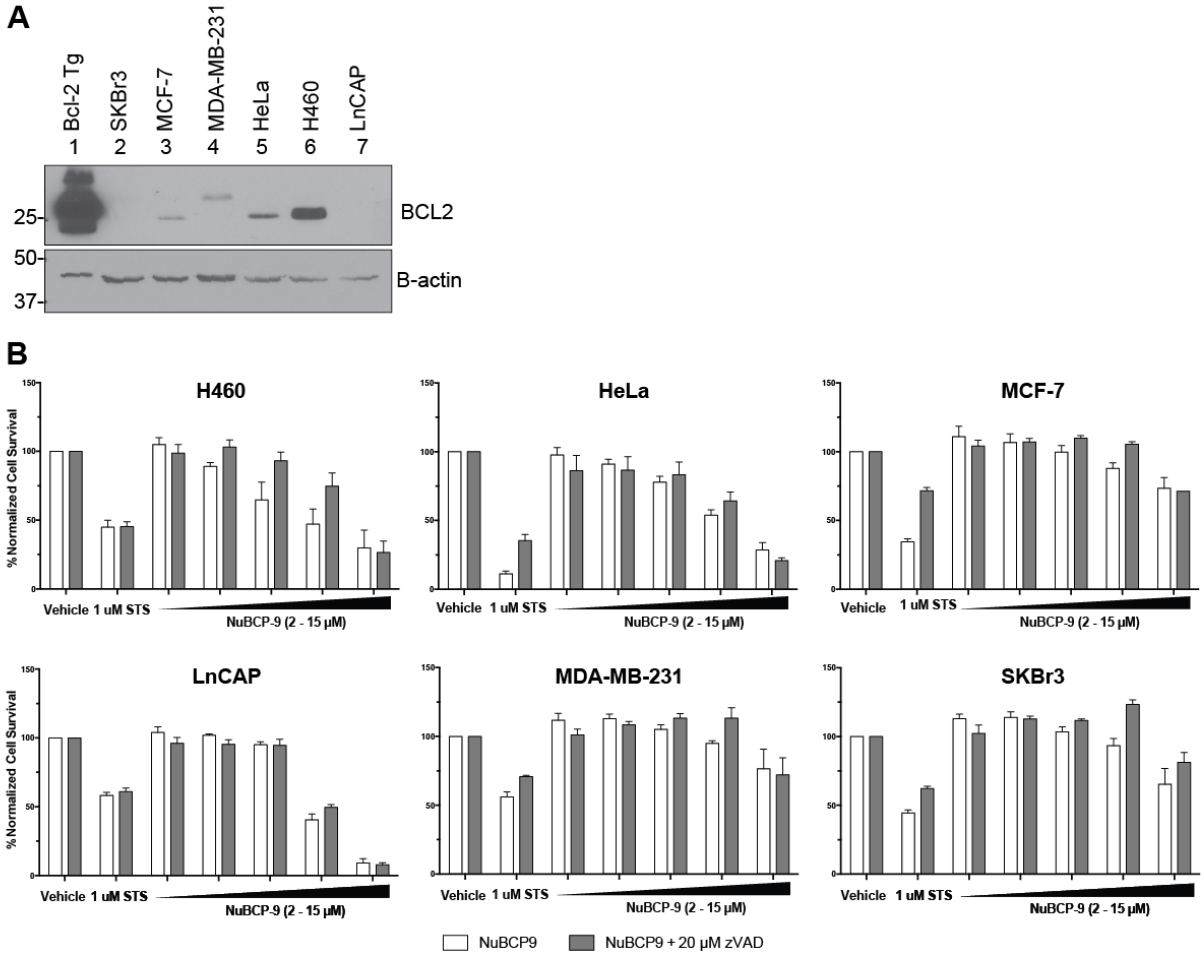

Figure 1. Lack of correlation between Bcl-2 expression and NuBCP-9 apoptotic activities. *A,* Western blot analysis comparing endogenous Bcl-2 from six different cancer cell lines. Lysates from T cells overexpressing the transgene for human wild-type Bcl-2 (Bcl-2 Tg) was used as a positive control. *B,* Each cancer cell line was incubated with the indicated concentration of STS or NuBCP-9 in the presence or absence of a pan-caspase inhibitor zVAD-fmk for 24 hours. Cell viability was measured by CellTiter-Glo. Results shown are referenced mean ± SD values to the vehicle control and are represented of three combined experimental repeats performed in triplicate.

FIGURE 2

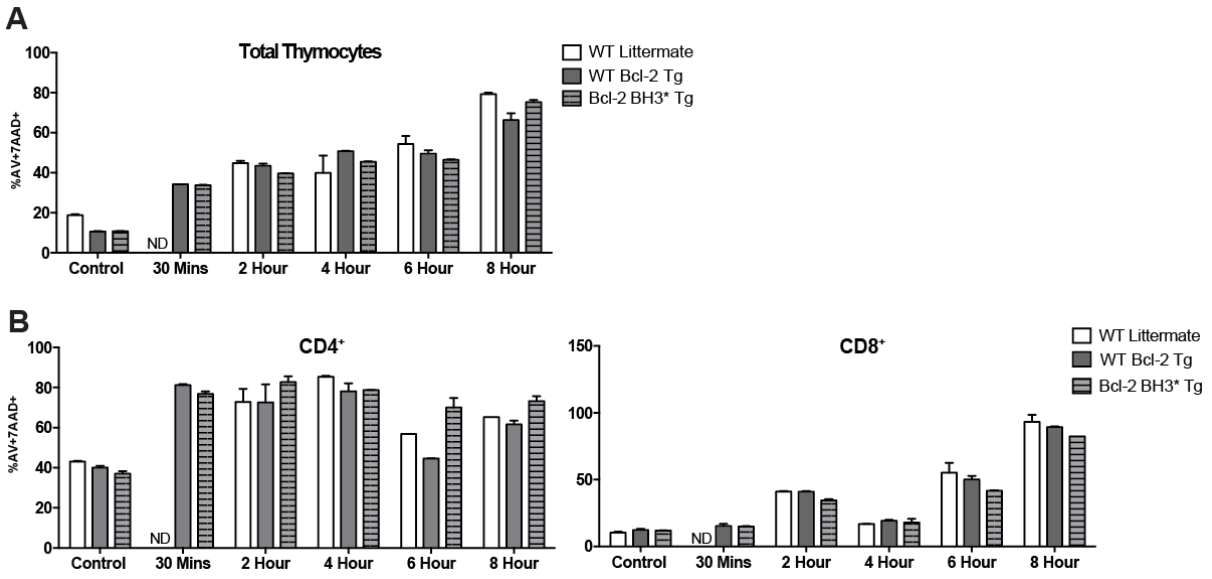

Figure 2. Viability in T cells expressing a Bcl-2 protein with a mutated BH3 domain after NuBCP-9 treatment. Viability was assessed by Annexin V and 7-AAD in thymocytes (A) or CD4 versus CD8 T cells obtained from peripheral lymph nodes (B) after indicated time with 10 μM NuBCP-9. The addition of DMSO was used as a control. *A,* Total thymocytes from each genotype were incubated with 10 μM NuBCP-9. *A*, Thymocytes were incubated with 10 μM of NuBCP-9 for indicated time. *B*, Flow cytometric analysis of CD4 (left panel) versus CD8 (right panel) T cells obtained from peripheral lymph nodes that were incubated with 10 μM NuBCP-9 for indicated time. Data are representative of two independent experiments performed in triplicate and shown as percentage of Annexin V^+ and $7AAD^+$ (%AV+7AAD+).

APPENDIX B

TAT-Bcl-2 Blocking Peptide

INTRODUCTION

In chapter 1, we uncovered residues within Bcl-2 BH4 domain, Y18 and Y21, that was sufficient to interact with Nur77 and Nor-1. The role of the BH4 domain in Bcl-2 has been reported to be anti-apoptotic. This led us to speculate that a Bcl-2 BH4 peptide could be sufficient to block multiple forms of apoptosis as previously shown with peptide derived from Bcl-x[136-138]. In addition, we also reasoned that a peptide containing Y18 and Y21 could also inhibit Nur77-mediated apoptosis by competitively bind to Nur77/Nor-1 and block the interaction with Bcl-2. Thus, we generated a FITC-conjugated cell penetrating peptide fused to the residues that correspond with Bcl-2/11-35. We aptly named this new peptide, Bcl-2 blocking peptide or TAT-BBP.

RESULTS

TAT-BH4 incorporates into cells

To gain a better understanding of the TAT-BBP cell penetrating peptide, I first assessed the ability of the peptide to incorporate into the HeLa cells by microscopy. HeLa cells that were incubated with the peptide for 2 hours were then interrogated for the presence of FITC. Indeed, I could detect FITC in HeLa cells that were incubated with TAT-BBP Specifically, the localization was predominately nuclear with defined puncta (Figure 1A).

I also assessed the efficiency of TAT-BBP incorporation by FACS. To this end, OVCAR3 cells were incubated with the TAT-only control or TAT-BBP peptide for 2 hours and uptake was measured by the presence of FITC. Incorporation of the TAT-only peptide into these cells was evident at both 330 μM and 660 μM concentrations (solid line, Figure 1B). Surprisingly, the TAT-BBP peptide was able to incorporate into these cells to a greater efficiency (dotted line, Figure 1B). In the same experiments except using HeLa cells, similar results were obtained (Figure 1C). Taken together, the TAT-BBP peptide is able to penetrate the cells and preferentially localizes in the nucleus.

TAT-BH4 does not protect from chemical inducers of apoptosis

The BH4 domain of the anti-apoptotic Bcl-2 family members is involved in the function to prevent apoptosis. In prior publications, the use of a TAT-BH4 peptide derived from Bcl-X was shown to protect cells from apoptosis by x-rays, cytokine withdrawal, and staurosporin[139]. We wondered if the TAT-BBP peptide could provide similar protection. To test whether TAT-BBP peptide could protection, we employed the use of two apoptotic inducers: staurosporin (STS) and etoposide (VP16). OVCAR3 cells were incubated with 1 μM of STS in the presence of either TAT-only or TAT-BBP peptides and cell death was measured by 7AAD staining. As expected, cells treated with 1 μM of STS were able to elicit cell death. In the presence of the TAT-only peptide, cell death was elicited to a similar level of cell treated with 1 μM of STS. Surprisingly, TAT-BBP peptide was unable to rescue cells from death by 1 μM STS (left panel, Figure 2A). Similar results were obtained using etoposide (right panel, Figure 2A). In addition, these results could be recapitulated in HeLa cells (Figure 3). Taken together, these results suggest that the TAT-BBP peptide is unable to provide additional protection from chemical inducers of apoptosis.

TAT-BH4 does not protect from Nur77-mediated apoptosis

To test whether TAT-BBP could protect from Nur77-mediated apoptosis, thymocytes were stimulated with CD3 and CD28 in the presence of TAT-only or TAT-BBP peptide. After stimulation, cell death was measured by cellular uptake of 7AAD through FACS analysis. Interestingly, thymocyte stimulated with strong CD3/D28 stimulus were not rescued from cell death in the presence of TAT-BBP as thymocyte cell death was indistinguishable from that of the presence of the control peptide (Figure 3).

DISCUSSION

The purpose of these experiments was to generate a possible tool to study negative selection, specifically, transiently block Nur77-mediated death during negative selection to understand the contributions of Nur77-mediate death in maintaining T cell tolerance. It is surprising, however, why the peptide did not provide additional protection against apoptosis against chemical inducers of apoptosis while a similar TAT-BH4 derived from Bcl-x peptide can offer protection is unclear. Additionally, it is also unknown why TAT-BBP could not protect thymocytes from TCR-induced cell death.

Perhaps a likely reason for the failure of this peptide to prevent apoptosis is because of its nuclear localization. The microscopy experiments revealed that the TAT-BBP localized predominately to the nucleus. Because of this, TAT-BBP may not be able to provide protection at the mitochondria. Like TAT-BH4, TAT-BBP was unable to rescue thymocyte undergoing TCR-mediated apoptosis.

Further, the proper folding of the alpha helix that comprises the BH4 domain may also be necessary to provide protection. The Bcl-2 BH4 residues we used to generate the CPP were core BH4 residues, and reports using N-terminal residues to the BH4 domain were important for proper folding and activity[136,137,140,141]. Thus, generating a peptide containing these additional residues may provide protection in our model and an avenue to improve this peptide's anti-apoptotic function.

MATERIALS AND METHODS

Mice

The use of C57BL/6 wild-type (WT) mice were compliant with and approved by the UC Berkeley Animal Care and Use Committee (ACUC*).*

Cells

HeLa and OVCAR cells were maintained at 37˚C in in RPMI 1640 supplemented with 10% FBS, 2 mM L-glutamine, non-essential amino acids, 5 x 10^{-5} M 2-mercaptoethanol and 1 mM sodium pyruvate (cRPMI). Each cell line was periodically tested negative for mycoplasma.

Generation of TAT-BBP

The sequence for the TAT-only peptide was derived from nine-amino acids within the protein transduction domain of HIV and is as follows: FITC-Ahx-CRKKRRQRRR-NH2. The amino acids corresponding to Bcl-2/11-35 were synthesized and conjugated C-terminally to the TAT cell-penetrating peptide interspersed by beta-alanine residues. The final sequence for the TAT-BBP peptide is as follows: FITC-Ahx-CRKKRRQRRR-

(ß-Ala)-NREIVMKYIHYKLSQRGYEWDAGDV-NH2. Both cell penetrating peptides were synthesized by Peptide 2.0. Purity of the synthesized peptide was >95% as determined by high performance liquid chromatography and mass spectrometric analysis.

Confocal microscopy

Hela cells (7×10^4) were seeded into 4-well microscope chambers slides (Thermoscientific), and incubated with TAT-only or TAT-BBP peptide for two hours. Cells were washed with PBS, then fixed with 4% paraformaldehyde. Fixed cells were washed with PBS and permeabilized with 0.5% Triton X-100. Triton X-100 was removed and blocked with %5 bovine serum albumin (BSA). Block was removed by washing with PBS. DAPI was added to stain nuclei. Slides were mounted using VectorShield (Vector Inc.). Confocal images were obtained using Zeiss LSM 510 META NLA AxioImager, then analyzed by Image J software.

7-aminoactinomycin D staining by flow cytometry

Single cells suspensions of HeLa or OVCAR3 cells or single cell suspensions from thymocytes were obtained as previously described elsewhere. Cells were seeded at 1-5 x 10^5 cells per well in a 96-flat bottom plate. Cells were pre-incubated with TAT-only or TAT-BBP peptide for one hour prior to adding staurosporin (STS; Sigma-Aldrich) or etoposide (VP16; Sigma-Aldrich) for 24 hours. For thymocyte death assays, thymocytes were pre-incubated with the peptide following stimulation with PMA/Ionomycin or CD3/CD28. Cells were harvested, washed with 1X PBS, resuspended in Annexin V binding buffer (100 mM HEPES, pH 7.4; 140 mM NaCl; 2.5 mM $CaCl_2$), and then incubated with 7AAD (BD Pharmingen) or a specific antibody to PE-Annexin V (eBiosciences).

FIGURES
FIGURE 1
A

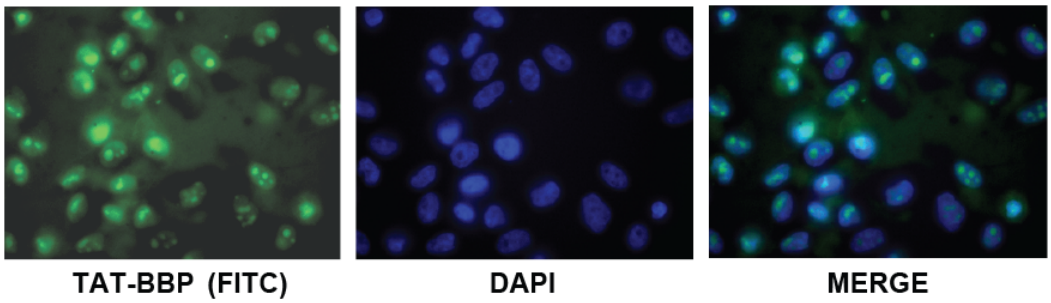

B

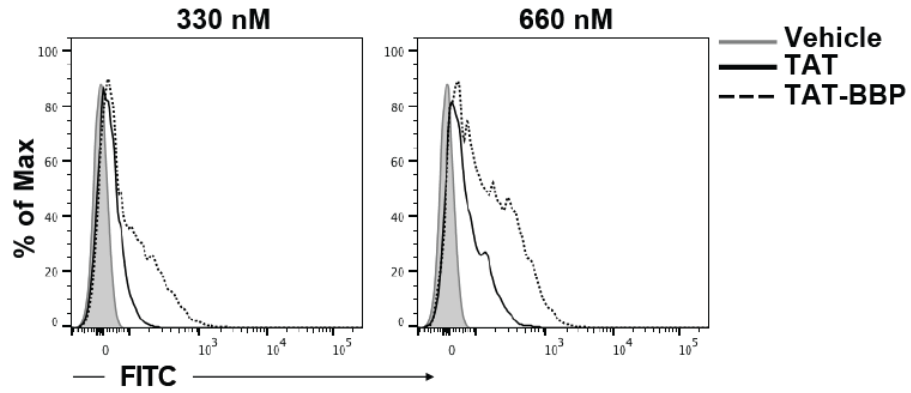

C

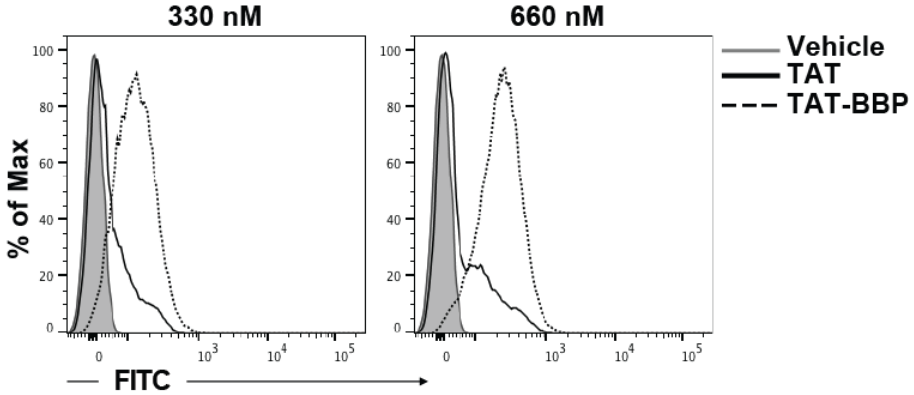

Figure 1. Incorporation of TAT-BBP peptide into cells. *A,* Localization of TAT-BBP peptide in the nuclear compartment. HeLa cells were incubated with 330 nM of TAT-BBP peptide for 24 hours, fixed on microscope slides and stained with DAPI. Images were captured using confocal microscopy and images were merged. *B-C,* FACS analysis of OVCAR3 (B) or HeLa (C) cells using two indicated concentrations of TAT-only or TAT-BBP peptide.

FIGURE 2

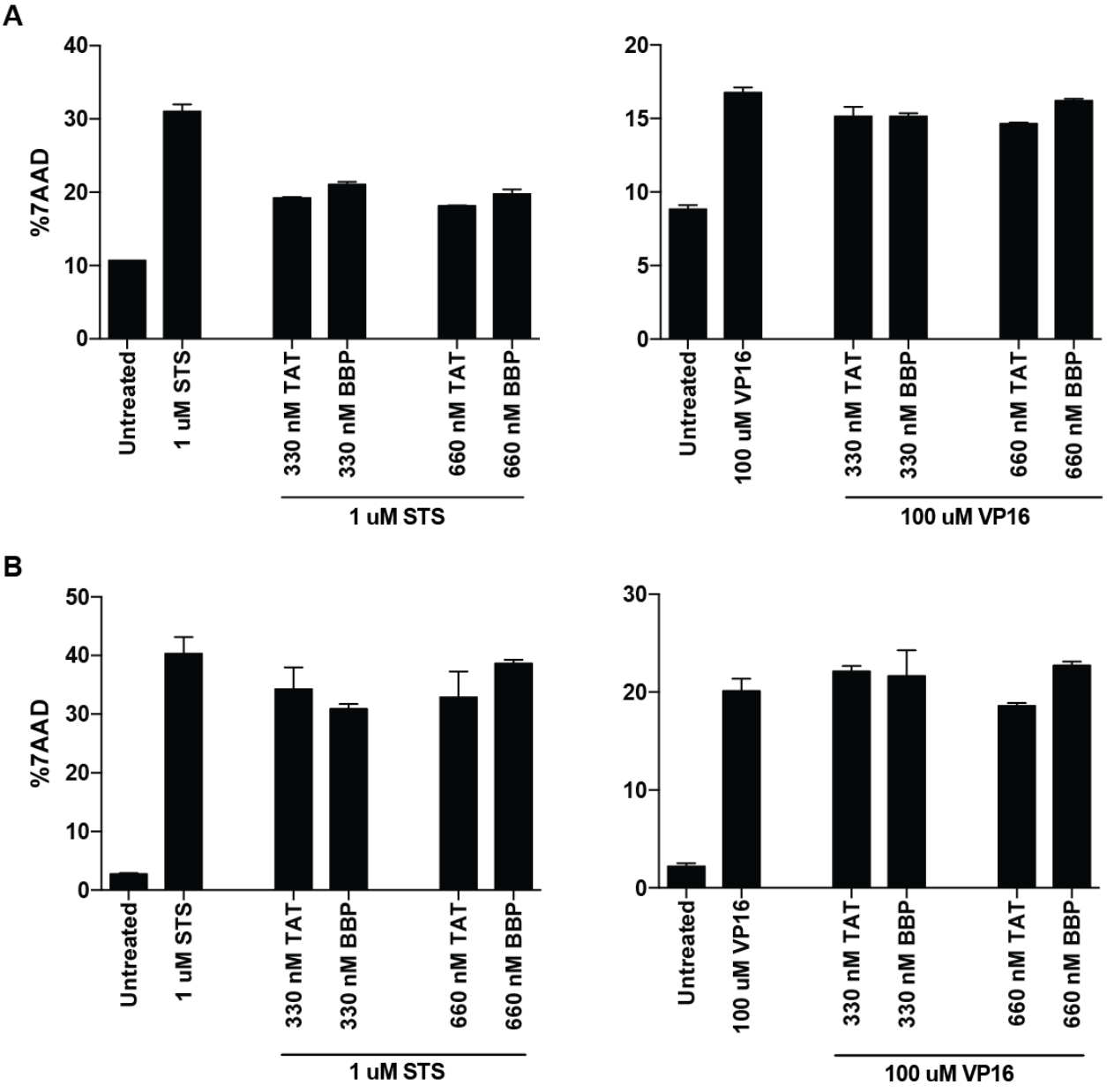

Figure 2. TAT-BBP does not provide addition protection against cell death. Cell death was measured by 7-aminoactinomycin D (7AAD) staining by FACS analysis. OVCAR3 (A) or HeLa (B) cells were pre-incubated with the TAT-only or TAT-BBP peptide then subjected to 1 μM of STS (left panels) or 100 μM VP16 (right panels). Data shown are raw percentage values of cells that stained positive for 7AAD.

FIGURE 3

A

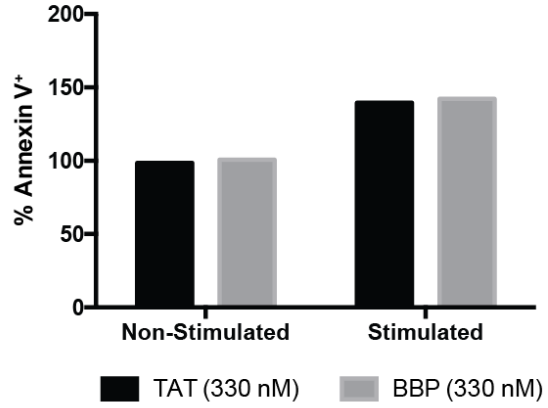

Figure 3. TAT-BBP does not protect against Nur77-mediated cell death. Thymocytes were obtained in wild-type mice and pre-incubated with indicated concentration of TAT-only or TAT-BBP peptide prior to stimulating with 10 µg/mL CD3 and 2 µg/mL CD28 for 18 hours. Cell death was measured using Annexin V and analyzed by FACS. Data shown here are normalized to non-stimulated samples.